ROCK COMPOSITION, LEACHATE QUALITY AND SOLUTE RELEASE AS A FUNCTION OF PARTICLE SIZE FOR THREE WASTE ROCK TYPES: AN 18-YEAR LABORATORY EXPERIMENT

December 2013

Minnesota Department of Natural Resources
Division of Lands and Minerals
500 Lafayette Road, Box 45
Saint Paul, MN 55155-4045

ROCK COMPOSITION, LEACHATE QUALITY AND SOLUTE RELEASE AS A FUNCTION OF PARTICLE SIZE FOR THREE WASTE ROCK TYPES: AN 18-YEAR LABORATORY EXPERIMENT

December 2013

Zach Wenz
Kim Lapakko
David Antonson

Minnesota Department of Natural Resources
Division of Lands and Minerals
500 Lafayette Road, Box 45
St. Paul, MN 55155-4045

TABLE OF CONTENTS

EXECUTIVE SUMMARY

Results from this study benefit the state of Minnesota in two fundamental ways. First, this experiment provides a large data set that can be used to validate experimental data collected by mining companies and their consultants as required by Minnesota Rule 6132.100. Second, this experiment design afforded development of a mathematical model that can predict (with some limitations) the composition of water draining from existing and future Duluth Complex waste rock stored on the Earth's surface. This model is a powerful tool that can be used to inform the state of Minnesota's environmental review and mine permitting processes for future mining projects. Furthermore, the potential for particle size experiments to aid environmental impact predictions and guide waste rock handling during mining operations and reclamation demonstrate the importance for this type of study to be included in waste rock characterization studies required for issuance of mine permits.

In this study three different rock types were characterized and different particle size samples of each rock type were subjected to laboratory dissolution tests for as long as 18 years to evaluate rock reactivity as a function of particle size. The rock types examined were norite (from the Duluth Complex, Mesaba prospect), diatreme, and mudstone. Each rock type was crushed and separated into a series of different particle size fractions ranging in size from <0.053 to 19 mm. Each size category from each rock type was analyzed for solid phase composition and subjected to humidity cell testing.

The particle size experiment provided insight into four key concepts that should be evaluated to assess the potential for proposed mining operations to impact the environment. These key concepts are 1) sulfide enrichment in fines, 2) leachate pH and sulfate release rate dependence on particle size, 3) sulfide mineral grain size distribution, and 4) long term leachate composition.

First crushing of rock can lead to enrichment of sulfide minerals in some particle size fractions. For norite, in which dominant sulfide mineral is softer than the host rock silicate minerals, the sulfur content of the smallest particle size sample was about twice that of the bulk sample. Thus, rates of sulfide mineral oxidation and the consequent acid production are enhanced not only by increased sulfide mineral specific surface area (area per unit mass) but also by increased sulfide mineral content of this fraction.

Second, the norite samples showed a systematic variation between both leachate pH and sulfate release rate and particle size. This relationship can be quantified and used to predict release rates for field scale waste rock piles. In addition, it indicates that the fine particles are dominant contributors to reactions in field scale rock piles.

Third, the substantial shift in pH and sulfate release rates observed between the 0.149-0.5 and 0.5-2.0 norite samples indicates that reducing norite rock particle size to less than 0.5 mm leads to near complete exposure of the majority of the sulfide mineral surfaces. Knowing this critical particle size in conjunction with a waste rock piles overall particle size distribution provides a gauge for the amount of highly reactive rock.

Fourth, the particle size experiment showed that essentially all the sulfide was reacted in particles finer than 0.5 mm, but for increasingly larger particles only a fraction of the sulfide was reacted over the reported experiment timespan. This demonstrates that not all sulfide minerals in a waste rock pile are readily available for reaction. Reaction of a considerable amount of these minerals will be controlled by the weathering and subsequent break down of the silicate mineral assemblage in which the sulfide minerals occur. The time required to dissolve silicates is orders of magnitude greater (thousands to tens of thousands of years for millimeters of weathering rind development (Colman and Pierce, 1981) than that for carbonates or sulfides.

1. EXPERIMENT HISTORY

The particle size experiment was designed to evaluate the dependence of leachate composition on rock particle size. To investigate this dependence the Minnesota Department of Natural Resources (MN DNR) began running a series of 25 rock dissolution tests in December, 1993 for three different rock types of six different particle size fractions and one blank. As of January 2013, only nine dissolution tests are active. Six of the active dissolution tests are of particular importance to the state of Minnesota because these samples are representative of some rock types of the Duluth Complex which host one of the largest Cu-Ni-Au-PGE deposits in the world. Data from this study can significantly aid development of waste characterization work plans, environmental review, and mine permitting for ore deposits hosted in the Duluth Complex.

Data collected from the particle size experiment previously were reported in Lapakko et al. (1995, 1998, and 2006). These reports contain detailed information of the experiment design, rock chemical composition (elemental concentrations, mineralogy, acid generation potential (AP), neutralization potential (NP), and empirical neutralization potential (ENP)), and comparative analysis of the leachate composition of the different rock types and size fractions. In general, these reports documented a particle size control on the percentage of acid generating and neutralizing components and a particle size dependence on sample leachate composition. This report is an update of the previous reports and presents an additional 500 weeks of data for trend analysis as well as additional interpretation of the chemical and physical processes responsible for the measured leachate compositions.

2. INTRODUCTION

Laboratory and field experiments designed to predict the composition of waste rock leachate commonly require particle size and/or volume reduction from full scale mining operations. Humidity cell kinetic tests are a common laboratory procedure used to determine solute release rates for tailings and waste rock. For waste rock, the laboratory tests require orders of magnitude reduction in grain size. For example, full scale mining operation waste rock piles contain rock ranging from clay (<0.004 mm) to boulder size (>256 mm), whereas the ASTM D5744-13 humidity cell test (ASTM International, 2013) requires material crushed to < 6.3 mm (0.25 in).

Mineral reaction rates have long been known to be in part dependent on the available surface area for reaction. Because solute release rates are related to surface area and total mineral surface area for a crushed rock sample is a function of the distribution of particle sizes, solute release rates are likewise dependent on particle size. The surface area of a sphere can be calculated by equation 1, where d = diameter. Specific surface area (eq. 2) relates surface area to mass by incorporating sample density, where ρ = density and d = diameter. From equation 2 the specific surface are is shown to be inversely proportional to particle diameter. Table 2.1 lists the surface area and specific surface area for a range of particle sizes demonstrating that few fine particles have much greater surface area per unit volume than large particles. For the particle size experiment, the smallest size sample had a specific surface area about 500 times that of the largest size sample. Thus, mass normalized solute release rates for laboratory humidity cell tests are inherently greater than that for operational scale waste rock piles.

$$SA_{sphere} = \pi d^2 \qquad \text{(eq.1)}$$

$$A_{s\ sphere} = \pi d^2/\rho(\pi d^3/6) \quad = 6/(\rho d) \qquad \text{(eq. 2)}$$

Reactions resulting in mineral dissolution and acid generation or neutralization are fundamentally related to the available surface area (mineral surface area exposed for reaction) of the minerals and consequently

particle size. The following text is an abbreviated discussion of mineral dissolution reactions relevant to the present study. A more thorough discussion of aqueous geochemistry fundamentals and geochemistry of acid mine drainage can be found in Plumlee and Logsdon (1999) and Jambor and Blowes (1994). The main sulfides in the rocks from this experiment include pyrite (FeS_2), pyrrhotite ($Fe_{1-x}S$), chalcopyrite ($CuFeS_2$) and cubanite ($CuFe_2S_3$). Oxidation of these minerals leads to acid generation through reactions 1-4. The rates of reaction and resultant acid production is dependent on mineral composition and crystal form, surface area exposure, availability of oxygen and water, fluid pH, and microbial activity.

$$4FeS_{2(s)} + 15O_{2(aq)} + 14H_2O_{(l)} = 4Fe(OH)_{3(s)} + 8SO_{4(aq)}^{2-} + 16H_{(aq)}^{+} \quad \text{(rxn. 1)}$$

$$8Fe_{1-x}S_{(s)} + [18 - 6x]\, O_{2(aq)} + [20 - 12x]H_2O_{(l)} = [8 - 8x]Fe(OH)_{3(s)} + 8SO_{4(aq)}^{2-} + 16H_{(aq)}^{+} \quad \text{(rxn. 2)}$$

$$4CuFeS_{2(s)} + 17O_{2(aq)} + 10H_2O_{(l)} = 4Fe(OH)_{3(s)} + 8SO_{4(aq)}^{2-} + 4Cu_{(aq)}^{2+} + 8H_{(aq)}^{+} \quad \text{(rxn. 3)}$$

$$\tfrac{8}{3}CuFe_2S_{3(s)} + \tfrac{52}{3}O_{2(aq)} + \tfrac{40}{3}H_2O_{(l)} = \tfrac{16}{3}Fe(OH)_{3(s)} + 8SO_{4(aq)}^{2-} + \tfrac{8}{3}Cu_{(aq)}^{2+} + \tfrac{32}{3}H_{(aq)}^{+} \quad \text{(rxn. 4)}$$

Acid generated by reactions 1 to 4 can be neutralized by reaction with carbonate and silicate minerals. For the particle size experiments the main minerals contributing to acid neutralization are calcite ($CaCO_3$), dolomite ($CaMg(CO_3)_2$), plagioclase ($CaAl_2Si_2O_8$, anorthite end member), and olivine ($MgSiO_4$, forsterite end member) through reactions 5 to 8. In general, the rate of dissolution for silicate minerals is orders of magnitude slower than that for carbonate minerals. Thus, despite reactions 5-8 showing two moles of acid neutralized for each mole of calcium or magnesium release, carbonates will neutralize an equivalent amount of acid faster.

$$CaCO_{3(s)} + 2H_{(aq)}^{+} = H_2CO_{3(aq)} + Ca_{(aq)}^{2+} \quad \text{(rxn. 5)}$$

$$CaMg(CO_3)_{2(s)} + 4H_{(aq)}^{+} = 2H_2CO_{3(aq)} + Ca_{(aq)}^{2+} + Mg_{(aq)}^{2+} \quad \text{(rxn. 6)}$$

$$CaAl_2Si_2O_{8(s)} + 2H_{(aq)}^{+} + H_2O_{(l)} = Ca_{(aq)}^{2+} + Al_2Si_2O_5(OH)_{4(s)} \quad \text{(rxn. 7)}$$

$$Mg_2SiO_4(s) + 4H_{(aq)}^{+} = 2Mg_{(aq)}^{2+} + SiO_{2(s)} + 2H_2O_{(l)} \quad \text{(rxn. 8)}$$

Because acid generating and acid neutralizing reactions occur at the mineral surface, any material covering the surface will affect the rate at which the reactions will occur. Mineral surfaces can become coated through precipitation of other minerals and by surface reactions that leach certain elements but leave non-reactive material at the mineral surface. For example, dissolution of anorthite (rxn. 7) results in forming the clay mineral kaolinite ($Al_2Si_2O_5(OH)_4$) which can lead to development of a coating on the plagioclase surface resulting in decreased plagioclase reactivity.

For sulfide oxidation, the formation of ferrihydrite ($Fe(OH)_3$; rxn. 1-4) during sulfide oxidation can form an oxide coating on the sulfide mineral surface. This is a common phenomenon seen for weathered sulfide minerals and has led to the application of the shrinking core model (Levenspiel, 1972) for sulfide oxidation. The shrinking core model is a mathematical expression of the sulfide oxidation rate as a function of sulfide particle size and thickness of an oxyhydroxide coating on the sulfide mineral surface. Increasing oxide coating thickness results in decreased oxidation rates. The decrease in sulfide oxidation rate occurs because as an oxide coating thickens oxygen must diffuse through a greater coating thickness. Diffusion is a much slower process than the reaction of oxygen at a fresh sulfide mineral surface. Applications of the shrinking core model to dissolution of sulfide minerals associated with mine wastes

have been presented by Davis and Ritchie (1986 and 1987), Nicholson et al. (1990) and Gerke et al. (1998). Photomicrographs and schematics depicting development of the oxidation coating on sulfide minerals are presented by Jambor (2003) and Jambor and Blowes (1998).

3. METHODS

The rock types diatreme, mudstone, and norite were selected for this experiment. The diatreme and mudstone samples were received by the MN DNR through request to the Western Governors' Association member states from undisclosed locations. The samples received were approximately < 15 cm (–6 inches), and were subsequently crushed to a 25.4 mm (–1 inch) particle size. The norite sample was collected from the FL-6 field test pile of the AMAX field study (Lapakko et al., 2004) and was similarly crushed to a 25.4 mm particle size. The crushed bulk samples were separated on a Ro-Tap® sieve shaker to collect the following six particle size fractions: 1) < 0.053 mm (–270 mesh), 2) 0.053 -0.149 mm (+270/–100 mesh), 3) 0.149 - 0.5 mm (+100/–35 mesh), 4) 0.5 - 2.0 mm (+35/–10 mesh), 5) 2.0 - 6.35 mm (+10 mesh/–0.25 inch), and 6) 6.35 - 19 mm (+0.25/–0.75 inch). After separation, the various size fractions were wet sieved (to remove residual fine particles) and dried. The diatreme and mudstone size fractions were then oven dried at about 38°C, and the norite was air dried. The drying times ranged from one to three days. The reactor and humidity cell experiments have been conducted by the MN DNR at the Hibbing Minnesota laboratory following the methods of Lapakko and Antonson (1994) and Lapakko and White (2000), respectively. The Lapakko and White (2000) method was subsequently revised slightly, adopted as Option B of ASTM D5744-07 and is included in the updated ASTM D5744-13 (ASTM International, 2013).

3.1 Analytical Methods

3.1.1 Solid Phase Composition

Solid-phase chemical analyses were conducted by ACME Analytical Laboratories Ltd., McSwiggen and Associates, and Midland Research. Whole rock total sulfur, sulfate, sulfide, and carbonate content were determined for each of the particle size fractions. Total sulfur content for equivalent particle size fractions between the ACME and Midland Research are significantly different for some particle size fractions for the norite and mudstone. The difference between these measurements is likely due to non-representative sampling for chemical analysis. Mineral modal abundance and composition was determined for the 2.0-6.35 mm fractions and the 6.35-19 mm particle size fraction for the mudstone. Solid phase compositional data is presented in Appendix 1.

ACME Analytical Laboratories Ltd.—. Total sulfur and carbon were determined by infrared adsorption using a LECO C244 Carbon-Sulfur analyzer. To determine total sulfur, the sample was crushed to < 100 µm and heated to >1650 °C. A second split was ignited to 800 °C to decompose sulfides and drive off sulfur as sulfur dioxide allowing the remaining concentration of sulfur as sulfate to be measured. Sulfur as sulfide was calculated by subtraction. Evolved carbon dioxide concentration was measured by dissolving the samples in $HClO_4$ followed by warming to 70 °C to release CO_2. Whole rock elemental composition was determined by inductively coupled plasma spectroscopy (ICP; Jarrel Ash Atom Corp Model 975) on samples crushed to < 100 µm, fluxed with $LiBO_2$, heated to 1050 °C, and dissolved in HNO_3.

McSwiggen and Associates—. Mineral modal abundances and mineral compositions for the three rock types were determined by x-ray analysis using a JEOL 8600 microprobe with an average accelerating voltage of 15 kV and average beam current of 20 nA. Microprobe analyses were calibrated using mineral standards. Mineral modal abundances were determined from at least 100 spot analyses on thin sections.

Midland Research—. Preliminary mineral identification and mineral modal abundances were conducted using X-ray diffraction (XRD; Philips Electronic Instruments Inc.) in conjunction with chemical analyses. The carbonate minerals present were identified by XRD, and checked by scanning electron microscopy (SEM; Amray model 1200B) and energy dispersive spectroscopy (EDS; Noran Instruments model 2010). For some samples, standard transmitted light petrographic techniques (Zeiss petrographic microscope) were used to verify x-ray analysis determined mineralogy.

3.1.2 Aqueous Phase Composition

Leachate volume (by weight), pH, alkalinity (if pH > 6.3) or acidity, and specific conductance were measuring in the MN DNR Hibbing laboratory. An Orion SA 720 pH meter, with a Ross combination pH electrode (8165), was used for pH determinations. Alkalinity and acidity were analyzed using standard titration techniques (APHA, 1992). A Myron L conductivity meter was used to determine specific conductance. Samples taken for SO_4 and metals analyses were filtered through a 0.45-micron filter. Sulfate concentrations before week 16 were determined at the MN DNR Hibbing laboratory using an HF Scientific DRT-100 nephelometer for the barium sulfate turbidimetric method (APHA, 1992). Sulfate concentrations measured between weeks 16 and 32 were analyzed using ICP, at the Midland Research Center. Subsequently, SO_4 concentrations were determined at the Minnesota Department of Agriculture (MDA) in St. Paul, MN. Sulfate concentrations exceeding five mg/L were determined using a Technicon AA2 automated colorimeter. Lower concentrations were determined using a Dionex ion chromatograph and, after week 257, a Lachat QuickChem 8000. Metals samples were acidified with 0.2 mL of analytical grade nitric acid per 50 mL sample. Metals analyses performed before week 32 were conducted at the MN DNR Hibbing laboratory using a Perkin Elmer 603 atomic absorption spectrophotometer in flame mode. Subsequent analyses were conducted at MDA. The concentration of Ca, Mg, Na, and K were determined on a Varian 400 SpectrAA. Data were checked by examining concentration variation over time, relationships of concentrations with conductance, and charge balance. Aqueous phase compositional data are presented in Appendix 2.

3.2 Humidity Cell and Reactor Experimental Procedure

The <0.053, 0.053-0.149, and 0.149-0.5 mm particle size samples were placed in 'MN DNR reactors' (Lapakko, 1988; Fig. 3.1A) whereas the larger size samples were placed in humidity cells (Fig. 3.1B). Additional detail on the sample container apparatuses and methods can be found in Lapakko et al. (2004). For particle sizes finer than 0.5 mm, the sample mass was 75 g and the rinse volume was 200 mL. For the larger particle size samples, the sample mass was 1000 g and the rinse volume was 300 mL for the norite and 400 mL for the diatreme and mudstone. Due to a limited sample mass of diatreme, the 6.35-19 mm particle size sample was omitted, and only 500 g of the 2.0-6.35 mm size fraction was used in the experiment and was rinsed with 200 mL.

Two peripheral experiments were conducted to examine the effects of changing the ratio of rock mass to rinse water volume and increasing the degree of evaporation. For the alternate rock mass and rinse water volume periphery experiment a 225 g sample of the 0.149-0.5 mm particle size samples of each rock type was run in a humidity cell and rinsed with 200 mL of water. Standard (covered) and uncovered humidity cells and reactors were compared using the 6.35-19 mm particle size sample of the mudstone and the 0.053-0.149, 0.5-2.0, and 6.35-19 mm particle size samples of the norite. Sample mass, rinse volume, and water to rock ratios for each of the humidity cells and reactors are listed in Table 3.1.

To ensure oxidation products were removed prior to beginning the experiment the solids were rinsed four to seven times. This rinse water was analyzed for specific conductance to provide an indicator of the decreasing masses of reaction products removed from the solids. The cumulative volume and solute released from this rinsing procedure is included in Appendix 2 as week 0. After the initial rinse procedure

the reactors and humidity cells were rinsed weekly. The rinse procedure allowed ten minutes of contact time before the water was drained into a receiving flask. Between rinses the solids were stored in the reactors in a room in which temperature and humidity were controlled. Temperature ranged from 20.3 to 28.9 °C with a mean of 24.2 °C and a standard deviation of 1.4 °C. Relative humidity over the same period ranged from 42% to 75% with a mean of 58% and a standard deviation of 4%.

Between week 0 and 1 the reactors were left uncovered and weighed on a daily basis to determine the variation in water retained over time. Due to varying degrees of drying among the humidity cells and reactors, it was determined that the covers should be left on the reactors between rinses, except for the <0.053 mm particle size sample of the diatreme and the mudstone, which did not drain readily (see pg. 12 Lapakko et al., 2004). The water remaining on top of these solids was decanted by pipet from the reactor and added to the leachate before analysis. The percentage of the total volume decanted from the<0.053 mm diatreme and mudstone samples for the first 30 weeks was on average 62% and 39%, respectively. Based on the weekly mass measurements and the presence of moisture on the inside walls of the covered reactors, it was assumed that the relative humidity was near 100 percent.

Rinse water pH ranged from 4.9 to 7.7 with an average of 6.1 and standard deviation of 0.4. The specific conductivity of the rinse water ranged from 0.1 to 8 µS with an average value of 0.9 µS and standard deviation of 0.9. These pH and conductivity measurements are the result of the reverse osmosis purification system for experiment rinse water.

3.3 AP(S_T), NP(CO_2), and ENP(pH 6) Calculations

The acid generation potential (AP(S_T)) of each sample was determined using equation 3. The percent AP(S_T) depleted was calculated based on the difference between the whole rock sulfur content and cumulative mass of SO_4 released. Neutralization potential (NP(CO_2)) was determined using equation 4 which assumes all CO_2 is associated with Ca and Mg, which will overestimate NP(CO_2) if there is Fe and/or Mn bearing carbonates. The percent NP(CO_2) depleted was calculated based on the difference between the whole rock calcium and magnesium carbonate content (as g $CaCO_3 \cdot$(kg rock)$^{-1}$) and cumulative mass of Ca and Mg released. For the diatreme sample, the carbonate mineralogy associated with the initial investigation (bulk chemistry, SEM, and XRD) indicated siderite and calcite contents of 3.2 and 0.5 wt%, respectively. However, the microprobe analyses indicated siderite ($FeCO_3$), rhodochrosite ($MnCO_3$), and/or kutnahorite ((Mn, Ca) CO_3) with varying modal abundances. Four methods were used to determine the fraction of CO_2 that was associated with the Ca and Mg (Lapakko et al., 2004) which yielded an average value of 27%. The percent NP(CO_2) expended was then calculated based on the difference between whole rock CO_2 concentration and cumulative mass release of Ca and Mg.

$$AP(S_T)\left(g\ CaCO_3 \cdot kg_{rock}^{-1}\right) = wt\%\ S \times \frac{100.0869\ g\ CaCO_3}{32.065\ gS} \times \frac{10\frac{gS}{kg_{rock}}}{wt\%\ S}$$

$$= wt\%\ S \times 31.21 \qquad \text{(eq.3)}$$

$$NP(CO_2)\left(g\ CaCO_3 \cdot kg_{rock}^{-1}\right) = wt\%\ CO_2 \times \frac{100.0869\ g\ CaCO_3}{44.0095\ gCO_2} \times \frac{10\frac{gCO_2}{kg_{rock}}}{wt\%\ CO_2} =$$

$$= wt\%\ CO_2 \times 22.74 \qquad \text{(eq. 4)}$$

Empirical neutralization potentials (ENP(pH 6)) were calculated to determine the acid-neutralizing mineral dissolution prior to leachate pH decreasing below 6.0 and remaining in this range. The acid-neutralizing mineral dissolution was calculated as the sum of the cumulative Ca and Mg released

(expressed as g $CaCO_3 \cdot (kg\ rock)^{-1}$) prior to leachate pH decreasing below 6.0. The ratio of ENP(pH 6) to NP(CO_2) was used to calculate the fraction of NP(CO_2) corresponding to the amount of Ca and Mg carbonate dissolution required to maintain a pH $\geq$ 6.0. Calcium and Mg can also be released by dissolution of minerals other than carbonates, such as sulfates. For samples containing calcium or magnesium sulfates, especially those for which leachate pH exceeded 6 for only a few weeks, the ENP(pH 6) value may include a substantial fraction of Ca and Mg from sulfate mineral dissolution.

3.4 Data Interpolation

Generally, the reactors and humidity cells were rinsed every week and the leachate volume, pH and specific conductivity (SC) were measured. For weeks when leachate volume, pH, and SC were not determined values were linearly interpolated from the previous and subsequent measured values. Concentrations of Ca, Mg and SO_4 were measured less frequently than volume, pH and SC and thus required a higher percentage of interpolation throughout the dataset. Because of the infrequency of elemental concentration measurements, anomalous values can significantly affect mass calculations if the anomalies occur during the periods of highest release rates (generally the first two hundred weeks). To limit this effect, anomalous values were replaced using the same process as that used for weeks during which data were not collected.

The concentration of K, Na, Al, Fe and trace elements (e.g. Cu, Co, Ni) were measured the least frequent (see Appendix 2) such that linear interpolation would be subject to considerable error. Thus, cumulative mass releases for K, Na, Al, Fe and trace elements were not performed. Despite a significant number of weeks requiring interpolated values, measurement frequency was greatest early in the experiment when the various measurement values changed the fastest. Later in the experiment (after about week 335) sampling frequency was lower and solute concentrations were much more stable. Consequently, error introduced by extrapolation in the latter period of the experiment is relatively small.

4. RESULTS

Comprehensive compositional and mineralogical analyses were performed on each of the rock types and in some instances individual particle size samples. The mineral modal abundances of the rocks are summarized in Table 4.1 and the compositions of each rock type and particle size sample are summarized in Table 4.2.

4.1 Mineralogy and Petrology

4.1.1 Norite

The norite sample is from the Mesaba Cu-Ni prospect hosted within the Partridge River Intrusion of the Duluth Complex, northeastern Minnesota. The primary minerals are plagioclase, olivine, hypersthene, biotite, cordierite, augite, ilmenite and sulfides. The sulfide minerals include pyrrhotite, chalcopyrite, and cubanite. The sulfide minerals commonly occur interstitial to the coarser grained silicate minerals. Less frequently the sulfides occur as inclusions in the silicate minerals (Figs. 4.1A to C). Alkali feldspar and calcite were also identified in the norite and may represent post crystallization alteration. Only two calcite grains were observed during microprobe analysis and their diameters were about 30 and 50 μm. Assuming the 6.35-19 mm size sample is representative of the bulk rock composition and all solid-phase CO_2 (Table 4.3) is present as calcite, the bulk calcite content could range from <0.02 to 0.05 wt% based on these limited measurements.

4.1.2 Diatreme

The diatreme primarily consists of fine to medium grain quartz and K-feldspar, with minor muscovite, carbonate, and pyrite. Chemical analyses indicate the diatreme contains anomalously elevated concentrations of Au, Ag, Pb and Zn, indicating a weakly mineralized origin. The carbonate minerals included Mn-rich siderite ($Fe_{1.5}$ $Mn_{0.23}$ $Ca_{0.14}$ $Mg_{0.12}$ $(CO_3)_2$), rhodochrosite ($Mn_{0.96}$ $Fe_{0.77}$ $Mg_{0.15}$ $Ca_{0.14}$ $(CO_3)_2$), and ferroan kutnahorite ($Mn_{0.89}$ $Ca_{0.51}$ $Fe_{0.42}$ $Mg_{0.18}$ $(CO_3)_2$). Petrographic analysis indicated medium to fine grained sulfide minerals occurred as both disseminated grains and in veinlets (Fig. 4.2). Subsequent microprobe analysis confirmed the presence of disseminated sulfide and carbonate minerals occurring as both coarse and fine grains (Figs. 4.2A to C). Positively identified sulfide minerals include pyrite and galena. Sphalerite was inferred to be present based on high Zn solid phase and leachate concentrations.

4.1.3 Mudstone

The mudstone primarily consisted of fine-grained quartz, K-feldspar, undifferentiated mica, carbonates, and pyrite (Figs. 4.3A to I). Chemical analyses indicate the mudstone contains anomalously elevated concentrations of As, Au, Sb, and Hg, indicating a weak epithermal mineralization style. The carbonates included dolomite ($Ca_{1.06}$ $Mg_{0.83}$ $Fe_{0.06}$ $Mn_{0.05}$ $(CO_3)_2$) and siderite ($Fe_{1.80}$ $Mg_{0.18}$ $Mn_{0.02}$ $(CO_3)_2$). Petrographic and microprobe image analysis indicated that pyrite occurred in four different textural settings. These textures, in order of decreasing abundance, include: (1) 0.5 to 1's mm size agglomerates of anhedral and subhedral pyrite grains on the order of 0.04 mm in diameter, intergrown with silicate minerals; (2) euhedral grains roughly 0.05 to 0.45 mm in diameter; (3) in 0.02 to 0.2 mm wide veins, variably intergrown with other minerals; and (4) as framboids 0.005 to 0.095 mm in diameter (see Fig. 4.3A, and Figs. 4.3D-H). Carbonates occurred as disseminated masses and veins with quartz (Figs. 4.3B, C, G and I). The carbonate veins did not contain cavities. Microprobe examination revealed dolomite masses (diameter ~ 0.2 mm) inter-grown with quartz, feldspar, and muscovite and dolomite inter-grown with potassium feldspar in a vein about 0.2 by 0.8 mm.

4.2 Particle Size Fractions Sulfur Content and Sulfide Grain Size Distribution

Total sulfur (S_T) content determined by Acme and Midland Research are in general agreement for most particle size fractions for each rock type except for the 0.053-0.149 mm norite and 2-6.35 and 6.35-19 mm norite and mudstone samples (Table 4.3). The lower Midland Research S_T wt% value for the norite 0.053-0.149 mm particle size sample is proved erroneous with respect to the total sulfur released from the sample in the laboratory experiment (see section 4.5.1). For the remaining discrepancies, it is not clear which value is correct because either the experiments were discontinued early or the release rate is sufficiently slow that the cumulative release is a small fraction of the total sulfur content precluding comparison. Sample heterogeneity may have also been a factor in creating the sulfur concentration discrepancies, that is, compositional differences between samples submitted for analysis and samples used in the experiment.

In general, the total sulfur content of the norite samples increased with decreasing particle size. This sulfide enrichment in fines is similar to that found for larger volumes of Duluth Complex rock excavated from an exploration shaft (Lapakko et al., 2004 and Lapakko, 1994). In contrast, the total sulfur content of the mudstone samples was greatest in the two largest particle size fractions. The combination of these two apparent trends suggests that the rock type and relative hardness of minerals in a rock may contribute to which minerals will become enriched or depleted in different particle size fractions during crushing. In the case of the norite, pyrrhotite is much softer and has lower tenacity than the plagioclase and olivine comprising the majority of the rock (Table 4.4). Thus, during crushing pyrrhotite is more susceptible to breaking down into smaller particles than the other minerals. In the case of the mudstone, pyrite is much

harder than the mica and carbonate minerals, which may result in enrichment of pyrite in the coarser particle fractions.

In addition to hardness, the relative mineral size distributions are also a likely cause for enrichment of certain minerals in different particle size fractions due to the tendency of rock to break along mineral grain boundaries. For example, if a rock with an average mineral groundmass grain size of 1 mm and average sulfide grain size of 0.5 mm were crushed, the < 1 mm sized sulfides would become concentrated in fractions < 1 mm. For the norite, the sulfide grain size measurements exhibit an exponential distribution (Fig. 4.4). Of seven cross section sulfide grain measurements five had diameters less than 0.5 mm, suggesting sulfide mineral diameters were generally smaller than 0.5 mm. Thus, not until the average particle size is 0.5 mm in diameter would significant sulfide enrichment in the finer fractions occur, which is supported by the compositional data showing sulfide enrichment for particle sizes less than 0.5 mm (Table 4.3). In addition, complete surface exposure of the majority of sulfides would only occur for the fractions <0.5 mm. The measured mudstone sulfide minerals similarly exhibit an exponential distribution (Fig. 4.5) though there are a greater amount of larger sulfides. Because some of the sulfide minerals are harder and/or coarser grained than the other mineral phases, sulfides were likely preferentially retained in the larger particle size fraction during crushing. The diatreme sample exhibits a uniform sulfide size distribution (Fig. 4.6), which is consistent with the similar total sulfur contents for each particle size (except for the smallest particle size sample). The uniform distribution of sulfides and silicates likely contributed to the similar sulfur contents among all but one of the diatreme size fractions.

4.3 AP(S_T), NP(CO_2), and ENP(pH 6)

Different particle sizes from the same rock are variably affected by the relative exposure of acid-producing and acid-neutralizing mineral surface areas and, consequently, the relative rates of acid production and neutralization. This variability can be explained by three consequences of particle size reduction. First, particle size reduction can preferentially concentrates softer minerals in finer size fractions (Table 4.2; Lapakko, 1994; Lapakko et al., 2006). Second, as particle size decreases the specific surface area (surface area per unit mass) of particles increases (see Table 2.1). Third, as particle size decreases towards the average mineral grain size of the rock more particles are composed of a single mineral increasing the surface area for reaction. For example, if the average sulfide diameter of a rock is 1 mm, crushed fractions ≤ 1 mm will have complete exposure of the sulfide mineral surface. In contrast, larger particle sizes can contain multiple minerals such that the individual mineral surface area is not entirely exposed reducing exposure to oxygen and water. For example, the surface area of a one cubic millimeter mineral would be 100% exposed for a sample with a particle size less than one millimeter and a decreasing percent surface area exposure for increasingly larger particle size samples. These morphologic changes introduced as a result of particle size reduction are apparent from the AP(S_T), NP(CO_2) and ENP(pH 6) values for all samples of the particle size experiment (Tables 4.5 and 4.6). Changes to AP(S_T) and NP(CO_2) are the result of consequence one whereas ENP(pH 6) is influenced by all three.

4.3.1 Norite AP(S_T), NP(CO_2), and ENP(pH6)

The AP(S_T) of the six particle size samples ranged from 13 to 47 g $CaCO_3$·(kg rock)$^{-1}$ and generally increased with decreasing particle size (Table 4.5). NP(CO_2) ranged from <0.11 to 7.0 g $CaCO_3$·(kg rock)$^{-1}$ and tended to increase as particle size decreased (Table 4.5). The ENP(pH 6) values ranged from 0.1 to 4.8 g $CaCO_3$·(kg rock)$^{-1}$ and increased with decreasing particle size (Table 4.6). Magnesium release contributed about 50% of the ENP(pH 6) for all samples. The magnesium contribution to the ENP(pH 6) indicates that either some Mg carbonate mineral is present (and was not detected) and/or

dissolution of Mg silicate minerals contributed to acid neutralization while pH remained above 6. Similarly, it is also likely that Ca silicate mineral dissolution contributed to the ENP(pH 6).

The AP(S_T) depleted ranged from 4% to 133% and generally increased with decreasing particle size. The greater than 100% AP(S_T) expended indicates the measured rock sulfur concentrations were lower than the samples used in the experiment. The NP(CO_2) depleted, based on cumulative release of Ca and Mg, ranged from 147% to 7832% (Table 4.5). The greater than 100% depletion indicates Ca and Mg release was from both carbonate and silicate minerals.

4.3.2 Diatreme AP(S_T), NP(CO_2), and ENP(pH6)

The AP(S_T) values of the five size fractions ranged from 28 to 73 g $CaCO_3$•(kg rock)$^{-1}$ and NP(CO_2) from 4.5 to 10 g $CaCO_3$•(kg rock)$^{-1}$ (Table 4.5). The <0.053 and 2.0-6.35 mm particle size samples had the two lowest AP(S_T) and NP(CO_2) values on average 46% and 77% less than the other samples, respectively. Thus, unlike the norite, there was no consistent relationship between particle size and AP(S_T) or NP(CO_2) values.

The 0.053-0.149, 0.5-2.0, and 2.0-6.35 mm fractions were the only size fractions tested for 943 weeks. The percent AP(S_T) depletion from the finest fraction was roughly 70%, and corresponding depletions for the two larger fractions ranged from roughly 10% to 20% (Table 4.5). The percent NP(CO_2) depletion for the 943 week samples ranged from about 70% to 120%. The greater than 100% NP(CO_2) depletion indicates that the silicate mineralogy may have contributed to acid neutralization for the <0.053 and 0.053-0.149 mm samples (Table 4.5).

The ENP(pH 6) for the <0.053 mm particle size sample was reported as greater than 6.2 because leachate pH did not decrease below 6. The respective ENP(pH 6) values for the 0.053-0.149, 0.149-0.5, 0.5-2.0, and 2.0-6.35 mm particle size samples were 7.5, 8.0, 8.1, and 4.8 g $CaCO_3$·(kg rock)$^{-1}$. These ENP(pH 6) values represent 88-97%, 85-91%, 80-81%, and 55-59% of the respective particle size sample NP(CO_2) (Table 4.6). Thus, the fraction of NP(CO_2) that reacted to neutralize acid and maintain leachate pH ≥ 6.0 generally decreased as particle size increased. The Ca and Mg carbonate minerals present in the finer fractions were apparently more readily available for reaction than those in the larger particles. For these four samples, Mg release contributed about 60% to 70% of the ENP(pH 6) suggesting that the overall carbonate mineral assemblage was on average Mg-rich.

4.3.3 Mudstone AP(S_T), NP(CO_2), and ENP(pH 6)

The AP(S_T) for the six particle size fractions ranged from 80 to 110 g $CaCO_3$•(kg rock)$^{-1}$. NP(CO_2) ranged from 18 to 45 g $CaCO_3$•(kg rock)$^{-1}$. Neither the AP(S_T) nor NP(CO_2) showed any systematic variation with particle size (Table 4.5).

The leachate pH of the two largest particle size samples of mudstone were continuously below 4.5, despite having NP(CO_2) values from 21-45 g $CaCO_3$•(kg rock)$^{-1}$. The average leachate Ca/Mg ratio of these two samples was 1.11. This ratio is within the range of the dolomite Ca/Mg ratio (1.02-1.46) indicating Ca and Mg release was predominately from dissolution of dolomite. These two samples had NP(CO_2) depletions ranging between 27 and 92% for the 134 week period of record (Table 4.5). However, the rate of NP(CO_2) dissolution was too slow to maintain leachate pH of at least 6.

The 0.053-0.149, 0.149-0.5, and 0.5-2.0 mm samples did produce leachate pH below 6 resulting in ENP(pH 6) values ranging from 19 to 37 g $CaCO_3$·(kg rock)$^{-1}$. The fractions of NP(CO_2) available for maintaining leachate pH ≥ 6.0 was between 97 to 117% for these particle size samples (Table 4.5). While

leachate pH was above 6, the average Ca/Mg ratio was 1.3, which is in excellent agreement with the average Ca/Mg molar ratio of the dolomite (1.06/0.83 = 1.28). The quantitative agreement between the observed neutralization and the NP present as dolomite and similar Ca/Mg molar ratios between dolomite and leachate indicate dolomite was largely responsible for acid neutralization above a pH of 6.

The limited capacity of some carbonates to neutralize acid has been previously observed for Fe- and Mg-bearing carbonates (Lapakko, 1993) and as a result of low specific surface area (Lapakko, 1998 and Lapakko et al., 2002). For these mudstone samples, the dolomite surface exposure in the smaller particle sizes was apparently greater than that of the larger particle sizes allowing more dolomite dissolution and associated acid neutralization. The smaller particle sizes would also tend to retain more water, facilitating increased transport of acidic reaction products from sulfide mineral surfaces to dolomite surfaces between sample rinses. In contrast, the large particle size samples drained more freely, due to larger pore spaces, thus limiting interaction between mineral surfaces during the weekly rinse cycle. The rates of Ca release from the larger samples typically ranged from 0.9 to 1.2 times those of magnesium (Table 4.7). This is less than the average Ca/Mg ratio reported for dolomite indicating that magnesium may have been contributed by a phase other than dolomite, for example siderite or mica.

4.4 Leachate Composition and Release Rate Time Series Trends

Compositional and solute release rate trends over the experiment timespan provide useful information about chemical reactions occurring and the rate of these processes. Of particular importance are the 1) leachate pH, reflecting the balance of acid producing and acid neutralizing reactions; 2) SO_4 release rate, reflecting the rate of sulfide mineral oxidation and the associated acid production; and 3) calcium and magnesium release rates, reflecting the dissolution of calcium and magnesium carbonates and silicate minerals and the associated acid neutralization. Also of importance is the release of trace elements, due to their potential toxicity.

4.4.1 Norite Time Series Trends

pH.— Leachate pH for the norite samples varied over time and can be grouped into three time series trends (Fig. 4.7). Trend one includes the three smallest particle size samples and is characterized by a sharply decreasing pH to a value of about 5 by week 100, reaching minimum pH values between 4 and 4.2 near week 200, and steadily increasing after week 400 to values above 5 by week 600. Trend two includes the 0.5-2.0 and 2.0-6.35 mm samples and is characterized by pH slowly decreasing below 5 by about week 400 and generally remaining below 5 to week 94 (end of record). Trend three is represented by the largest particle size sample from which pH decreased and plateaued. Values decreased from an initial value of about 6.5 to consistently below 6 after week 400 and subsequently fluctuated between 5.5 and 6.

These three trends can be explained by the physical and chemical properties of the different particle size fractions. For trend 1 the initial drop in pH is the result of relatively rapid acid generation from oxidation of large sulfide surface area afforded by the fine-grained sulfides in the three smallest particle size samples. Silicate mineral surface areas were also relatively large in the fine-grained fraction. However, the dissolution rates of these minerals, and the attendant acid neutralization, were inadequate to maintain pH at the higher levels observed for the large particle size fractions (Fig. 4.7). This suggests that size reduction preferentially enhanced sulfide mineral surface area relative to silicate mineral surface area (see also Lapakko et al., 2006).

The later increase in pH after a minimum value had been reached likely represents substantial depletion of reactive sulfide minerals available for oxidation. For the two smallest particle size samples a stabilized pH of 6.5 was maintained for over 200 weeks and suggests an apparent steady state has been reached. For the

two finest samples this apparent steady state is likely the result of near complete sulfide mineral oxidation, as indicated by high cumulative mass depletion of sulfur near the same time interval (see Fig. 4.28). For the 0.149-0.5 mm fraction the degree of sulfide mineral depletion was lower. Additional factors affecting the increase in pH (and decrease in SO_4 release rates) for this sample (and larger size fractions) include partial sulfide mineral oxidation with remnant sulfides being protected within the rock matrix and oxidation inhibition due to surface coatings on the remaining sulfide minerals. Consequently sulfide mineral oxidation declined substantially after week 600 (Fig. 4.8), and the silicate minerals present neutralized the small amounts of acidity from the rinse water and that generated from the remaining reactive sulfide.

For trend 2, the larger size samples have an overall smaller surface area and mass of sulfide that resulted in a slower pH decrease and greater minimum leachate pH, as that of trend 1. The stabilization of trend 2 at a pH of about 5 after week 500 may represent a similar scenario to pH stabilization of trend 1. Conceivably a quasi-steady state was reached, likely the result of diffusion-limited sulfide oxidation and neutralizing silicate mineral dissolution reactions. For trend 3, the relatively stable pH trend for the entirety of the experiment indicates the natural acidity of the rinse water and slow acid generation by sulfide oxidation (Fig. 4.8) were neutralized by reaction with silicate minerals.

Sulfate.— Leachate from all samples exhibited an overall decrease in SO_4 release rate through about week 700 after which SO_4 release appeared to stabilize (Fig. 4.8). For the two smallest particle size samples there were SO_4 release rate peaks centered near weeks 100, 200, 300 and 400. The 0.149-0.5 mm size sample exhibited small SO_4 release rate peaks near weeks 100 and 200 and the 0.5-2.0 mm size sample showed a small SO_4 release rate peak at week 300. The SO_4 release rate peaks at 200 and 400 weeks coincided with periods of lowest pH for the three smallest particle size samples. The SO_4 release rate peaks at week 100 had no clear association with pH minima but this SO_4 peak did coincide with the initial leachate pH decrease. The correlation of low pH and elevated SO_4 release for these three size fractions is consistent with biological mediation of the sulfide mineral oxidation reaction. However, the ratio of the minimum to maximum SO_4 release rates from year 2 to the year of minimum pH was typically within a factor of two, indicating that any influence of biological mediation was fairly small. For the <0.053 and 0.053-0.149 mm samples SO_4 concentrations were at or below detection limit (0.5 mg/L) by week 928 and 781 (except for one detection at week 860 of 0.83 mg/L for the 0.053-0.149 mm particle size sample). The 2.0-6.35 and 6.35-19 mm samples showed an apparent SO_4 release rate increase from about week 900 to 943.

Major Cations.— Similar to the SO_4 release rate trend, the Ca release rate was initially high and gradually declined through about week 700 after which the Ca release rate was more stable (Fig. 4.9). The two smallest particle size samples had Ca release rate peaks centered at weeks 200 and 400, coincident to two of the SO_4 release rate peaks but less pronounced. The correlation in release rate trends between SO_4 and Ca indicates dissolution of calcium bearing mineral(s) to neutralize acid generated by sulfide oxidation. Magnesium release rates for the 0.053-0.149 and 0.149-0.5 mm samples are on average greater than the Ca release rate through about week 200 (Fig. 4.10). After week 200 the Mg release rate for the three smallest size samples rapidly declined to values below the Ca release rates. The 0.5-2.0 mm particle size sample exhibits about a factor of two greater Mg release rate over Ca release rate. The two largest particle size samples have roughly equivalent Ca and Mg release rate values and trends.

Trace Elements.— In general release rates for trace elements, which occur as major components in sulfide minerals, namely Cu, Ni and Co, sharply decreased over time for all particle size samples after a minimum pH has been reached (Figs. 4.11, 4.12, and 4.13). The three smallest particle size samples exhibited a rapid increase in Cu release rates to about week 100, which was the period pH decreased rapidly. After week 100, Cu release rates were relatively stable through week 500 after which the Cu release rate decreased rapidly, similar to the change in SO_4 release rate. The Cu release rate trend is

roughly the inverse of that for pH suggesting a strong pH control for Cu release. In contrast, the Co and Ni release rates monotonically decreased over time similar to the Ca and Mg release rate trends. The Cu releases rates for the three largest particle size samples increased until about week 450 after which the rates gradually declined.

4.4.2 Diatreme Time Series Trends

pH.— Leachate pH for all the diatreme particle size samples exhibits a generally decreasing pH trend through week 400 (Fig. 4.14). At week 400 leachate from all particle size samples had a pH of about 6 ± 0.5. After week 400 leachate pH from each of the samples exhibited different pH trends that differ from relationships between pH and particle size observed for the norite samples. The <0.053 mm particle size sample did not exhibit any significant pH change through week 466 when the experiment was discontinued. In contrast, leachate pH for the 0.053-0.149 mm particle size sample dropped sharply below about 4 by week 500 and gradually decreased to a pH of 3.4 through week 943. The 0.149-0.5 mm particle size sample leachate pH sharply dropped from 5.8 at about week 500 to 4.4 by week 531 when the experiment was discontinued. The leachate pH trend for the 0.149-0.5 mm particle size sample is similar to that for the 0.053-0.149 particle size sample except that the rapid pH decline was about 100 weeks later. The leachate pH trend of the 0.5-2 mm particle size sample exhibited no sharp decline in pH. Instead, pH gradually decreased from 6.3 to 5.6 between weeks 400 and 800 after which the pH appeared to stabilize at about 5.5. The leachate pH trend for the largest particle size fraction (2-6.35 mm) declined steadily after about week 200 from 7.5 to 4.1 through week 943.

For the 0.053-0.149 and 0.149-0.5 mm particle size groups the acid neutralization potential of the samples was eventually exceeded by the acid production of the sulfides. The leachate pH trend for the 0.5-2 mm sample appears to be stabilizing at a value of about 5.5. The steady decline in leachate pH for the largest particle size sample and lower pH in comparison to the 0.5-2.0 mm particle size sample suggests the carbonate mineral exposure may be limited by particle size. This limitation could be due to inclusion of carbonate grains within the larger rock particles meaning the carbonate grains are on average < 2 mm in diameter for this particle size sample. The NP:AP ratio for the two largest particle sizes are between 0.16 and 0.18 indicating that at some point the leachate should become acidic. However, the leachate pH time series for these samples show a gradual decline in pH instead of a rapid decrease in pH exhibited by the 0.053-0.149 and 0.149-0.5 mm size samples. It is not clear why leachate pH for the largest diatreme sample has exhibited a gradual pH trend unlike all the other rock types and particle sizes.

Sulfate.— The <0.053 particle size sample SO_4 release rate is generally stable from about week 50 to 400 when the rate approximately doubles thru week 465 (Fig 4.15). The 0.053-0.149 mm particle size leachate exhibited an increasing SO_4 release rate trend of about a factor of three from about week 200 to 450, after which the SO_4 release rate gradually increased thru week 943. The 0.149-0.5 mm particle size sample shows a gradually increasing SO_4 release rate from week 100 to week 500 after which the rate rapidly increased by over a factor of three. The 0.5-2 mm particle size sample exhibits a gradual SO_4 release rate increase from about week 100 through week 943. Leachate from the 2-6.35 mm particle size sample has remained relatively constant from about week 150 to week 875 after which the rate increased by about a factor of 2.

Major Cations.— The diatreme sample has relatively low Ca and Mg concentrations and elevated K concentrations (Table 4.2). The low Ca and Mg rock contents are evident in the solute release rate plots. For instance, the <0.053 and 0.053-0.149 mm particle size sample leachate concentration for Mg were at or below detection (0.1 mg/L) by weeks 376 and 621. In addition, neither the Ca nor Mg release rate time series plots exhibit similar trends to the SO_4 release trend as was the case with the norite samples (Figs. 4.16 and 4.17). Lack of correlation between SO_4 and Ca and/or Mg release rates suggests that some other cation is balancing the negative charge produced from the SO_4. It is possible K and Na are significant

contributors to the overall charge balance, but because Na and K were not regularly measured, especially later in the experiment (Appendix 2), it is not possible to determine if there release rates increased while SO_4 release increased for the 0.053-0.149 and 0.149-0.5 mm samples.

Trace Elements.— Lead and Zn release rates follow a trend similar to SO_4 release rates for the respective particle size sample (Fig 4.18 and 4.19). The increase in Pb and Zn release rate coincides with decreasing pH suggesting solubility driven control, presumably from dissolution of galena and sphalerite. No other trace elements were detected at a high enough concentration and/or frequency to identify trends.

4.4.3 Mudstone Time Series Trends

pH.— The abundance of fine clay and mica minerals slowed rinse water from draining through the <0.053 mm sample. This led to discontinuing this sample after week 134. Over this period of record, leachate pH remained near neutral. For the remaining five samples two basic pH trends were observed (Fig. 4.20). Trend one is characterized by an extended period of pH fluctuating between 7 and 8 followed by a rapid decline to a pH less than 3. The change to acidic leachate occurred at weeks 360, 440, and 230 for the 0.053-0.149, 0.149-0.5, and 0.5-2.0 mm samples. Trend two is characterized by an initial acidic leachate pH of about 4 that decreases to about 3 by week 15 and remains at a pH of 3 ± 0.5 through week 167. The lower pH and decreased time to acidity for the larger particle size samples is the opposite trend observed for the norite. The faster onset to acidic leachate for the larger particle size samples is likely due to the higher total sulfur content (Table 4.3).

Sulfate.— Leachate from the mudstone samples had on average the highest release rates for circumneutral pH, as expected given the greater sulfide content of the rock (Fig. 4.21). In general, the SO_4 release rates are inversely related to pH. Sulfate release rate trends for the 0.053-0.149 and 0.149-0.5 mm samples are similar and show an early elevated release rate followed by an extended period of stable release and then up to about a factor of 40 increase when leachate pH rapidly turned acidic. The 0.5-2 mm particle size sample initially has a relatively high release rate to week 50 after which the release rate lowers quickly and is maintained at a lower rate until about week 230 when the rate increases again, upon leachate becoming acidic, through week 283. After week 283 the SO_4 release rate decreases as pH slightly increases. The two largest size fractions show generally decreasing SO_4 release rates over the 167 weeks of data collection.

Major Cations.— Mudstone leachate release rates for Ca and Mg generally exhibit trends similar to those of SO_4 (Figs. 4.22 and 4.23).

Trace Elements.— The concentration of Sb was greatest for leachate pH greater than 7 and decreased by over a factor of 10 upon rapid acidification of sample leachate (Fig 4.24). Leachate concentrations of Cr and Zn showed the opposite behavior, that is, concentration increased with decreasing pH (Figs 4.25 and 4.26). Leachate concentrations of As exhibited both behaviors with As concentration increasing above a pH of about 7, generally below detection (2 μg/L) between about pH 3 and 7, and again increasing below a pH of 3 (Fig 4.27). Collectively, the observed trace element pH relationships are consistent with $Fe(OH)_3$ sorption theory described by Dzomback and Morel (1990).

4.5 Cumulative Mass Release and Average Release Rates

The cumulative mass of sulfur released in conjunction with the initial sulfur content was used to determine the amount of sulfur remaining. The mass of remaining sulfur in the experiment samples along with the SO_4 release rate provides insight into the variables controlling leachate pH over different time intervals. Cumulative mass release plots can also be used to evaluate the change in SO_4 release rate over time. A greater than 100% mass released indicates that the rock material analyzed for bulk chemical

composition was not representative of the sample used in the humidity cell experiment. Alternatively, if the rock sample analyzed for chemical composition had higher sulfur content than the dissolution experiment sample then the calculated percent sulfur lost would be erroneously low. Table 4.7 lists calculated average release rates by year for each rock type and particle size sample.

4.5.1 Norite Cumulative Mass Release and Average Release Rates

Cumulative percent sulfur released for the smallest to largest particle size samples through 943 weeks are 98, 134, 69, 40, 14, and 4 based on the Midland Research S_T concentrations and 104, 104, 71, 40, 18, and 8 based on the ACME analytical laboratory S_T concentrations (Fig. 4.28). The two smallest particle size samples appear to have exhausted all sulfide minerals initially present whereas the 0.149-0.5 mm size sample appears to have reached a point of stabilized low SO_4 release. It is conceivable the larger particles within the 0.149-0.5 mm sample may be exhibiting oxygen diffusion decreased rates, that is, the smaller sulfide particle surfaces have been completely oxidized whereas the larger exposed sulfide particles have developed an oxide coating that is limiting SO_4 release due to an oxygen limited diffusion rate. The three largest particle size samples have more consistent total sulfur concentrations and all exhibit a stable slow sulfur depletion trend.

The SO_4 release rates from the two smallest particle size samples decreased by about a factor of 100, whereas the 0.149-0.5 mm particle size decreased by a factor of about 50 (Fig. 4.8). Although these samples exhibited changing SO_4 release rate trends, on a log scale a relatively stable long term release rate is distinguishable from about week 10 to 300. After about week 300, decreased sulfide content and possibly development of oxyhydroxide coatings resulted in rapidly decreasing SO_4 release rates. Therefore, to calculate average SO_4 release rates for these samples only the values between weeks 10 and 300 were used. This 290 week period, represent the average release rates prior to sulfur depletion limiting the release rate. Although the three largest sized samples do not exhibit significant changes in SO_4 release rate over time, for consistency, the same time interval was selected for calculating long term release rates. The long term SO_4 release rates for the norite samples in increasing size order are 9.53×10^{-1}, 7.29×10^{-1}, and 6.06×10^{-1}, 1.31×10^{-2}, 4.81×10^{-2}, and 1.46×10^{-2} mmol·kg^{-1}·wk^{-1}, respectively.

Ca and Mg release rates exhibit a more gradual decrease than SO_4, likely due to the much greater concentration of these elements in the norite (Figs. 4.9 and 4.10). Annual release rates for Ca and Mg are listed in Table 4.7.

4.5.2 Diatreme Cumulative Mass Release and Average Release Rates

Cumulative percent sulfur released, calculated from the Midland Research sulfur data, for the 0.053-0.149, 0.5-2.0, and 2.0-6.35 mm samples through 943 weeks are 70, 11, and 20, respectively (Fig 4.29). These values are very similar to the cumulative release based on the ACME S_T values (Table 4.5). The three smallest diatreme particle size samples exhibit relatively constant SO_4 release after an initial high rate and prior to pH dropping below 6. This period encompasses weeks 50 to 300 and average SO_4 release rates for the <0.053, 0.053-0.149, and 0.149-0.5 mm samples over this range are 3.34×10^{-2}, 1.41×10^{-1}, and 8.31×10^{-2} mmol·kg^{-1}·wk^{-1}, respectively. The 0.053-0.149 particle size sample showed an additional relatively constant SO_4 release rate after pH dropped below about 3.5 (about weeks 550 to 943). The average SO_4 release over this period is 7.64×10^{-1} mmol·kg^{-1}·wk^{-1}, roughly an order of magnitude greater than the release rate for pH > 6. The 0.5-2.0 and 2.0-6.35 mm samples maintained relatively constant SO_4 release rates despite pH decreasing by 2 to 3 units over the duration of the experiment. The SO_4 release rates for these two larger sized samples over weeks 100-943 are 6.84×10^{-2} and 9.00×10^{-2} for the 0.5-2.0 and 2.0-6.35 mm size samples.

Unlike the norite, Ca and Mg release rates were more variable than the SO_4 release rate. Because of this variation no large scale average release rates were calculated. Annual release rates for Ca and Mg from the diatreme are listed in Table 4.7.

4.5.3 Mudstone Cumulative Mass Release and Average Release Rates

The mudstone <0.053, 2.0-6.35, and 6.35-19 mm samples were discontinued week 134 and had cumulative percent sulfur depletion, calculated from the Midland Research sulfur data, of 13%, 34%, and 15% (Fig. 4.30). The 0.053-0.149, 0.149-0.5, and 0.5-2.0 mm samples were discontinued on weeks 385, 483, and 335, respectively and had respective cumulative sulfur releases of 35%, 44%, and 53% (Fig. 4.30). The short 134 week collection period for the <0.053, 2.0-6.35, and 6.35-19 mm samples limits the potential range for identifying large scale release rates. However, SO_4 release rates from week 57 to 134 are relatively stable for these particle size samples and can be used to calculate average SO_4 release rates, in increasing particle size, of 1.35×10^{-1}, 1.91×10^{0}, and 6.10×10^{-1} $mmol\cdot kg^{-1}\cdot wk^{-1}$. For the remaining samples SO_4 release was relatively stable from week 57 to before pH dropped below about 6.5. This period is different for the 0.053-0.149, 0.149-0.5, and 0.5-2.0 mm samples and can be represented by the following week intervals of 57-300, 57-400 and 57-200, respectively. The average SO_4 release rates for the 0.053-0.149, 0.149-0.5, and 0.5-2.0 mm samples from the above mentioned time intervals are 4.13×10^{-1}, 3.08×10^{-1}, and 7.56×10^{-1} $mmol\cdot kg^{-1}\cdot wk^{-1}$, respectively.

Ca and Mg release rates were more variable than SO_4 precluding deriving long term average release rates. Annual release rates for Ca and Mg from the mudstone are listed in Table 4.7.

4.6 Standard (Covered) and Uncovered Samples

Leachate from uncovered duplicate samples was measured to determine if water retention in the cells affected leachate pH and solute release rates for equivalent particle sizes. This experiment included the norite 0.053-0.149, 0.5-2.0, and 6.35-19 mm size samples and the mudstone 6.35-19 mm size sample. Leachate from the largest uncovered norite particle size humidity cell did not show significantly different pH values or SO_4 release rates over a 128 week period in comparison to the equivalent particle size standard humidity cell (Fig. 4.31 and 4.32). The norite 0.5-2.0 mm standard and uncovered samples exhibited similar pH trends through week 111 after which the uncovered reactor leachate pH dropped to an average value of 5.2 whereas the standard reactor maintained an average pH of 5.7 from weeks 28 to 134 (Fig. 4.33). The norite 0.5-2.0 mm samples also exhibited similar SO_4 release trends for about 50 weeks, after which the uncovered sample leachate increased in SO_4 release rate by an average factor of 1.3 (Fig 4.34). Leachate pH for the norite 0.053-0.149 mm uncovered sample remained near a pH of about 5.4 from week 15 to 132 whereas the leachate pH for the standard sample dropped below 5 at week 80, to 4.4 by week 107, and then slowly declined to 4.3 at week 134 (Fig. 4.35). Leachate from the standard and uncovered 0.053-0.149 mm samples showed similar SO_4 release rates through about week 44, after which SO_4 release rates from the standard sample were up to three times those of the uncovered sample (Fig. 4.36).

Leachate pH from the standard and uncovered mudstone samples (6.35-19 mm) exhibited a different trend behavior. The pH of leachate from the standard sample decreased from about 4 to 3 from week one to 11 and then stabilized at about 3.2 (Fig. 4.37). Leachate pH from the uncovered sample decreased more gradually from a value of about 3.7 to 2.7 from week one to 79 after which pH stabilized near 2.7. Sulfate release from the standard and uncovered mudstone samples were similar up to week 41, after which SO_4 release from the uncovered sample was up to 4.5 greater than that of the standard sample (Fig. 4.38).

4.7 Different Sample Masses

The 0.149-0.5 mm samples for each rock type were placed into both reactors (75 g samples) and humidity cells (225 g samples) to assess the effect of different water:rock ratios on leachate composition. The 225 g sample humidity cells ran for 134 weeks. Both sample masses received the same rinse volume (200 mL) resulting in a factor of three lower water:rock ratio for the 225 gram samples (Table 3.1). Leachate pH for the norite humidity cell and reactor were similar until about week 72 when pH began to drop faster for the reactor resulting in a pH difference of about a 0.5 pH unit by week 134 (Fig. 4.39). Sulfate release rate increased by up to a factor of two after week 74 for the reactor (Fig 4.40). Leachate pH for the diatreme and mudstone samples was on average slightly lower for the reactors (Figs. 4.41 and 4.43). Diatreme SO_4 release rates between the humidity cell and reactor exhibited no consistent differences (Fig 4.42). Mudstone SO_4 release rate for both humidity cell and reactor were similar up to week 56 after which the reactor rates increased by up to a factor of 2 (Fig. 4.44). For all rock types, the lower fluid pH and greater SO_4 release rates for the 75 g samples may have been due to the greater efficiency of larger volumes of water to remove more oxidized surface coatings.

5. DISCUSSION

5.1 Particle Size Control of SO_4 Release Rate

For the norite samples, the average SO_4 release rate increased with decreasing particle size. The smallest particle size sample had a SO_4 release rate 65 times that of the coarsest sample, clearly demonstrating the finest material is significantly more reactive (Table 5.1). Figure 5.1 shows the average norite sample SO_4 release rate as a power function of particle size. Mathematically this relationship is defined by equation 5, were x is the average particle size diameter in millimeters. In theory, equation 5 could be used to calculate SO_4 release rate for particle sizes greater than 19 mm, although the confidence of extrapolating beyond the experimental data is not certain. However, because release rates for the finer particles are orders of magnitude greater than even the 6.35-19 mm particle size category it is likely larger particles would have a small additional contribution to the overall load generated by most waste rocks. Sulfate release is the result of rinsing oxidation products and the sulfide oxidation rate is predominantly controlled by the exposed surface area. This exposure is a function of rock particle size and physical characteristics of both sulfide mineral grains and host rock mineral grains that are specific to individual rock types. Thus, equation 5 is unique to the norite rock examined in this experiment.

$$SO_4\ release\ rate\ (mmol \cdot kg^{-1} \cdot wk^{-1} \cdot S_T wt\%^{-1}) = 0.16 \times x^{-0.52} \quad \text{(eq. 5)}$$

5.2 Geochemistry of Pyrrhotite Oxidation Rate

Williamson and Rimstidt (1994) showed the pyrite oxidation rate by oxygen decreases slightly as pH decreases to the point Fe^{3+} is the dominant Fe-species after which the rate of pyrite oxidation increases with decreasing pH. Similarly, leachate from the norite samples exhibited both positive and negative correlations between SO_4 release rate and pH (Fig. 5.2). Figure 5.3 shows how SO_4 release and pH changed on an annual basis for the norite <0.053 mm particle size sample, which exhibited the same trend as the 0.053-0.149 and 0.149-0.5 mm samples. From 1993 to 1995 there was a positive correlation between pH and SO_4 release rate, and from 1996 to 1997 this correlation was negative. The positive correlation between SO_4 release rate and pH is characteristic of abiotic sulfide oxidation by $O_{2(aq)}$ whereas the negative correlation is characteristic of oxidation by Fe^{3+} (Fig. 5.4). The similar patterns suggest the rate dependence of pyrrhotite oxidation on pH and oxidant is similar to that of pyrite oxidation. This similarity is somewhat expected, because availability of Fe^{3+} is fundamentally dependent on pH (Fig. 5.5).

From 1998 to 2008 the negative correlation between pH and SO_4 release rate continued, but occurred at a pH greater than that for which Fe^{3+} is highly soluble, possibly indicating that the SO_4 release decrease was no longer controlled by availability of oxidant (Fig. 5.2). Instead, the SO_4 release decrease may have been due to a decrease in available sulfide surface area and/or the oxidation reaction becoming diffusion limited. The former inference is supported by sulfur depletion calculations indicating over 50% of the sulfur had been released by the beginning of 1998. From 2009 to 2011 SO_4 release rates rapidly decreased and were consistently below detection limit by the end of 2011. Leachate pH from the larger particle sizes decreased slowly over the first 400 to 500 weeks then stabilized (Fig. 4.7). Sulfate release rates from these three size fractions decreased slowly through about week 650 and then stabilized at a rate roughly 40 to 50 percent of that in year 2 (Fig. 4.8, Tables 4.7, 4.8, 4.9).

In contrast to the norite, diatreme and mudstone samples did not exhibit consistent, systematic variations of pH and SO_4 release rate with particle size (Figs. 5.6 and 5.7). However, the 0.053-0.149 mm diatreme and all the mudstone samples (except the <0.053 mm sample) do exhibit a relationship between leachate pH and SO_4 release rate. For the diatreme sample SO_4 release rate gradually increased as pH decreased over a pH range from 3 to 8 (Fig. 4.14, 4.15, 5.6). The two mudstone samples show a marked increase in SO_4 release rate upon pH decreasing below about 4 (Fig. 4.20, 4.21, 5.7).

5.3 Standard and Uncovered Samples

Leachate pH and SO_4 release rates for the uncovered samples (both reactors and humidity cells) differed from those of associated standard (covered) samples. The trends observed were dependent on particle size. The differences observed are attributed to a greater degree of evaporation for uncovered samples.

For the 0.053-0.149 mm norite, the uncovered reactor produced higher pH after week 70 and lower SO_4 release after about week 40 (Figs. 4.35 and 4.36, respectively). Lapakko and Berndt (2009) reported similar behavior for tailings generated from Duluth Complex rock. They speculated that the lower SO_4 release rate under evaporating (uncovered reactor) conditions was due to either 1) slower oxidation rates for the period during which these reactors were dry (roughly half the weekly cycle) or 2) inhibited mediation of oxidation by neutrophilic bacteria due to the dryer conditions. Irrespective of the cause, slower sulfide mineral oxidation resulted in less acid production resulting in a greater leachate pH.

For the 6.35-19 mm mudstone samples the opposite trend was observed. That is, the uncovered humidity cell yielded lower leachate pH (Fig. 4.37) and greater SO_4 release (Fig. 4.38) after about week 40. This may be the result of decreased acid neutralization resulting from decreased transport of acidic reaction products to neutralizing mineral surfaces. In addition, the lower pH and greater SO_4 release of the uncovered sample could also be resultant from enhanced breakdown of the larger particles from a more extreme wetting and drying cycle. This enhanced breakdown would expose sulfides that were previously encased in the large particles.

The 0.5-2.0 and 6.35-19 mm norite samples did not display any substantial differences between standard and uncovered samples (Figs. 4.31 to 4.34). However, the on average slightly lower pH and greater SO_4 release of the uncovered samples could be resultant from decreased transport of acidic reaction products to neutralizing mineral surfaces.

5.4 Different Sample Masses

Leachate from the 225 g samples had on average a lower SO_4 release rate and higher pH than the 75 g samples (Figs 4.39 to 4.44). The 225 g samples had a water to rock ratio one third of the 75 g samples indicating a possible W:R ratio control on leachate pH and SO_4 release rate (Table 3.1). The norite

samples exhibited the greatest variability in pH and SO_4 release rate between the different mass samples (Figs. 4.39 and 4.40). It is unclear why the larger mass samples had lower SO_4 release and higher pH.

5.5 Application of the Laboratory Data for Prediction

Humidity cell tests are commonly used to estimate release rates from mine wastes for predicting environmental impact from mining operations. These estimates commonly apply humidity cell release rates as mass dependent rates. However, because mineral reaction rates are strongly surface area dependent and humidity cells have a much larger specific surface area (area/unit mass) than most mine waste rock piles, direct application of the humidity cell data would generally lead to gross overestimation of mine waste release rates.

The overestimated rates are commonly modified by uncertain, unitless, parameters named 'scale factors' (eq. 6). Scale factors are intended to account for the differences between the laboratory and field environment (e.g., particle size, water contact, temperature, etc.). The accuracy in applying scale factors is limited because many of the differences between the lab and exact field environments are unknown. Therefore, selecting reasonable scale factors inherently includes numerous assumptions and commonly results in a wide range of values to encompass the uncertainty. If the particle size of the laboratory and field material is known then release rates can be applied to individual particle size fractions eliminating the need for a particle size scale factor.

$$Field_{rate} = Lab_{rate} \times Scale\ Factor(s) \qquad \text{(eq. 6)}$$

The norite samples from the particle size experiment were collected from the AMAX FL-6 field test pile. The AMAX FL-6 test pile was an approximately 1000 tonne rock pile, for which leachate composition and flow were measured for 16 years. Rock from the AMAX test piles were previously characterized for composition and particle size distribution (Lapakko et al., 2004). The similar rock type and well characterized particle size distribution of the AMAX FL-6 rock pile and the norite samples from the particle size experiment provide the opportunity to account for surface area differences between the laboratory and field experiments effectively limiting a major variable between laboratory and field rock character. Accounting for a dominant variable between the laboratory and field allows a more accurate calculation for extrapolating laboratory data to the field environment.

Predicting the annual SO_4 release rate of the AMAX FL-6 waste rock pile can be performed using equation 7. To make this calculation, the average particle size diameter (i) from each AMAX FL-6 particle size category was determined by taking the average of the end range values (Table 5.2, column 2). Next the SO_4 release rate for each average particle size (i) is calculated from equation 5 (Table 5.2, column 3). Then each particle size SO_4 release rate is multiplied by the mass fraction of each AMAX particle size category (Table 5.2, column 5) and summed.

$$SO_4 release\ rate_{field} = \sum_{(i)} SO_4 release\ rate_{lab(i)} \times mass\ fraction_i \qquad \text{(eq.7)}$$

For the AMAX FL-6 waste rock pile, SO_4 release rate field measurements and values predicted by equation 7 can be compared to evaluate the prediction technique. Figure 5.8 shows that the laboratory predicted values are both greater and less than the field measured rates. For the first three years, the laboratory prediction over estimates the field values whereas the prediction underestimates for the following years (except 1990, which had an anomalously low total leachate flow measurement, see Lapakko et al. (2004)). Excluding data from 1990 the prediction calculation on average under predicts by a factor of 0.6.

Some of the difference between laboratory prediction and field measurements can be attributed to the influence of pH on SO_4 release rates. Inspection of the AMAX field data shows that leachate was not consistently acidic until after the third year which coincides with the point at which the prediction underestimates the field values. Because the average laboratory release rates for the particles greater than 6.35 mm had leachate pH values of about 6 and the AMAX FL-6 waste rock pile had an average pH of about 4.5 the predicted release rate for the AMAX rock particles greater than 6.35 mm may inherently lead to under prediction. This is due to the increased rate of sulfide oxidation at low pH resultant from ferric iron becoming the dominant oxidant (see Fig. 5.4).

Figure 5.9 shows that pyrite oxidation rates increase by about a factor of two from a pH of 6 to 4.5. If pyrrhotite oxidation rates change similarly over this pH range then the calculated release rates for samples > 6.35 mm from the AMAX particle size fractions can be multiplied by two. Applying the factor of 2 rate increase to the 6.35 mm and larger particle size fractions results in an average under prediction factor of 0.9 (Fig. 5.10). This close SO_4 release rate prediction strongly suggests that particle size (a proxy for surface area) is a dominant variable for extrapolating laboratory release rates to large waste rock piles. This comparison suggests that variables such as temperature and water contact do not have as large an impact. However, the AMAX waste rock piles are orders of magnitude smaller than most mining operation waste rock piles. For larger waste rock piles (millions of tonnes) temperature and water contact would likely become more important factors that could limit the amount of reactive rock.

Applying the particle size data for predictions inherently requires a few simplifying assumptions. First, the SO_4 release rates calculated for the AMAX test piles leachate were calculated from only the period of sampling which did not always capture all of the leachate exiting the rock pile (on average 240 days per year; Lapakko et al., 2004). This collection period may incorporate oxidation products produced during the no flow winter months released during the spring melt. This could potentially result in SO_4 release rates that are greater than what would normally be determined from continuous flow. However, inspection of annual SO_4 concentration trends shows only in 1990 did the highest SO_4 concentrations occur during the spring. In general, the SO_4 concentration of FL-6 rock pile leachate increased through summer and then either decreased, fluctuated or rarely increased. Second, annual SO_4 release rate data from the AMAX field piles was not normalized to the individual particle size fractions (Table 5.2) S_T concentrations. Instead, the release rate was normalized by the bulk sulfur content of 0.8 wt % Third, the mineral grain size distribution and rock textures are assumed to be equal between laboratory and field samples.

5.6 Implications to Mine Waste Leachate Prediction and Rock Management

The particle size experiment provided insight into four key concepts that should be evaluated to assess the potential for proposed mining operations to impact the environment. These key concepts are 1) sulfide enrichment in fines, 2) leachate pH and SO_4 release rate dependence on particle size, 3) sulfide mineral grain size distribution, and 4) long term leachate composition.

First crushing of rock can lead to enrichment of sulfide minerals in some particle size fractions. In the case of norite were the dominant sulfide (pyrrhotite) is significantly softer than the silicate minerals, S_T increased by about a factor of two from the bulk composition to the smallest particle size sample. This was observed for both this laboratory experiment and the AMAX field rock piles (Lapakko et al., 2004). Knowing if sulfide is concentrated is an important consideration because concentrating sulfide minerals in the fines increases the SO_4 release rate due to a greater specific surface area and increased amount of reactant.

Second, the norite samples showed a marked difference in pH and SO_4 release rate among the different particle size fractions. This relationship can be quantified and used to predict release rates for field scale

waste rock piles. In addition, the fine particles largely drive the reaction progress in field scale rock piles. For example, the leachate pH from the AMAX FL-6 rock pile exhibited low pH leachate despite the < 0.5 mm material accounting for only 3.1 % of the total rock mass.

Third, the significant shift in overall greater pH and lower SO_4 release rates observed between the 0.149-0.5 and 0.5-2.0 norite samples is indicative of the sulfide mineral grain size distribution where the transition to particles less than 0.5 mm leads to near complete exposure of the majority of the sulfide mineral surfaces. Knowing this critical particle size in conjunction with a waste rock piles overall particle size distribution provides a gauge for the amount of highly reactive rock.

Fourth, the particle size experiment showed that for material ≤ 0.5 mm nearly all the sulfide was reacted. For increasingly larger particles a much smaller fraction of the sulfide was reacted over the reported experiment timespan. This demonstrates that not all of the sulfide in a waste rock pile is readily available for reaction and that a considerable amount of sulfide will be limited for release based on the weathering and subsequent break down of the silicate mineral assemblage for which the sulfide are enclosed. The time required to dissolve silicates is orders of magnitude greater (thousands to tens of thousands of years for millimeters of weathering rind development (Colman and Pierce, 1981)) than that for carbonates or sulfides.

6. RECOMMENDATIONS FOR FUTURE WORK

Interpreting the results and further developing the predictive capability of the particle size experiment could be benefitted by three specific follow up investigations. First, expand the limited measurements of sulfide and non-sulfide mineral grain sizes to aid interpretation of the chemical release behavior as a function of time and particle size. Second, conduct solid phase analysis of the discontinued samples and samples with below detection limit leachate SO_4 concentrations to compare the post experiment composition with cumulative mass released to determine, with greater certainty, what the initial sample composition was. Third, continuing the experiment for the Duluth Complex norite samples with leachate SO_4 concentrations above detection (four largest particle size samples) to learn how SO_4 release from large particles will progress and aid in determining the reactive time period for Duluth Complex rock.

ACKNOWLEDGEMENTS

Funding for this report and laboratory work since July 2011 was provided by Minerals Cooperative Environmental Research and Iron Ore Cooperative Research State programs plus industry match. Funding for laboratory work prior to July 2011 was provided by the State of Minnesota general fund, US Army Corps of Engineers (DACW45-02-P-0205), U.S. Environmental Protection Agency (USEPA) under Agreement no. CX-816270-01-0 administered by the Western Governors' Association (WGA), and USEPA Grant no. X-8200322-01-0. Laboratory dissolution experiments were conducted by Pat Geiselman, Anne Jagunich, Kate Willis, and Cal Jokela. Anne Jagunich and Andea Johnson contributed to data management.

REFERENCES

American Public Health Association (APHA), American Water Works Association, Water Environment Federation, 1992. Standard methods for the examination of water and wastewater, 18th ed. American Public Health Association, Washington, D.C.

ASTM International. 2013. D5744-13, Standard test method for laboratory weathering of solid materials using a humidity cell. American Society for Testing and Materials, West Conschohocken, PA. 23p.

Bucknam, C.H., White III, W., Lapakko, K.A. 2009. Standardization of Mine Waste Characterization Methods by ADTI-MMS. *In* Proc. Securing the Future and 8thICARD, June 22-26, 2009, Skellefteå, Sweden (CD ROM). 12 p.

Busenberg, E., Plummer, L.N. 1982. The kinetics of dissolution of dolomite in CO_2-H_2O systems at 1.5^o to 65^o C and 0 to 1 atm P_{CO2}. American Journal of Science, v. 282. p. 45-78.

Colman, S. M.. Pierce, K. L. 1981. Weathering rinds on andesitic and basaltic stones as a Quaternary age indicator, Western United States. USGS Professional Paper 1210, 56 p.

Davis, G.B. Ritchie, A. I. M. 1986. A model of oxidation in pyritic mine wastes: part 1: equations and approximate solution. Applied Mathematical Modelling, v. 10, p. 314-322.

Davis, G.B., Ritchie, A. I. M. 1987. A model of oxidation in pyritic mine wastes: part 3: import of particle size distribution. Applied Mathematical Modelling, v. 11, p. 417-422.

Dzombak, D. A., Morel, F. M. M. 1990. Surface complexation modeling, hydrous ferric oxide. Wiley, New York, 393 p.

Gerke, H.H., Molson, J.W., Frind, E.O. 1998. Modelling the effect of chemical heterogeneity on acidification and solute leaching in overburden mine spoils. Journal of Hydrology, v. 209, p. 166-185.

Jambor, J.L. 2003. Mine waste mineralogy and mineralogical perspectives of acid–base accounting. In Environmental Aspects of Mine Wastes (J.L. Jambor, D.W. Blowes, and A.I.M. Ritchie, eds.). Mineral. Association Canada, Short Course Volume 31, p.117-145.

Jambor, J. L., Blowes, D. W., eds. 1994. The environmental geochemistry of sulfide mine-wastes, Mineralogic Association of Canada Short Course, v.22, 438 p.

Jambor, J.L., Blowes, D.W. 1998. Theory and applications of mineralogy in environmental studies of sulfide-bearing mine waste. In Short Course Handbook on Ore and Environmental Mineralogy (L. J. and Vaughan, D.J. eds.). Mineralogical Association of Canada, v. 27, p. 367-401.

Jerz, J. K., Rimstidt, J. D. 2004. Pyrite oxidation in air. Geochimica et Cosmochimica Acta, v. 68, p. 701-714.

Lapakko, K. A. 1988. Apparatus for environmental leaching testing. U.S. Patent 4,783,318.

Lapakko, K.A. 1993. Evaluation of Tests for Predicting Mine Waste Drainage pH: Report to the Western Governors' Association. MN Dep. Nat. Resour., Div. of Minerals. St. Paul, MN. 76 p. plus appendices.

Lapakko, K. A. 1994. Comparison of Duluth Complex rock dissolution in the laboratory and field. In

International Land Reclamation and Mine Drainage Conference and the 3rd International Conference on the Abatement of Acidic Drainage, Pittsburgh, PA, April 24-29. p. 419-428.

Lapakko, K.A. 2003. Developments in Humidity-Cell Tests and their Application. In Environmental Aspects of Mine Wastes (J.L. Jambor, D.W. Blowes, and A.I.M. Ritchie, eds.). Mineralogical Association of Canada Short Course Volume 31. p. 147-164.

Lapakko, K.A., Antonson, D.A., Johnson, A.M., Folman, J.T. 2002. Laboratory drainage quality from mafic-intrusive, tuffaceous-sedimentary, and weathered waste rocks. Final Report on Contract BLM JSP012002 to the U.S. Bureau of Land Management Utah State Office. 81 p. plus appendices.

Lapakko, K.A., Antonson, D.A., Engstrom, J.N. 2004. Analytical screening of abandoned waste rock piles. Report on Contract No. DACW45-02-P-0212 to US Army Corps of Engineers by the Minnesota Department of Natural Resources. 91 p. plus appendices.

Lapakko, K. A., Antonson, D. A., Wagner, J. R. 1998. Mixing of alkaline solids with finely-crushed acid-producing rock. MN Dept. Nat. Resour., Div. of Minerals, St. Paul, MN. April 1998. 49 p. plus appendices.

Lapakko, K. A., Engstrom, J. N., Antonson, D. A. 2006. Effects of particle size on drainage quality from three lithologies. In proceedings, 7th International Conference on Acid Mine Drainage, St. Louis, Missouri, 33 p.

Lapakko, K. A., Haub, J. N., Antonson, D. A. 1998. Effects of Dissolution time and particle size on kinetic test results. Society for Mining, Metallurgy, and Exploration Preprint 98-114, 9 p.

Lapakko, K. A., Wessels, J., Antonson, D. A. 1995. Long term dissolution testing of mine waste. report to United States Environmental Protection Agency for grant # X-8200322-01-0, 85 p.

Levenspiel, O. 1972. Chemical Reaction Engineering, 1st edition, Wiley, New York, 578 p.

Nicholson, R. V., Gillham, R. W., Reardon, E. J., 1990, Pyrite oxidation in carbonate-buffered solution: 2. Rate control by oxide coatings. Geochimica et Cosmochimica Acta, v. 54, p. 395-402.

Plumlee, G.S., and Logsdon, M.J., eds., 1999. The environmental geochemistry of mineral deposits, Part A.: Processes, techniques, and health issues: Society of Economic Geologists, Inc., Reviews in Economic Geology, vol. 6A, 371 p.

Williamson, M.A., Rimstidt, J.D., 1994. The kinetics and electrochemical rate-determining step of aqueous pyrite oxidation. Geochimica et Cosmochimica Acta, v. 58, p. 5443-5454.

TABLES

Table 2.1 Particle Size Surface Area and Specific Surface Area

Particle size diameter (mm)	Particle size surface area (mm^2)	Particle size volume (mm^3)	Mass of one particle (g)	Specific surface area (mm^2/g)
0.001	3.14E-06	5.2E-10	1.57E-12	2.00E+06
0.0265	2.21E-03	9.7E-06	2.92E-08	7.55E+04
0.01	3.14E-04	5.2E-07	1.57E-09	2.00E+05
0.1	3.14E-02	5.2E-04	1.57E-06	2.00E+04
1	3.14E+00	5.2E-01	1.57E-03	2.00E+03
10	3.14E+02	5.2E+02	1.57E+00	2.00E+02
12.675	5.05E+02	1.1E+03	3.20E+00	1.58E+02
100	3.14E+04	5.2E+05	1.57E+03	2.00E+01
1000	3.14E+06	5.2E+08	1.57E+06	2.00E+00

A density of 3.0 g/cm3 was used to make the calculations.

Table 3.1 Humidity Cell and Reactor Sample Mass, Rinse Volume and Water to Rock Ratio

	mass of rock (g)					
	≤0.053	0.053-0.149	0.149-0.5	0.5-2.0	2.0-6.35	6.35-19
Norite	75	75	75 (225)	1000	1000	1000
Diatreme	75	75	75 (225)	1000	500	NA
Mudstone	75	75	75 (225)	1000	1000	1000
	rinse volume (mL)					
Norite	200	200	200	300	300	300
Diatreme	200	200	200	400	200	NA
Mudstone	200	200	200	400	400	400
	water:rock mass ratio					
Norite	2.67	2.67	2.67 (0.89)	0.3	0.3	0.3
Diatreme	2.67	2.67	2.67 (0.89)	0.4	0.4	NA
Mudstone	2.67	2.67	2.67 (0.89)	0.4	0.4	0.4

Table 4.1 Mineral Modal Abundances

Mineral	Norite	Mudstone	Diatreme
Plagioclase	43	--	--
Olivine	28	--	--
Pyroxene	11	--	--
Cordierite	5	--	--
Quartz	--	45	71
K-spar	--	27	16
Mica	5	13	9
Oxide	4	--	--
Carbonate	--	5	3
Sulfide	4	12	3
total	100	102	101

Table 4.2 Whole Rock Composition

Sample	Particle Size (mm)	S_T	S^{2-}	SO_4	C_T	CO_2	SiO_2	Al_2O_3	Fe_2O_3	MgO	CaO	Na_2O	K_2O	TiO_2	P_2O_5	MnO	LOI	FeO
norite	<0.053	1.41	1.13	0.28	0.25	0.14	43.69	13.85	18.64	8.23	6.45	1.58	0.95	2.47	0.45	0.17	2.1	
norite	0.053-0.149	1.11	0.76	0.35	0.18	0.61	44.58	14.65	18.92	8.18	6.25	1.82	1	2.46	0.22	0.16	0.4	
norite	0.149-0.5	1.24	0.8	0.44	0.15	0.06	45.01	14.98	17.68	8.67	6.6	1.91	0.89	1.73	0.18	0.15	1.2	
norite	0.5-2.0	0.87	0.52	0.35	0.13	<0.01	44.95	14.88	17.56	8.8	6.81	1.81	0.78	1.88	0.23	0.16	1.2	
norite	2.0-6.35	0.64	0.57	0.07	0.15	<0.01	45.5	15.24	17.09	8.78	6.96	1.79	0.79	1.95	0.25	0.17	0.7	
norite	6.35-19	0.43	0.31	0.12	0.08	0.02	45.52	15.11	16.76	9.51	7.58	1.62	0.67	1.8	0.25	0.17	0.9	
diatreme	<0.053	0.9	0.57	0.34	0.29	0.77	58.41	19.86	5.43	0.79	0.53	0.21	7.57	0.35	0.09	0.49	4.6	3.14
diatreme	0.053-0.149	1.88	1.53	0.35	0.45	1.45	67.97	12.86	5.12	0.47	0.87	0.67	6.91	0.16	0.1	0.58	2.7	2.54
diatreme	0.149-0.5	2.19	2.05	0.14	0.45	1.5	72.72	9.77	5.15	0.4	0.28	0.16	4.99	0.13	0.05	0.64	3.7	2.01
diatreme	0.5-2.0	1.87	1.69	0.18	0.51	1.72	74.61	9.52	4.68	0.43	0.36	0.14	4.36	0.16	0.07	0.76	3.6	2.34
diatreme	2.0-6.35	1.59	1.44	0.15	0.41	1.38	70.01	12.41	4.67	0.51	0.24	0.17	5.67	0.32	0.12	0.6	3.8	2.34
mudstone	<0.053	2.74	2.06	0.68	0.9	0.84	66.22	12.11	5.77	1.79	1.39	0.16	5.26	0.59	0.21	0.08	6	
mudstone	0.053-0.149	3.12	2.54	0.58	1.08	1.63	64.62	11.1	8.21	1.72	1.62	0.12	4.92	0.51	0.18	0.1	5.6	
mudstone	0.149-0.5	2.56	1.98	0.58	1.11	1.6	66.59	11.47	5.21	1.8	1.6	0.08	5.12	0.57	0.23	0.08	6.8	
mudstone	0.5-2.0	2.83	2.29	0.54	1.04	1.46	66.75	11.49	5.55	1.7	1.4	0.06	5.17	0.57	0.21	0.08	6.1	
mudstone	2.0-6.35	2.99	2.45	0.55	1.2	2.08	65.92	11.52	5.4	1.96	1.97	0.13	5.12	0.58	0.2	0.1	6.2	
mudstone	6.35-19	2.7	2.35	0.35	0.88	0.98	67.73	11.28	5.24	1.6	1.07	0.08	4.92	0.57	0.22	0.03	6.3	

Data from Acme

Table 4.3 ACME and Midland Sulfur and CO_2 wt% Comparison

sample	particle size (mm)	S_T[1] (wt%)	S_T[2] (wt%)	CO_2[1] (wt%)	CO_2[2] (wt%)
norite	<0.053	1.41	1.51	0.14	0.32
	0.053-0.149	1.11	0.87	0.61	0.1
	0.149-0.5	1.24	1.29	0.06	0.06
	0.5-2.0	0.87	0.88	<0.01	0.05
	2.0-6.35	0.64	0.83	<0.01	0.09
	6.35-19	0.43	0.93 (0.3*)	0.02	<0.01
diatreme	<0.053	0.90	0.95	0.77	0.96
	0.053-0.149	1.88	1.98	1.45	1.32
	0.149-0.5	2.19	2.34	1.50	1.6
	0.5-2.0	1.87	1.9	1.72	1.73
	2.0-6.35	1.59	1.5	1.38	1.46
mudstone	<0.053	2.74	2.83	0.84	0.88
	0.053-0.149	3.12	3.01	1.63	1.64
	0.149-0.5	2.56	2.61	1.60	1.68
	0.5-2.0	2.83	2.79	1.46	1.4
	2.0-6.35	2.99	3.52	2.08	1.27
	6.35-19	2.70	3.46	0.98	1.89

[1]= Acme analysis, [2]= Midland Analysis, *= original analysis

Table 4.4 Mineral hardness and average grain size

Rock Type	Mineral	Moh's Hardness	Absolute Hardness (g)	Average Grain Size
Norite	Pyrrhotite	4	21	fine
	Plagioclase	6	72	medium
	Olivine	6.5-7	100	medium
	Pyroxene	5-6	48-72	medium
Diatreme	Pyrite	6-6.5	72	fine-medium
	K-feldspar	6	72	fine-medium
	Quartz	7	100	fine-medium
	Mica	2-2.5	3	fine
	Carbonates	3-4	9-21	fine-medium
Mudstone	Pyrite	6-6.5	72	fine-medium
	Mica	2-2.5	3	fine
	Quartz	7	100	fine
	K-feldspar	6	72	fine
	Carbonates	3-4	9-21	fine-medium

Absolute Hardness as reported by sclerometer testing.

Table 4.5 Tabulation of AP(S_T) and NP(CO_2) values by rock type and particle size.

Sample	particle size (mm)	Weeks	S_T^1 (wt %)	S_T^2 (wt %)	CO_2 (wt %)	CO_2 (wt %)	Mass (mg)	AP^1	AP^2	NP^1	NP^2	% AP^1 depleted	% AP^2 depleted	% NP^1 depleted	% NP^2 depleted
norite	<0.053	943	1.41	1.51	0.14	0.32	75	44	47	3.0	7.0	105%	98%	880%	385%
	0.053-0.149	943	1.11	0.87	0.61	0.10	75	35	27	13	2.2	104%	133%	147%	897%
	0.149-0.5	943	1.24	1.29	0.06	0.06	75	39	40	1.3	1.3	71%	69%	1314%	1314%
	0.5-2.0	943	0.87	0.88	<0.01	0.05	1000	27	27	0.11	1.1	40%	40%	7832%	783%
	2.0-6.35	943	0.64	0.83	<0.01	0.09	1000	20	26	0.11	2.0	18%	14%	2641%	147%
	6.35-19	943	0.43	0.93	0.02	<0.01	1000	13	29	0.44	0.11	8%	4%	230%	919%
diatreme	<0.053	466	0.90	0.95	0.77	0.96	75	28	30	4.5	5.6	25%	23%	138%	110%
	0.053-0.149	943	1.88	1.98	1.45	1.32	75	59	62	8.5	7.8	74%	70%	107%	118%
	0.149-0.5	536	2.19	2.34	1.50	1.60	75	68	73	8.8	9.4	10%	10%	94%	88%
	0.5-2.0	943	1.87	1.9	1.72	1.73	1000	58	59	10	10	12%	11%	84%	83%
	2.0-6.35	943	1.59	1.5	1.38	1.46	500	50	47	8.1	8.6	19%	20%	72%	68%
mudstone	<0.053	134	2.74	2.83	0.84	0.88	75	86	88	18	19	13%	13%	102%	97%
	0.053-0.149	385	3.12	3.01	1.63	1.64	75	97	94	35	36	34%	35%	110%	109%
	0.149-0.5	483	2.56	2.61	1.60	1.68	75	80	81	35	37	45%	44%	117%	111%
	0.5-2.0	335	2.83	2.79	1.46	1.40	1000	88	87	32	30	52%	53%	112%	117%
	2.0-6.35	134	2.99	3.52	2.08	1.27	1000	93	110	45	28	39%	34%	56%	92%
	6.35-19	134	2.70	3.46	0.98	1.89	1000	84	108	21	41	19%	15%	51%	27%

[1]= Acme analysis, [2]= Midland Analysis

For values with < detection limit (DL) one-half the DL value was used.

Table 4.6 Tabulation of ENP(pH 6) values by rock type and particle size.

Sample	particle size (mm)	Weeks pH ≥6	Cumulative Ca release for pH ≥6 g Ca·(kg rock)$^{-1}$	Cumulative Mg release for pH ≥6 g Mg·(kg rock^{-1})	Cumulative Ca release for pH ≥6 g $CaCO_3$·(kg rock)$^{-1}$	Cumulative Mg release for pH ≥6 g $CaCO_3$·(kg rock)$^{-1}$	ENP	ENP % Ca	ENP % Mg	S_T[1] (wt %)	S_T[2] (wt %)	CO_2[1] (wt %)	CO_2[2] (wt %)
norite	<0.053	17	1.07	0.51	2.67	2.08	4.8	56%	44%	1.41	1.51	0.14	0.32
	0.053-0.149	8	0.21	0.12	0.52	0.47	1.0	52%	48%	1.11	0.87	0.61	0.10
	0.149-0.5	7	0.13	0.09	0.31	0.35	0.7	47%	53%	1.24	1.29	0.06	0.06
	0.5-2.0	18	0.07	0.04	0.18	0.18	0.4	50%	50%	0.87	0.88	<0.01	0.05
	2.0-6.35	31*	0.04	0.03	0.10	0.12	0.2	46%	54%	0.64	0.83	<0.01	0.09
	6.35-19	48*	0.03	0.02	0.06	0.08	0.1	45%	55%	0.43	0.93	0.02	<0.01
diatreme	<0.053	466	1.75	0.45	4.36	1.86	6.2	70%	30%	0.90	0.95	0.77	0.96
	0.053-0.149	415*	1.22	1.08	3.05	4.45	7.5	41%	59%	1.88	1.98	1.45	1.32
	0.149-0.5	427*	1.48	1.05	3.69	4.31	8.0	46%	54%	2.19	2.34	1.50	1.60
	0.5-2.0	544*	1.52	1.06	3.79	4.35	8.1	47%	53%	1.87	1.9	1.72	1.73
	2.0-6.35	403	0.59	0.80	1.46	3.29	4.8	31%	69%	1.59	1.5	1.38	1.46
mudstone	<0.053	134	4.13	2.01	10.30	8.25	18.6	56%	44%	2.74	2.83	0.84	0.88
	0.053-0.149	367	8.23	3.90	20.54	16.05	36.6	56%	44%	3.12	3.01	1.63	1.64
	0.149-0.5	449	8.56	3.90	21.35	16.03	37.4	57%	43%	2.56	2.61	1.60	1.68
	0.5-2.0	239	6.80	3.16	16.96	12.99	30.0	57%	43%	2.83	2.79	1.46	1.40
	2.0-6.35	0	--	--	--	--	--	--	--	2.99	3.52	2.08	1.27
	6.35-19	0	--	--	--	--	--	--	--	2.70	3.46	0.98	1.89

*= pH change was gradual. The week listed represents time prior to pH values below 6.0 for more than two consecutive measurements

For values with < detection limit (DL) one-half the DL value was used.

Table 4.7 Average Annual SO_4, Ca, Mg Release Rates ($mmol \cdot kg^{-1} \cdot wk^{-1}$). (Page 1 of 6)

Year	Norite (<0.053 mm)				Diatreme (<0.053 mm)				Mudstone (<0.053 mm)			
	min pH	SO_4	Ca	Mg	min pH	SO_4	Ca	Mg	min pH	SO_4	Ca	Mg
1993	7.11	1.84E+00	1.47E+00	5.82E-01	6.77	4.86E-01	4.45E-01	6.91E-02	7.22	3.35E+00	2.99E+00	1.80E+00
1994	4.70	9.93E-01	4.76E-01	3.81E-01	6.55	8.61E-02	9.06E-02	3.68E-02	7.07	2.79E-01	4.79E-01	3.47E-01
1995	4.44	8.39E-01	3.19E-01	3.54E-01	6.17	3.53E-02	5.52E-02	2.82E-02	7.23	1.56E-01	3.74E-01	3.04E-01
1996	4.19	9.52E-01	2.20E-01	2.16E-01	6.13	4.77E-02	5.00E-02	4.18E-02	7.15	9.38E-02	2.62E-01	2.21E-01
1997	4.00	1.49E+00	2.72E-01	1.81E-01	6.46	2.99E-02	3.79E-02	2.42E-02	NA	NA	NA	NA
1998	4.22	7.97E-01	2.12E-01	9.06E-02	5.94	2.76E-02	1.11E-02	1.74E-02	NA	NA	NA	NA
1999	4.45	5.37E-01	1.80E-01	6.87E-02	6.11	2.41E-02	7.45E-03	8.79E-03	NA	NA	NA	NA
2000	4.79	3.22E-01	1.31E-01	4.93E-02	6.21	2.47E-02	3.79E-03	6.53E-03	NA	NA	NA	NA
2001	4.50	5.63E-01	1.53E-01	4.92E-02	6.27	3.47E-02	8.05E-03	5.34E-03	NA	NA	NA	NA
2002	4.42	6.00E-01	1.59E-01	4.89E-02	5.84	7.44E-02	7.93E-03	5.64E-03	NA	NA	NA	NA
2003	4.54	4.46E-01	1.69E-01	4.85E-02	NA	NA	NA	NA	NA	NA	NA	NA
2004	4.74	2.86E-01	1.42E-01	3.40E-02	NA	NA	NA	NA	NA	NA	NA	NA
2005	5.09	2.00E-01	1.10E-01	2.81E-02	NA	NA	NA	NA	NA	NA	NA	NA
2006	5.70	1.14E-01	8.09E-02	2.29E-02	NA	NA	NA	NA	NA	NA	NA	NA
2007	6.09	5.79E-02	5.53E-02	2.12E-02	NA	NA	NA	NA	NA	NA	NA	NA
2008	6.42	3.54E-02	4.44E-02	2.05E-02	NA	NA	NA	NA	NA	NA	NA	NA
2009	6.49	2.25E-02	4.22E-02	2.21E-02	NA	NA	NA	NA	NA	NA	NA	NA
2010	6.39	1.61E-02	4.69E-02	2.32E-02	NA	NA	NA	NA	NA	NA	NA	NA
2011	6.53	1.07E-02	3.47E-02	1.91E-02	NA	NA	NA	NA	NA	NA	NA	NA

Table 4.7 Average Annual SO_4, Ca, Mg Release Rates ($mmol \cdot kg^{-1} \cdot wk^{-1}$) (Page 2 of 6).

Year	Norite (0.053-0.149 mm)				Diatreme (0.053-0.149 mm)				Mudstone (0.053-0.149 mm)			
	min pH	SO_4	Ca	Mg	min pH	SO_4	Ca	Mg	min pH	SO_4	Ca	Mg
1993	6.93	8.49E-01	4.62E-01	4.36E-01	6.69	3.68E-01	2.83E-01	1.92E-01	6.90	1.24E+01	1.88E+00	1.62E+00
1994	4.80	7.18E-01	2.74E-01	3.11E-01	6.74	1.59E-01	2.14E-01	2.00E-01	7.00	5.18E-01	5.89E-01	4.27E-01
1995	4.27	7.15E-01	2.36E-01	3.37E-01	6.52	1.48E-01	1.26E-01	1.85E-01	7.21	4.51E-01	6.56E-01	4.49E-01
1996	4.12	6.89E-01	1.48E-01	2.68E-01	6.68	1.47E-01	6.63E-02	1.69E-01	7.37	4.14E-01	7.12E-01	4.84E-01
1997	4.06	9.54E-01	1.63E-01	2.47E-01	6.42	1.48E-01	4.94E-02	1.18E-01	7.38	4.28E-01	5.91E-01	4.72E-01
1998	4.03	7.45E-01	1.46E-01	1.31E-01	6.43	1.11E-01	2.14E-02	5.98E-02	7.36	3.98E-01	4.33E-01	3.78E-01
1999	4.15	5.18E-01	1.27E-01	7.84E-02	6.21	1.64E-01	2.22E-02	4.40E-02	7.00	3.57E-01	3.40E-01	3.08E-01
2000	4.30	4.33E-01	1.08E-01	5.52E-02	6.28	1.77E-01	1.65E-02	2.50E-02	6.25	5.73E-01	4.05E-01	3.54E-01
2001	4.09	8.00E-01	1.32E-01	6.43E-02	5.93	2.21E-01	1.66E-02	1.21E-02	2.46	7.00E+00	8.45E-01	4.17E-01
2002	4.19	6.22E-01	1.40E-01	6.75E-02	4.56	4.00E-01	1.64E-02	1.08E-02	NA	NA	NA	NA
2003	4.44	3.07E-01	1.17E-01	4.54E-02	3.72	4.98E-01	1.88E-02	8.31E-03	NA	NA	NA	NA
2004	4.81	1.42E-01	9.00E-02	3.04E-02	3.53	5.91E-01	2.26E-02	1.49E-02	NA	NA	NA	NA
2005	5.03	8.49E-02	5.15E-02	2.13E-02	3.32	6.66E-01	2.25E-02	1.04E-02	NA	NA	NA	NA
2006	6.19	4.43E-02	3.60E-02	1.74E-02	3.49	7.03E-01	3.18E-02	5.32E-03	NA	NA	NA	NA
2007	6.38	2.13E-02	2.54E-02	1.67E-02	3.30	7.91E-01	3.08E-02	5.34E-03	NA	NA	NA	NA
2008	6.45	1.43E-02	2.09E-02	1.78E-02	3.32	8.12E-01	2.74E-02	5.33E-03	NA	NA	NA	NA
2009	6.49	6.62E-03	1.94E-02	1.85E-02	3.05	1.10E+00	2.47E-02	5.30E-03	NA	NA	NA	NA
2010	6.41	8.55E-03	2.49E-02	1.75E-02	3.24	6.60E-01	2.24E-02	5.33E-03	NA	NA	NA	NA
2011	6.41	6.70E-03	1.79E-02	1.68E-02	3.10	7.49E-01	1.38E-02	5.29E-03	NA	NA	NA	NA

Table 4.7 Average Annual SO_4, Ca, and Mg Release Rates ($mmol \cdot kg^{-1} \cdot wk^{-1}$) (Page 3 of 6).

Year	Norite (0.149-0.5 mm)				Diatreme (0.149-0.5 mm)				Mudstone (0.149-0.5 mm)			
	min pH	SO_4	Ca	Mg	min pH	SO_4	Ca	Mg	min pH	SO_4	Ca	Mg
1993	6.71	6.35E-01	2.96E-01	3.40E-01	6.81	2.40E-01	2.18E-01	1.23E-01	6.37	1.85E+01	1.66E+00	1.30E+00
1994	5.02	5.17E-01	1.49E-01	2.72E-01	6.89	9.13E-02	2.67E-01	2.02E-01	7.00	5.34E-01	5.77E-01	4.28E-01
1995	4.73	5.89E-01	1.39E-01	3.58E-01	6.87	7.18E-02	2.27E-01	2.39E-01	7.23	3.40E-01	6.05E-01	3.92E-01
1996	4.34	5.53E-01	1.22E-01	2.83E-01	6.96	6.71E-02	8.02E-02	1.42E-01	7.68	3.20E-01	6.11E-01	4.00E-01
1997	4.21	8.24E-01	1.15E-01	3.43E-01	6.69	8.36E-02	3.44E-02	8.91E-02	7.40	3.07E-01	5.69E-01	4.07E-01
1998	4.21	6.41E-01	9.07E-02	2.13E-01	6.47	9.56E-02	1.87E-02	5.65E-02	7.34	2.93E-01	3.64E-01	2.82E-01
1999	4.19	4.84E-01	8.46E-02	1.46E-01	6.35	1.04E-01	1.44E-02	3.19E-02	7.24	2.72E-01	3.24E-01	2.69E-01
2000	4.40	3.43E-01	7.65E-02	9.68E-02	6.45	9.82E-02	9.58E-03	2.58E-02	7.35	2.72E-01	3.03E-01	2.71E-01
2001	4.37	3.11E-01	6.78E-02	6.56E-02	6.04	1.19E-01	1.27E-02	1.61E-02	6.86	3.98E-01	3.15E-01	2.76E-01
2002	4.50	2.42E-01	5.76E-02	5.35E-02	5.67	1.58E-01	9.64E-03	9.18E-03	2.75	1.55E+00	5.23E-01	3.23E-01
2003	4.70	1.75E-01	5.31E-02	4.74E-02	4.41	2.53E-01	1.43E-02	1.46E-02	2.74	5.23E+00	3.70E-01	2.77E-01
2004	4.82	1.29E-01	3.94E-02	3.28E-02	4.30	6.70E-01	2.03E-02	4.45E-02	NA	NA	NA	NA
2005	4.76	1.01E-01	2.99E-02	2.75E-02	NA	NA	NA	NA	NA	NA	NA	NA
2006	5.13	7.79E-02	2.50E-02	2.32E-02	NA	NA	NA	NA	NA	NA	NA	NA
2007	5.29	6.08E-02	2.10E-02	2.18E-02	NA	NA	NA	NA	NA	NA	NA	NA
2008	5.51	5.63E-02	1.96E-02	2.06E-02	NA	NA	NA	NA	NA	NA	NA	NA
2009	5.67	5.00E-02	1.96E-02	2.37E-02	NA	NA	NA	NA	NA	NA	NA	NA
2010	5.72	3.79E-02	2.00E-02	2.22E-02	NA	NA	NA	NA	NA	NA	NA	NA
2011	5.77	3.00E-02	1.34E-02	1.65E-02	NA	NA	NA	NA	NA	NA	NA	NA

Table 4.7 Average Annual SO_4, Ca, and Mg Release Rates ($mmol \cdot kg^{-1} \cdot wk^{-1}$) (Page 4 of 6).

Year	Norite (0.5-2.0 mm)				Diatreme (0.5-2.0 mm)				Mudstone (0.5-2.0 mm)			
	min pH	SO_4	Ca	Mg	min pH	SO_4	Ca	Mg	min pH	SO_4	Ca	Mg
1993	6.56	1.38E-01	8.81E-02	9.37E-02	6.68	2.46E-01	1.03E-01	1.17E-01	5.42	1.76E+00	1.82E+00	1.53E+00
1994	5.41	1.72E-01	6.53E-02	7.71E-02	7.04	8.80E-02	1.10E-01	1.27E-01	6.78	2.51E+00	1.34E+00	1.02E+00
1995	5.38	1.13E-01	3.28E-02	6.31E-02	7.22	5.45E-02	1.29E-01	1.78E-01	6.80	9.73E-01	6.05E-01	4.49E-01
1996	5.30	1.17E-01	3.02E-02	6.51E-02	7.61	5.44E-02	1.18E-01	1.35E-01	7.27	6.64E-01	4.24E-01	3.13E-01
1997	5.17	1.38E-01	3.19E-02	7.74E-02	7.30	6.07E-02	1.24E-01	1.14E-01	6.67	5.67E-01	3.77E-01	2.69E-01
1998	5.09	1.30E-01	2.85E-02	7.40E-02	6.96	7.48E-02	9.05E-02	8.27E-02	3.23	8.65E-01	4.50E-01	3.23E-01
1999	4.98	1.24E-01	2.64E-02	7.35E-02	6.95	8.11E-02	5.46E-02	6.08E-02	2.21	2.32E+00	3.47E-01	2.32E-01
2000	4.89	1.22E-01	2.62E-02	7.34E-02	6.64	7.02E-02	3.25E-02	4.17E-02	2.58	1.01E+00	6.98E-02	6.28E-02
2001	4.80	1.31E-01	2.65E-02	7.68E-02	6.17	6.78E-02	2.24E-02	2.98E-02	NA	NA	NA	NA
2002	4.76	1.32E-01	2.51E-02	7.74E-02	6.02	6.77E-02	1.47E-02	2.23E-02	NA	NA	NA	NA
2003	4.69	1.21E-01	2.42E-02	7.57E-02	5.90	6.34E-02	1.04E-02	1.55E-02	NA	NA	NA	NA
2004	4.72	1.20E-01	2.26E-02	7.29E-02	5.69	6.46E-02	7.08E-03	1.07E-02	NA	NA	NA	NA
2005	4.72	1.16E-01	1.98E-02	6.39E-02	5.53	6.42E-02	4.69E-03	7.60E-03	NA	NA	NA	NA
2006	4.78	9.82E-02	1.76E-02	5.69E-02	5.70	6.35E-02	3.76E-03	5.58E-03	NA	NA	NA	NA
2007	4.71	9.07E-02	1.54E-02	4.29E-02	5.56	6.47E-02	2.62E-03	4.50E-03	NA	NA	NA	NA
2008	4.78	8.91E-02	1.31E-02	3.82E-02	5.54	7.14E-02	2.33E-03	4.14E-03	NA	NA	NA	NA
2009	4.67	8.40E-02	1.50E-02	4.89E-02	5.51	7.45E-02	2.25E-03	3.72E-03	NA	NA	NA	NA
2010	4.73	8.23E-02	1.59E-02	5.33E-02	5.38	7.67E-02	2.54E-03	3.29E-03	NA	NA	NA	NA
2011	4.73	9.19E-02	1.46E-02	4.99E-02	5.48	8.28E-02	2.16E-03	2.87E-03	NA	NA	NA	NA

Table 4.7 Average Annual SO_4, Ca, and Mg Release Rates ($mmol \cdot kg^{-1} \cdot wk^{-1}$) (Page 5 of 6).

Year	Norite (2.0-6.35 mm)				Diatreme (2.0-6.35 mm)				Mudstone (2.0-6.35 mm)			
	min pH	SO_4	Ca	Mg	min pH	SO_4	Ca	Mg	min pH	SO_4	Ca	Mg
1993	6.35	7.59E-02	3.12E-02	3.84E-02	6.32	2.02E-01	3.41E-02	9.15E-02	3.76	2.15E+00	1.14E+00	7.19E-01
1994	5.37	5.09E-02	2.17E-02	2.47E-02	6.63	1.89E-01	5.14E-02	1.11E-01	3.02	3.67E+00	1.55E+00	1.27E+00
1995	5.24	4.55E-02	1.76E-02	2.26E-02	6.53	1.13E-01	4.63E-02	1.10E-01	2.59	2.03E+00	6.38E-01	5.76E-01
1996	5.42	4.74E-02	1.70E-02	2.48E-02	7.36	9.64E-02	4.12E-02	1.07E-01	2.61	1.66E+00	3.76E-01	3.62E-01
1997	5.27	5.09E-02	1.69E-02	2.60E-02	7.09	8.34E-02	3.70E-02	8.44E-02	NA	NA	NA	NA
1998	4.99	5.03E-02	1.39E-02	2.34E-02	6.87	8.65E-02	3.05E-02	7.17E-02	NA	NA	NA	NA
1999	4.82	4.27E-02	1.10E-02	2.02E-02	6.42	8.05E-02	2.50E-02	5.29E-02	NA	NA	NA	NA
2000	4.77	4.34E-02	1.24E-02	2.23E-02	6.33	7.90E-02	2.26E-02	4.10E-02	NA	NA	NA	NA
2001	4.80	4.80E-02	1.18E-02	2.18E-02	5.89	9.28E-02	2.50E-02	3.72E-02	NA	NA	NA	NA
2002	4.82	3.75E-02	8.87E-03	1.82E-02	5.67	9.13E-02	1.88E-02	2.65E-02	NA	NA	NA	NA
2003	4.80	3.60E-02	9.74E-03	1.87E-02	5.30	9.32E-02	1.42E-02	1.83E-02	NA	NA	NA	NA
2004	4.82	3.45E-02	8.73E-03	1.76E-02	5.12	8.59E-02	9.70E-03	1.23E-02	NA	NA	NA	NA
2005	4.81	3.45E-02	7.86E-03	1.61E-02	4.98	1.03E-01	8.88E-03	1.07E-02	NA	NA	NA	NA
2006	4.90	2.85E-02	7.09E-03	1.41E-02	4.85	8.03E-02	5.99E-03	6.44E-03	NA	NA	NA	NA
2007	4.85	2.78E-02	6.62E-03	1.39E-02	4.67	8.78E-02	5.21E-03	5.77E-03	NA	NA	NA	NA
2008	4.91	2.62E-02	5.85E-03	1.24E-02	4.20	8.71E-02	4.64E-03	4.64E-03	NA	NA	NA	NA
2009	4.81	2.71E-02	6.30E-03	1.32E-02	4.39	8.61E-02	4.47E-03	4.16E-03	NA	NA	NA	NA
2010	4.85	2.81E-02	6.99E-03	1.40E-02	4.00	9.24E-02	4.95E-03	4.69E-03	NA	NA	NA	NA
2011	4.82	3.11E-02	7.63E-03	1.45E-02	4.02	1.19E-01	5.23E-03	4.09E-03	NA	NA	NA	NA

Table 4.7 Average Annual SO_4, Ca, and Mg Release Rates ($mmol \cdot kg^{-1} \cdot wk^{-1}$) (Page 6 of 6).

Year	Norite (6.35-19 mm)				Diatreme (6.35-19 mm)				Mudstone (6.35-19 mm)			
	min pH	SO_4	Ca	Mg	min pH	SO_4	Ca	Mg	min pH	SO_4	Ca	Mg
1993	5.75	5.88E-02	2.34E-02	3.39E-02	NA	NA	NA	NA	3.77	1.09E+00	4.76E-01	4.01E-01
1994	5.83	2.10E-02	8.77E-03	9.84E-03	NA	NA	NA	NA	2.87	1.71E+00	5.40E-01	5.90E-01
1995	5.87	1.50E-02	7.32E-03	8.64E-03	NA	NA	NA	NA	3.05	6.44E-01	2.36E-01	2.20E-01
1996	5.74	1.46E-02	7.12E-03	9.85E-03	NA	NA	NA	NA	3.07	5.41E-01	1.91E-01	1.59E-01
1997	5.66	1.37E-02	7.38E-03	7.92E-03	NA	NA	NA	NA	NA	NA	NA	NA
1998	5.74	1.25E-02	5.65E-03	7.13E-03	NA	NA	NA	NA	NA	NA	NA	NA
1999	5.67	1.19E-02	4.86E-03	5.41E-03	NA	NA	NA	NA	NA	NA	NA	NA
2000	5.65	1.08E-02	4.56E-03	5.24E-03	NA	NA	NA	NA	NA	NA	NA	NA
2001	5.76	1.15E-02	4.66E-03	4.35E-03	NA	NA	NA	NA	NA	NA	NA	NA
2002	5.69	9.67E-03	3.84E-03	3.64E-03	NA	NA	NA	NA	NA	NA	NA	NA
2003	5.65	9.36E-03	4.41E-03	4.55E-03	NA	NA	NA	NA	NA	NA	NA	NA
2004	5.16	9.67E-03	4.00E-03	4.27E-03	NA	NA	NA	NA	NA	NA	NA	NA
2005	5.46	8.77E-03	3.32E-03	4.00E-03	NA	NA	NA	NA	NA	NA	NA	NA
2006	5.74	7.65E-03	2.90E-03	3.18E-03	NA	NA	NA	NA	NA	NA	NA	NA
2007	5.13	8.37E-03	2.90E-03	3.96E-03	NA	NA	NA	NA	NA	NA	NA	NA
2008	5.62	8.20E-03	2.70E-03	3.90E-03	NA	NA	NA	NA	NA	NA	NA	NA
2009	5.47	7.26E-03	2.57E-03	3.70E-03	NA	NA	NA	NA	NA	NA	NA	NA
2010	5.47	7.52E-03	2.76E-03	3.92E-03	NA	NA	NA	NA	NA	NA	NA	NA
2011	5.61	8.56E-03	3.19E-03	4.92E-03	NA	NA	NA	NA	NA	NA	NA	NA

Table 5.1 Norite average SO_4 release rates.

Particle Size (mm)	average SO_4 release rate (mmol/kg/wk)	standard deviation	Rate Factor*
<0.053	9.53E-01	3.37E-01	65
0.053-0.149	7.29E-01	1.89E-01	50
0.149-0.5	6.06E-01	1.73E-01	42
0.5-2.0	1.31E-01	3.05E-02	9
2.0-6.35	4.81E-02	7.51E-03	3
6.35-19	1.46E-02	3.54E-03	1

* Rate factor is the factor increase of the average SO_4 release rate for each particle size to that of the largest particle size (6.35-19 mm).

Table 5.2 Tabulation of AMAX FL-6 prediction calculation.

size range (mm)	average (mm)	Calculated AMAX SO4 release rate (mmol/kg/wk/%S)	weight fraction AMAX	Weighted AMAX SO_4 release rate (mmol/kg/wk/%S)	Weighted AMAX SO_4 release rate $\times 2$ (mmol/kg/wk/%S)
152.4-304.8	228.6	9.49E-03	0.059	5.60E-04	1.12E-03
76.2-152.4	114.3	1.36E-02	0.135	1.84E-03	3.68E-03
38.1-76.2	57.15	1.95E-02	0.273	5.33E-03	1.07E-02
19.05-38.1	28.575	2.80E-02	0.192	5.37E-03	1.07E-02
6.35-19	12.675	4.27E-02	0.224	9.57E-03	1.91E-02
2.0-6.35	4.175	7.61E-02	0.061	4.64E-03	4.64E-03
0.5-2.0	1.25	1.42E-01	0.022	3.13E-03	3.13E-03
0.149-0.5	0.3245	2.87E-01	0.016	4.60E-03	4.60E-03
0.053-0.149	0.101	5.27E-01	0.008	4.22E-03	4.22E-03
< 0.053	0.0265	7.37E-01	0.007	5.16E-03	5.16E-03
			sum=	**4.44E-02**	**6.71E-02**

FIGURES

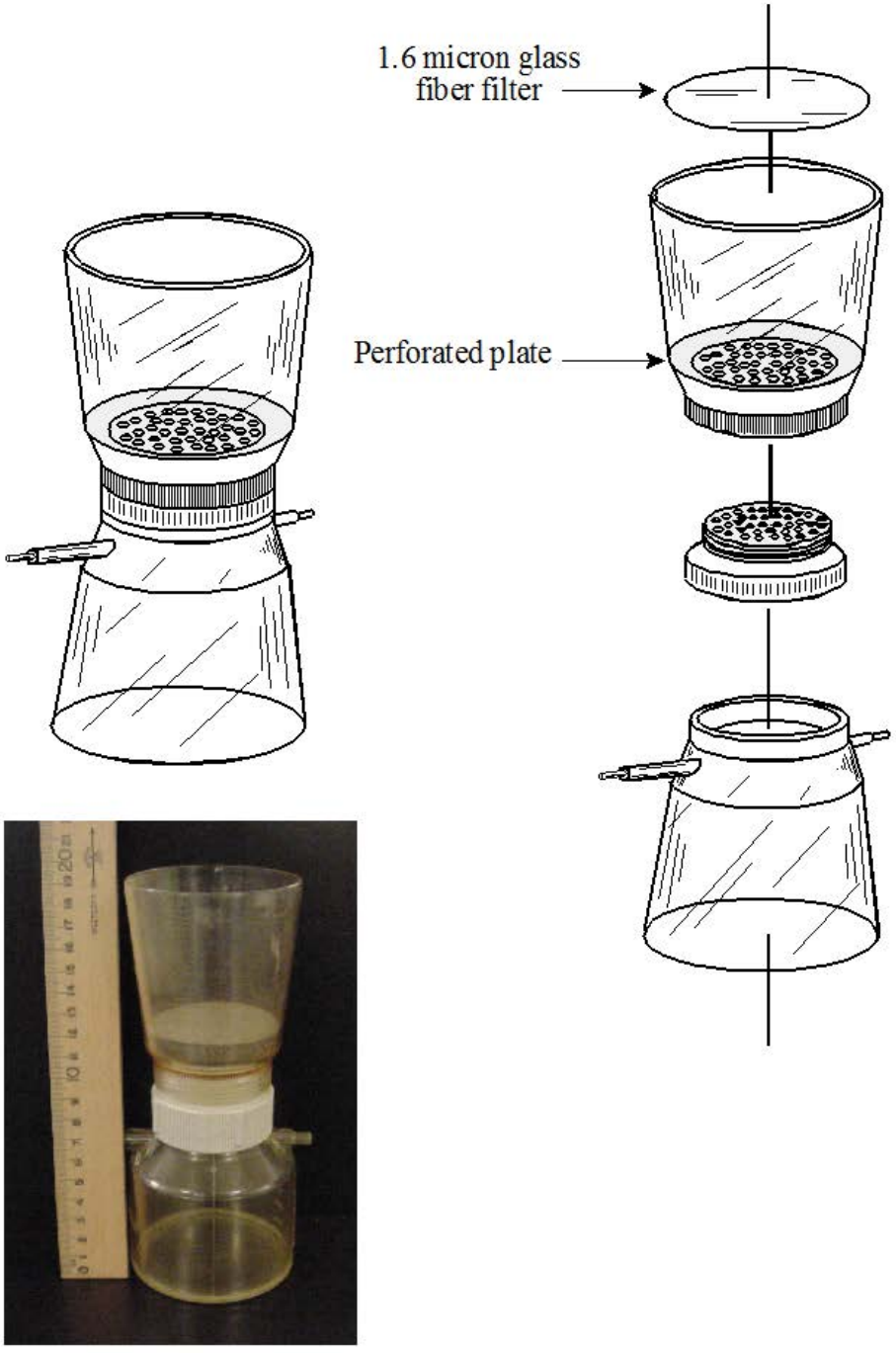

Figure 3.1A Schematic and image of reactor apparatus.

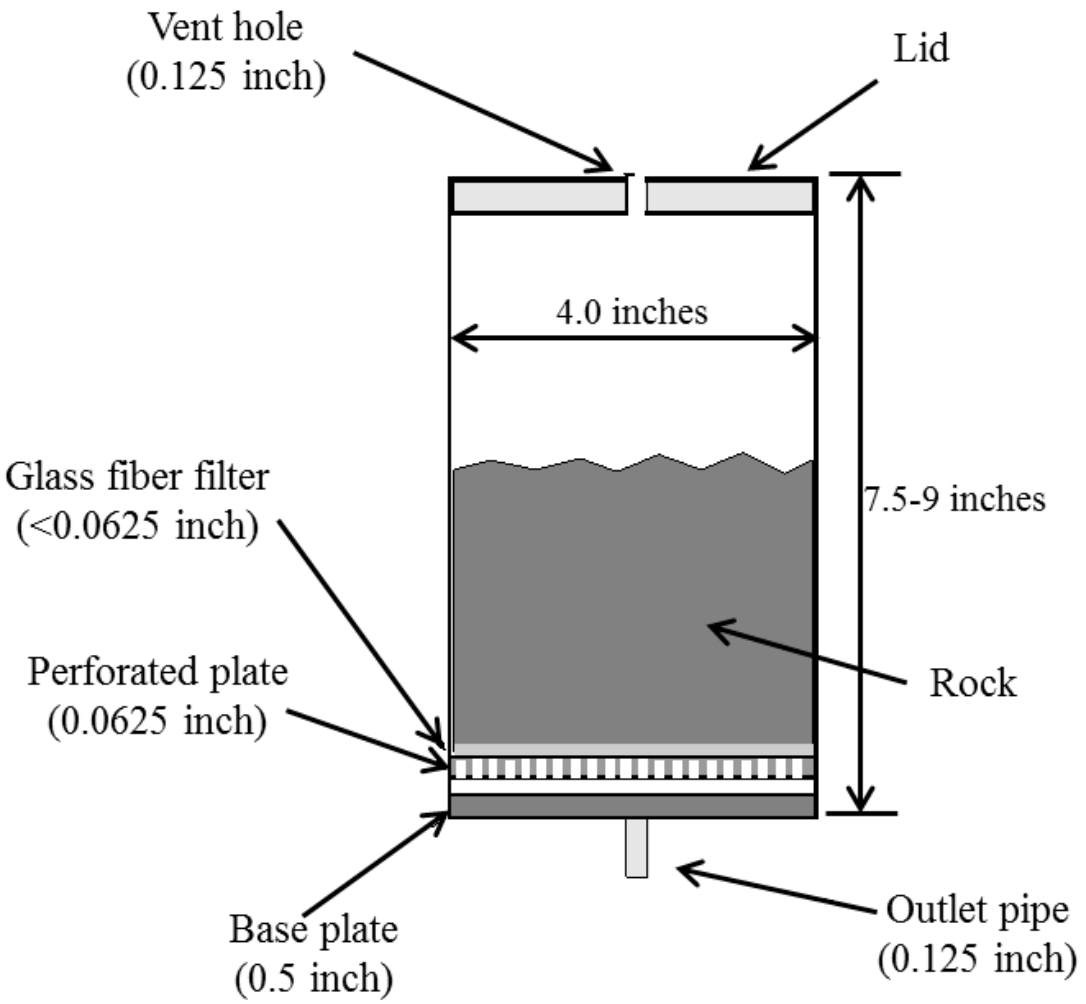

Figure 3.1B Schematic of humidity cell.

Norite: 2.0-6.35 mm sample

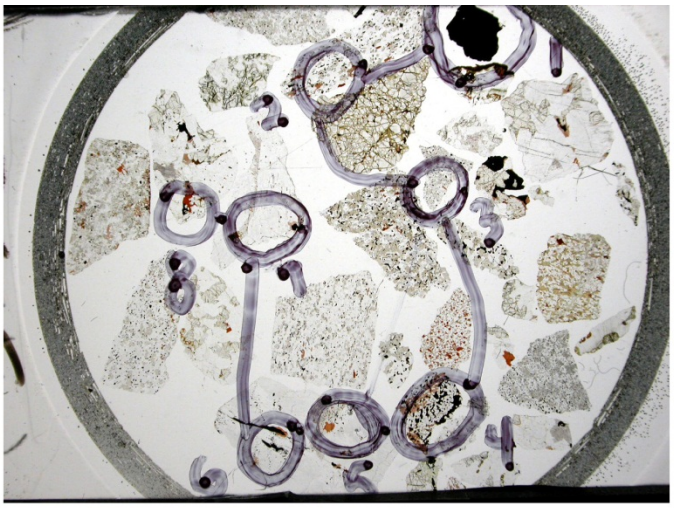

5 mm

Circle 1

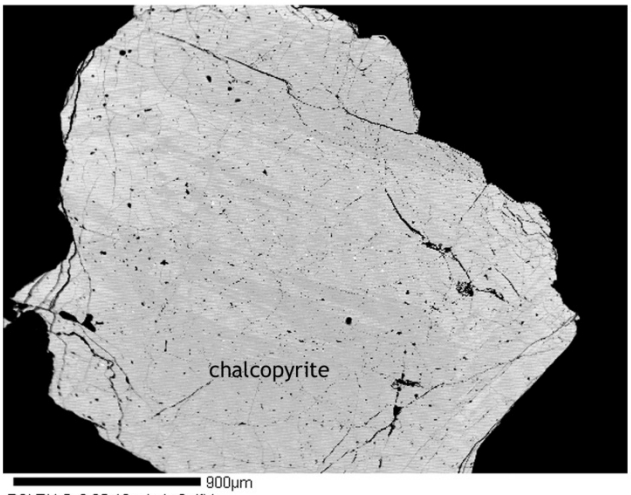

Circle 2

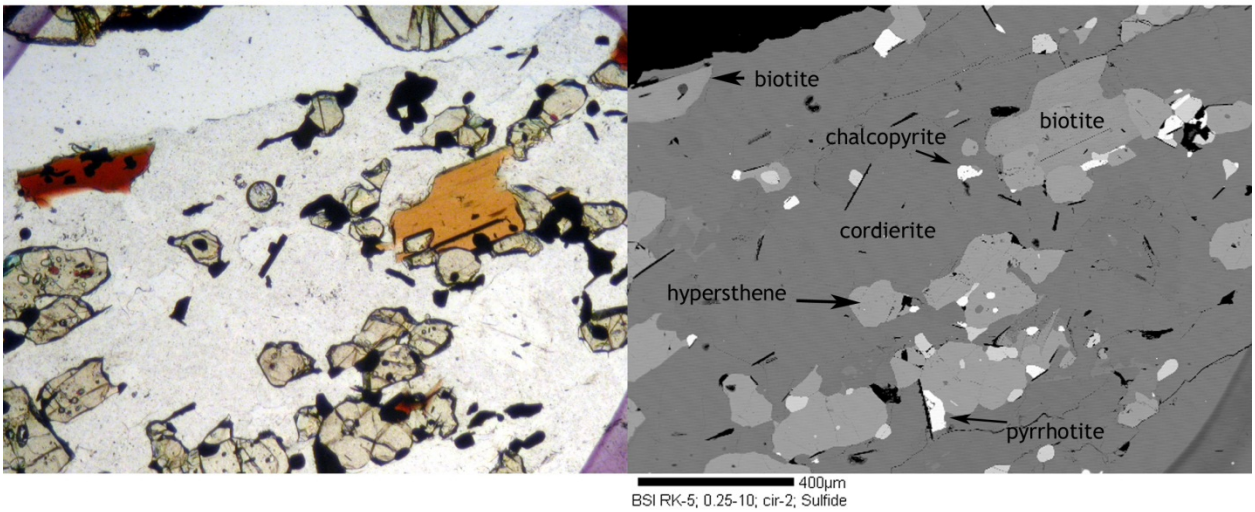

Figure 4.1A Norite images.

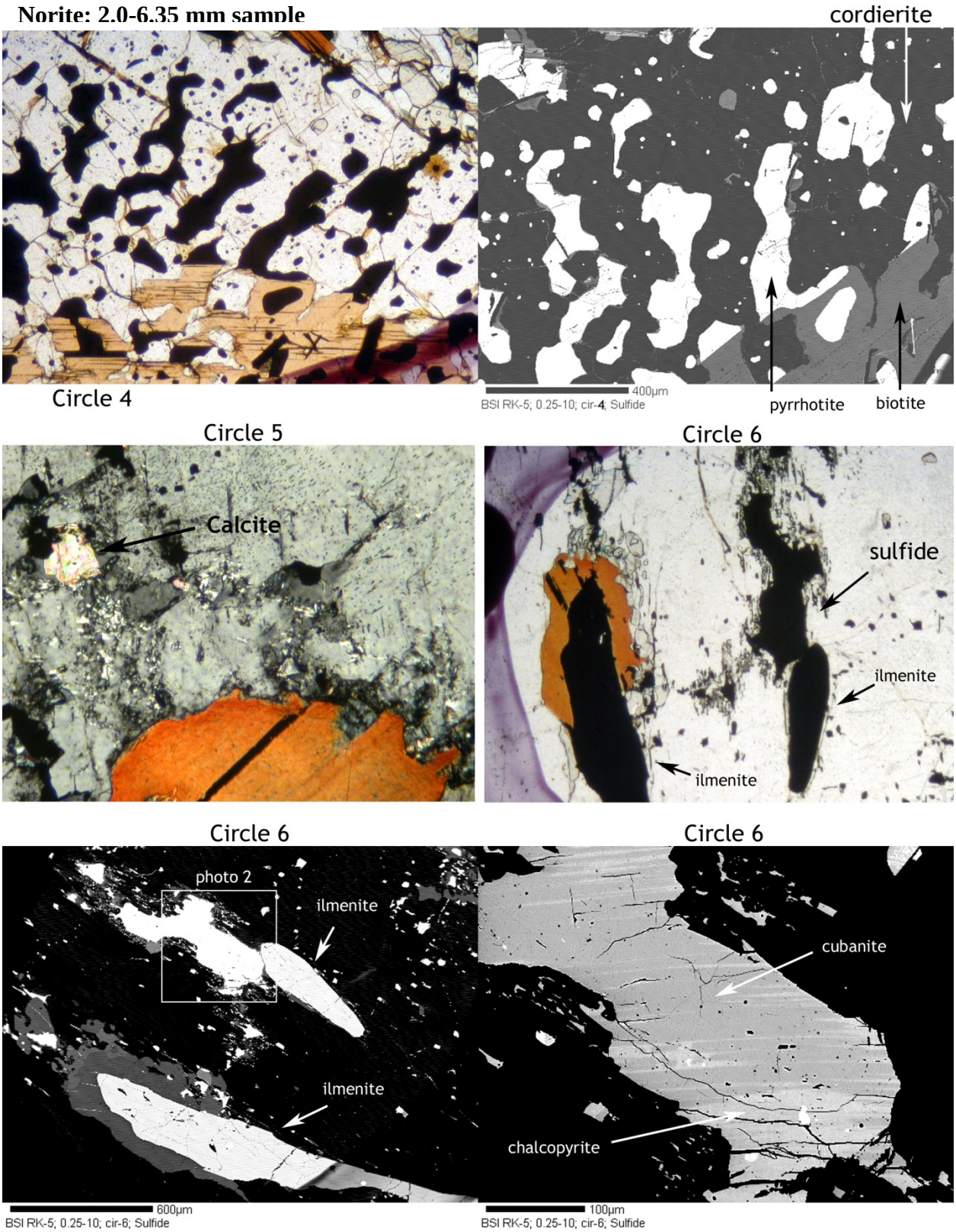

Figure 4.1B Norite images.

Norite: 2.0-6.35 mm sample

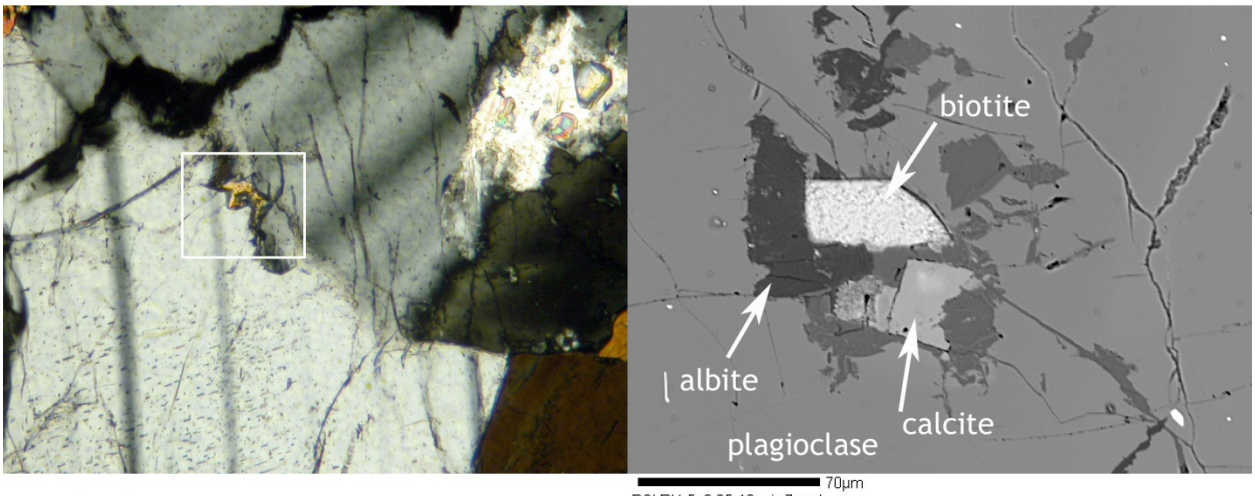

Circle 7

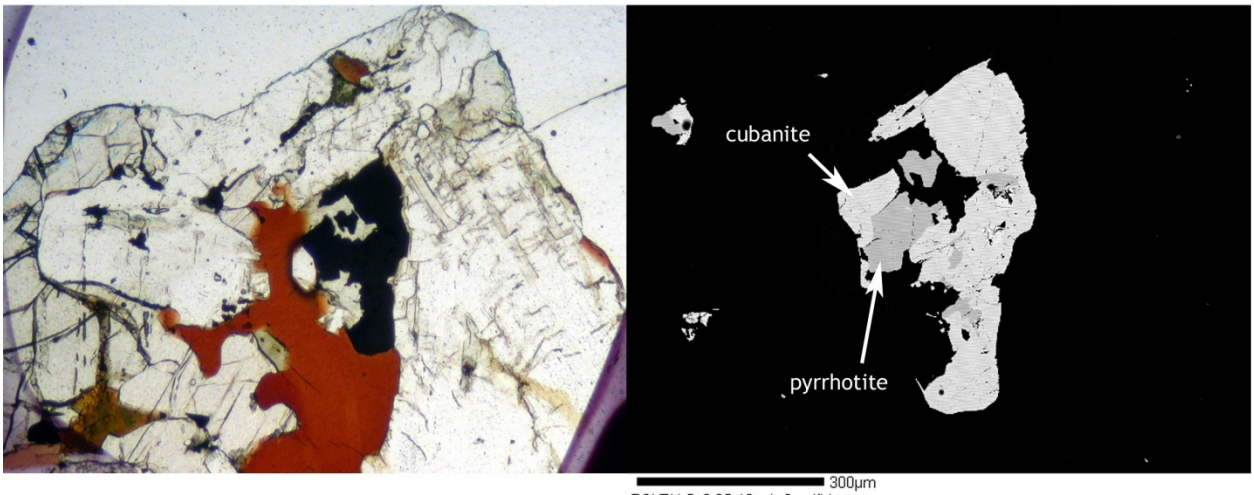

Circle 8

Figure 4.1C Norite images.

Diatreme 2.0-6.35 mm sample

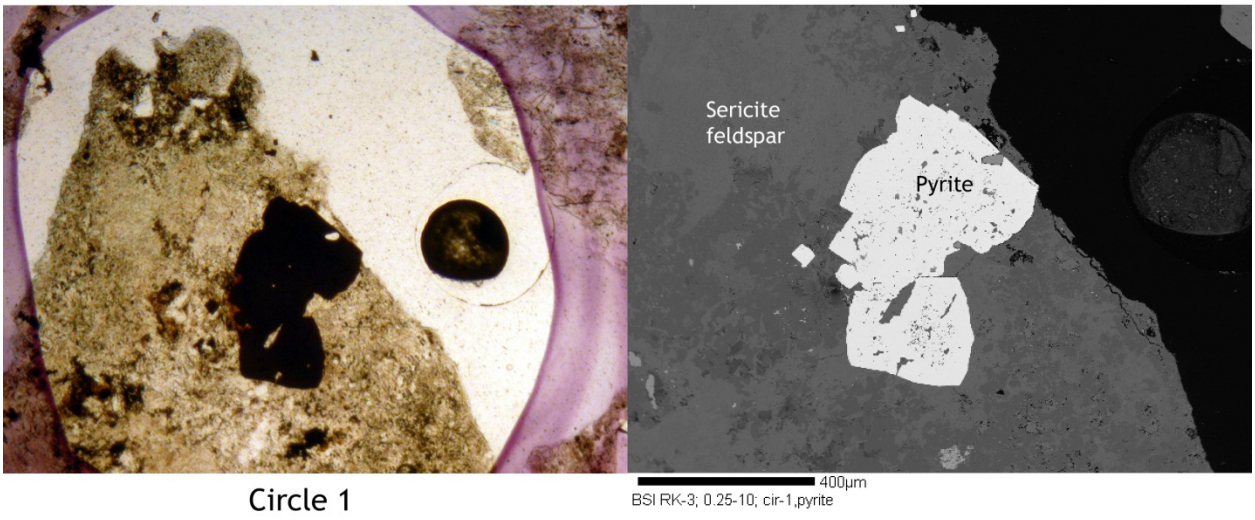

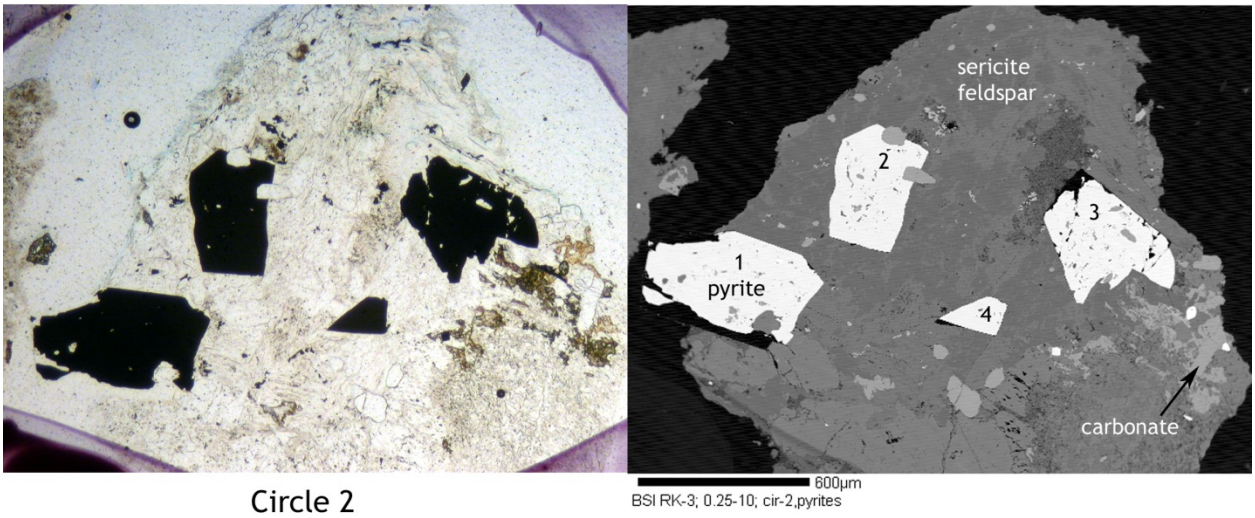

Figure 4.2A Diatreme images.

Diatreme 2.0-6.35 mm sample

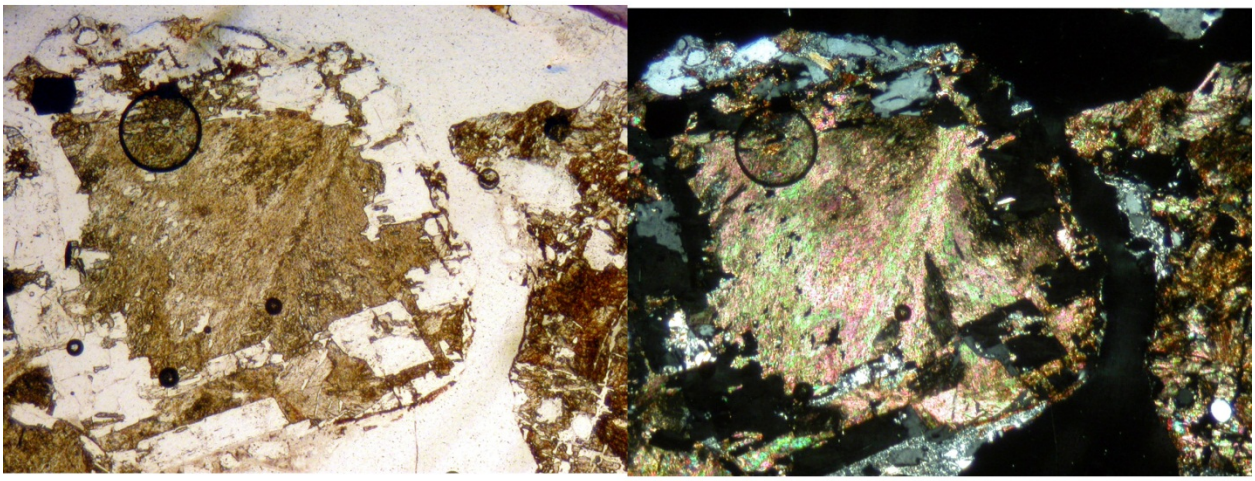

x-polarized light

Circle 3

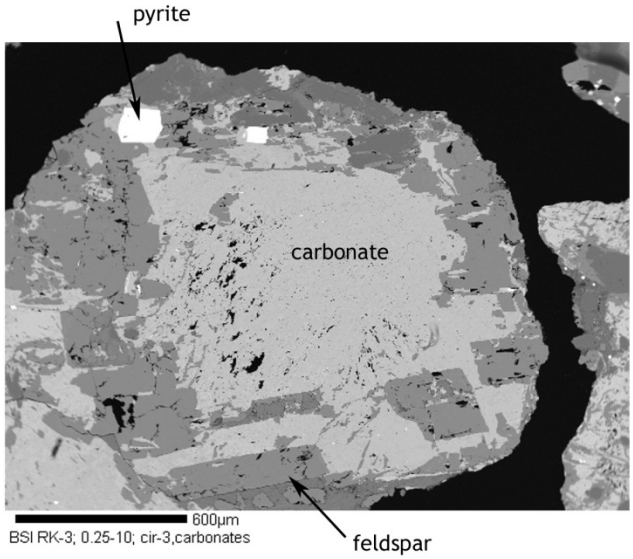

Figure 4.2B Diatreme images.

Diatreme 2.0-6.35 mm sample

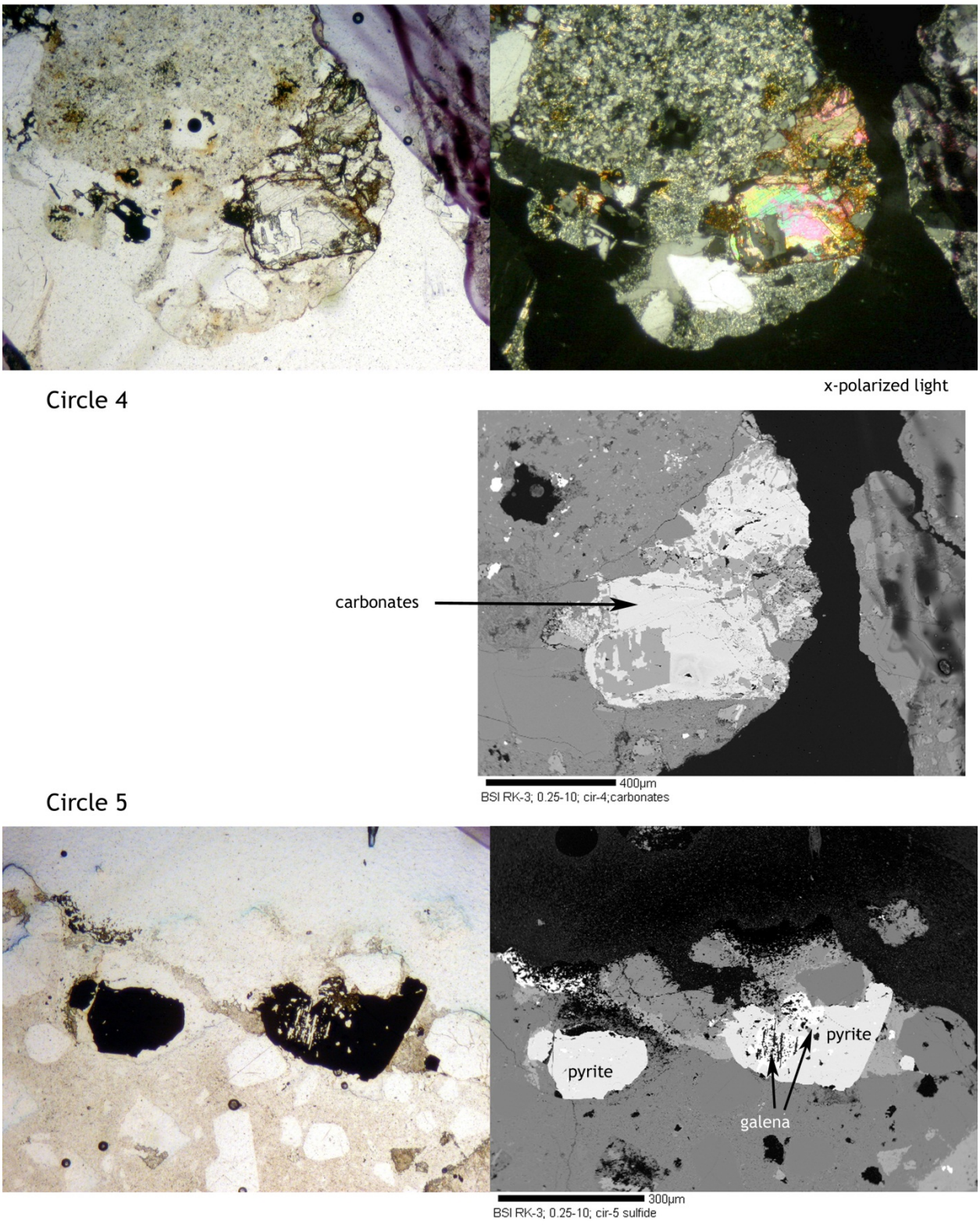

Figure 4.2C Diatreme images.

Mudstone 2.0-6.35 mm sample

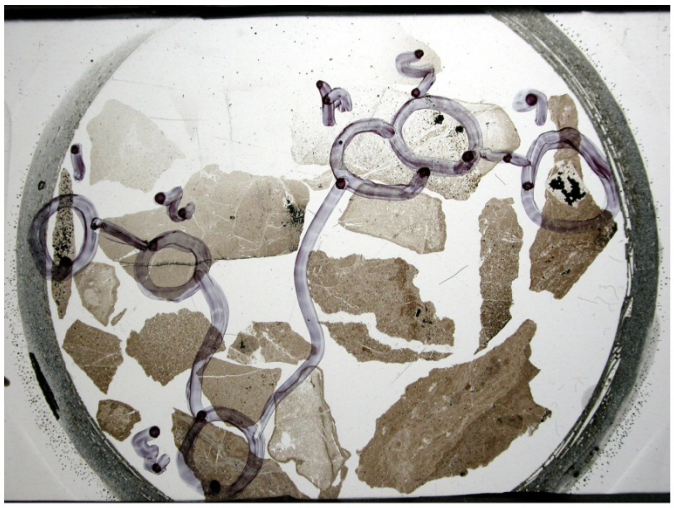

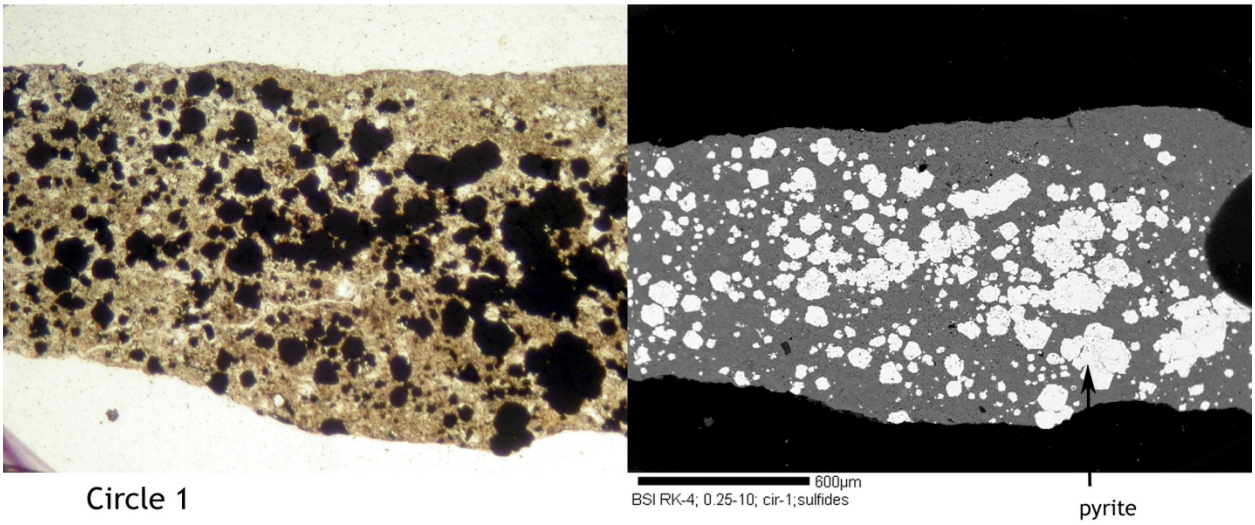

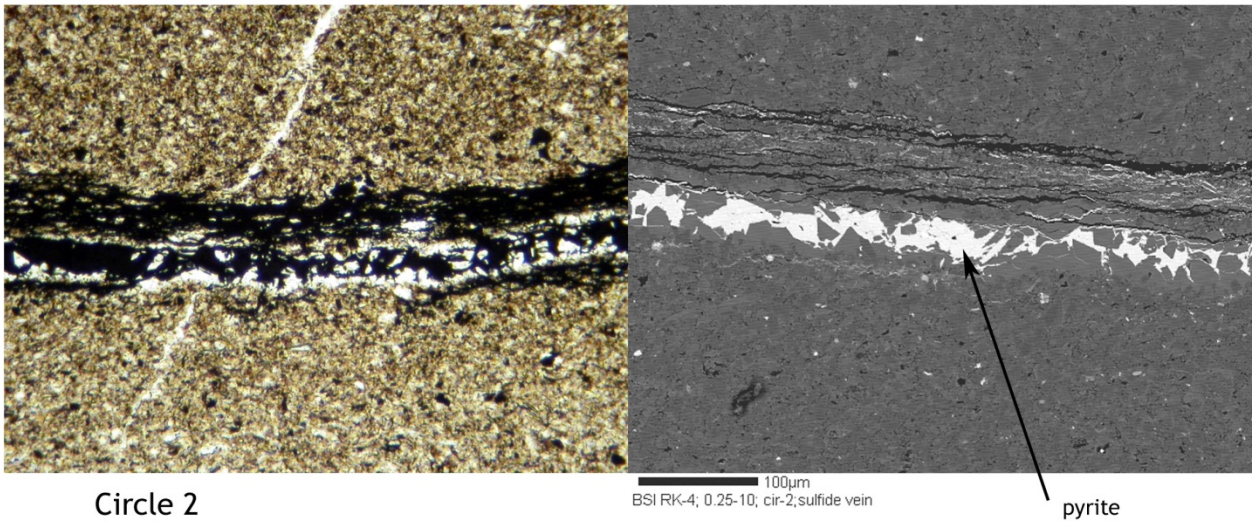

Figure 4.3A Mudstone images.

Mudstone 2.0-6.35 mm sample

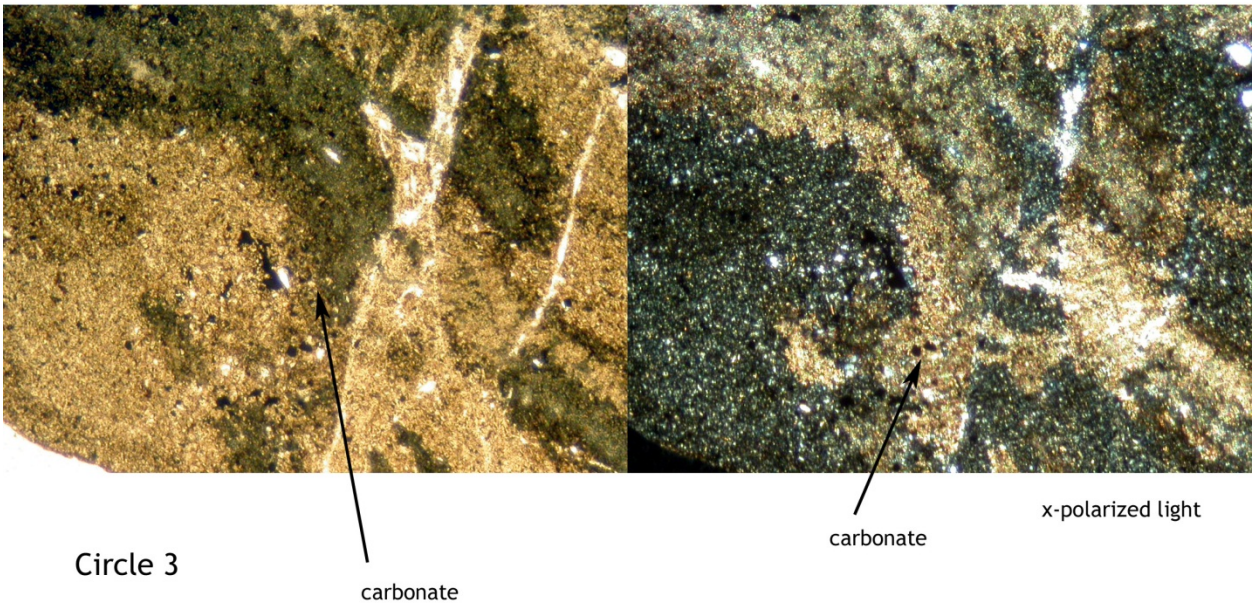

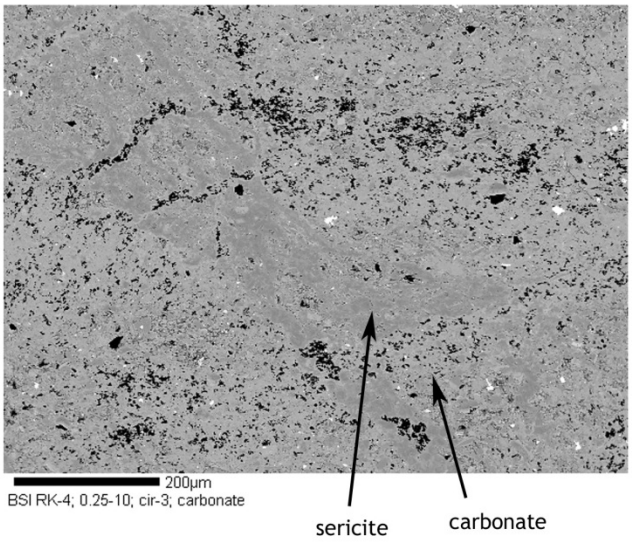

Figure 4.3B Mudstone images.

Mudstone 2.0-6.35 mm sample

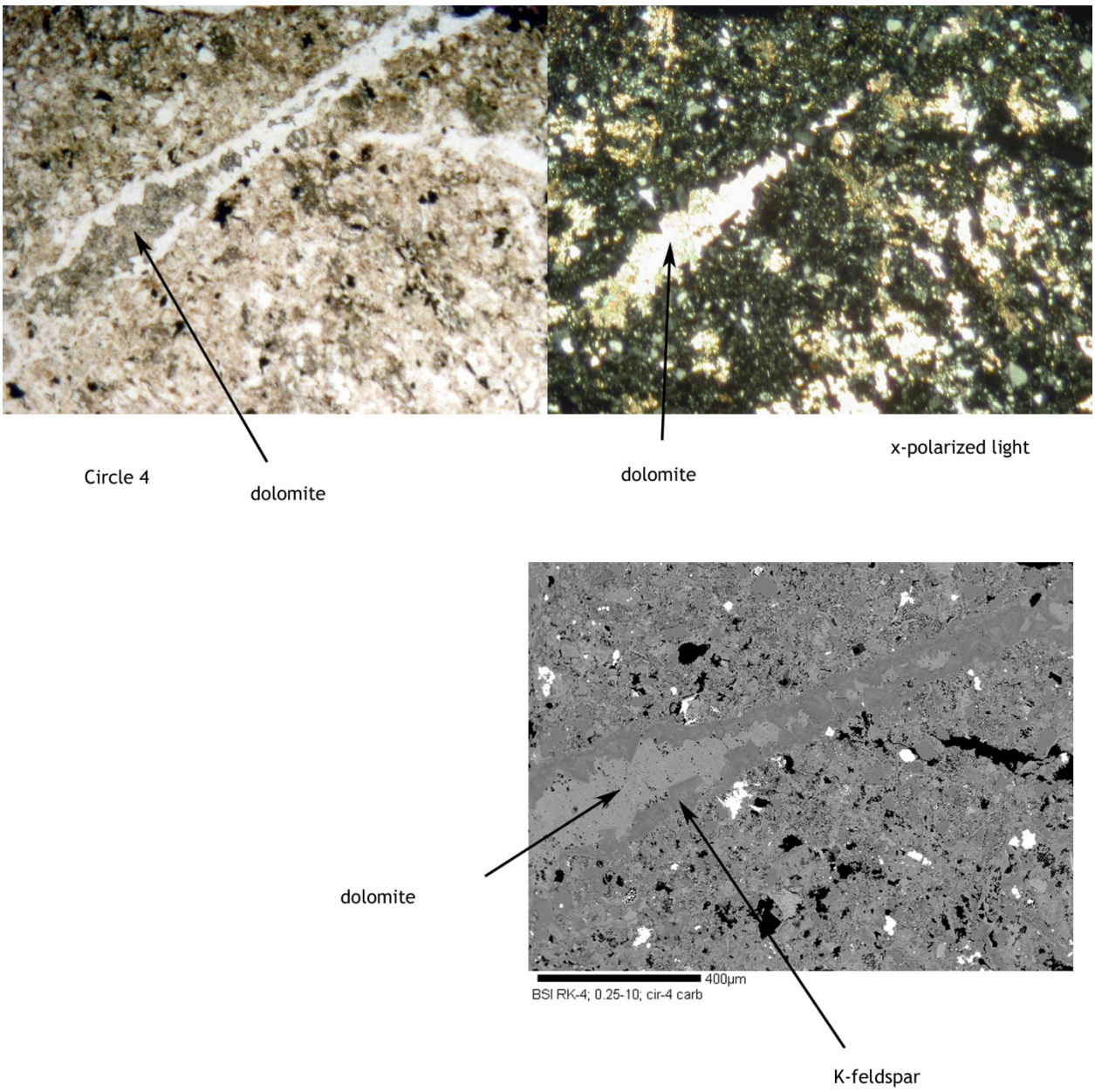

Figure 4.3C Mudstone images.

Mudstone 2.0-6.35 mm sample

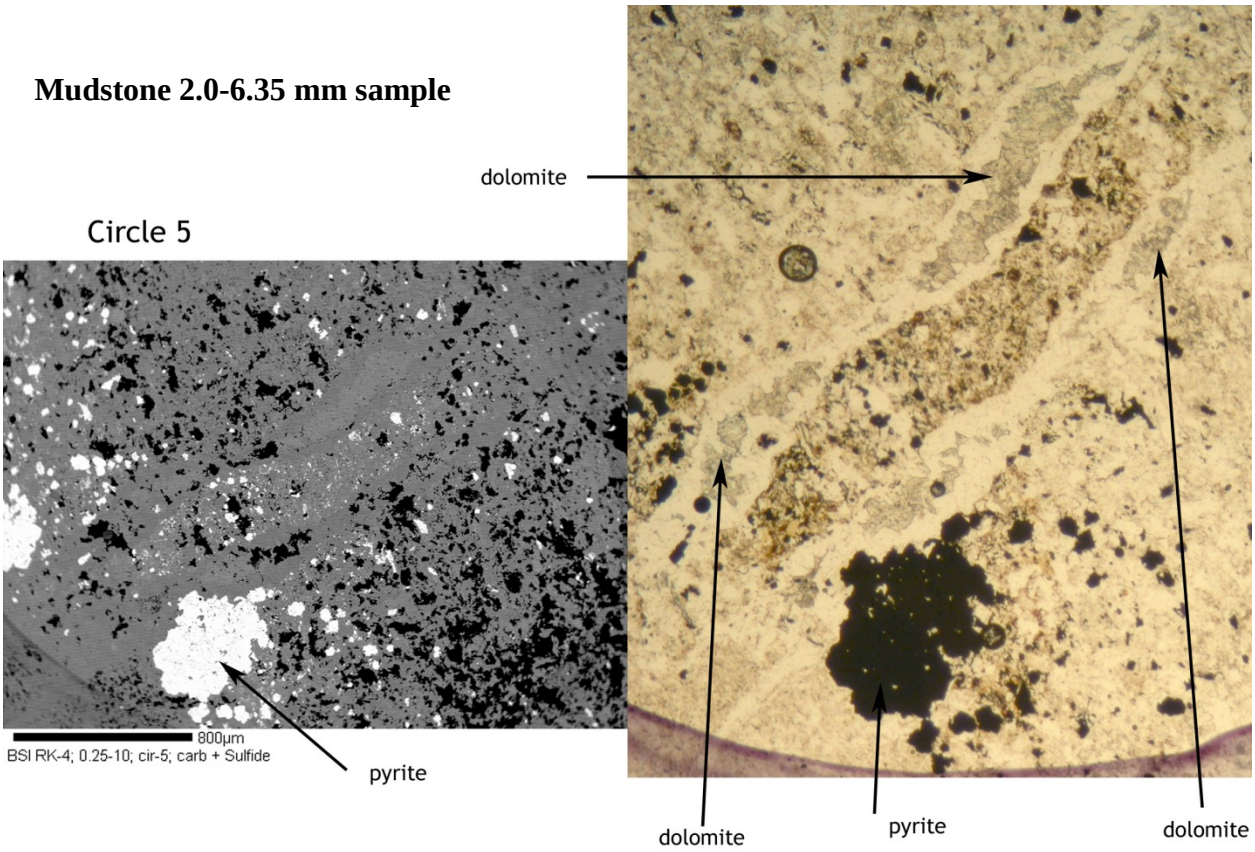

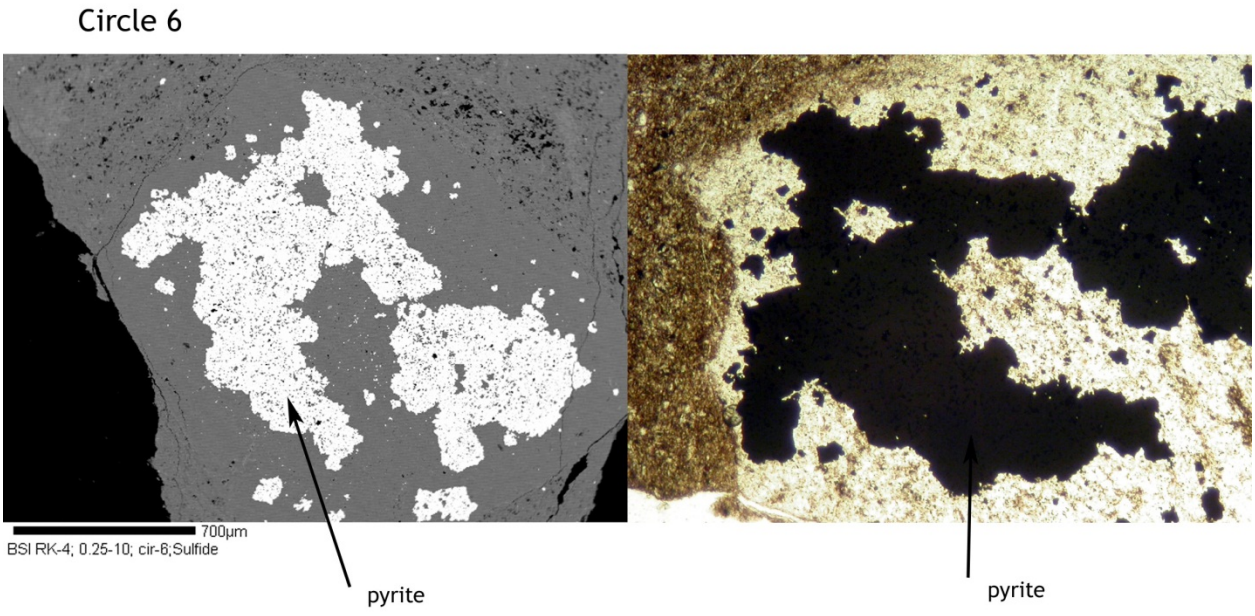

Figure 4.3D Mudstone images.

Mudstone

19 mm sample

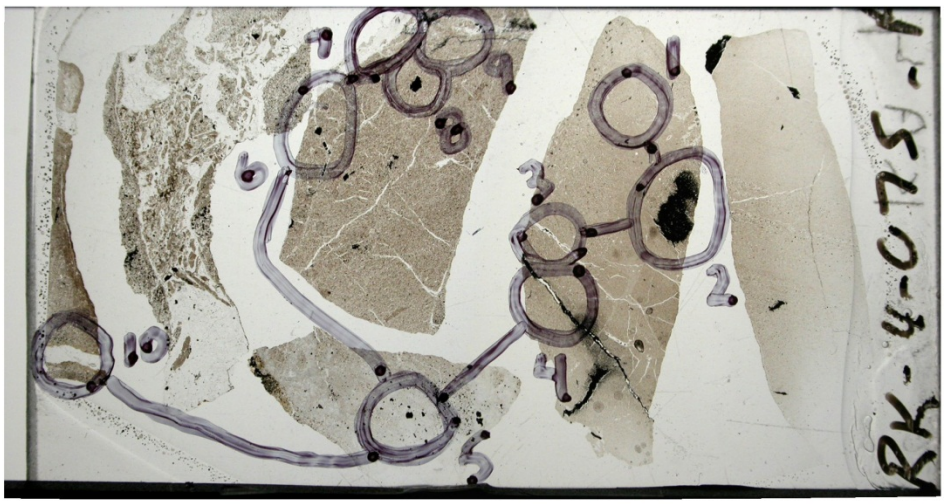

Circle 1

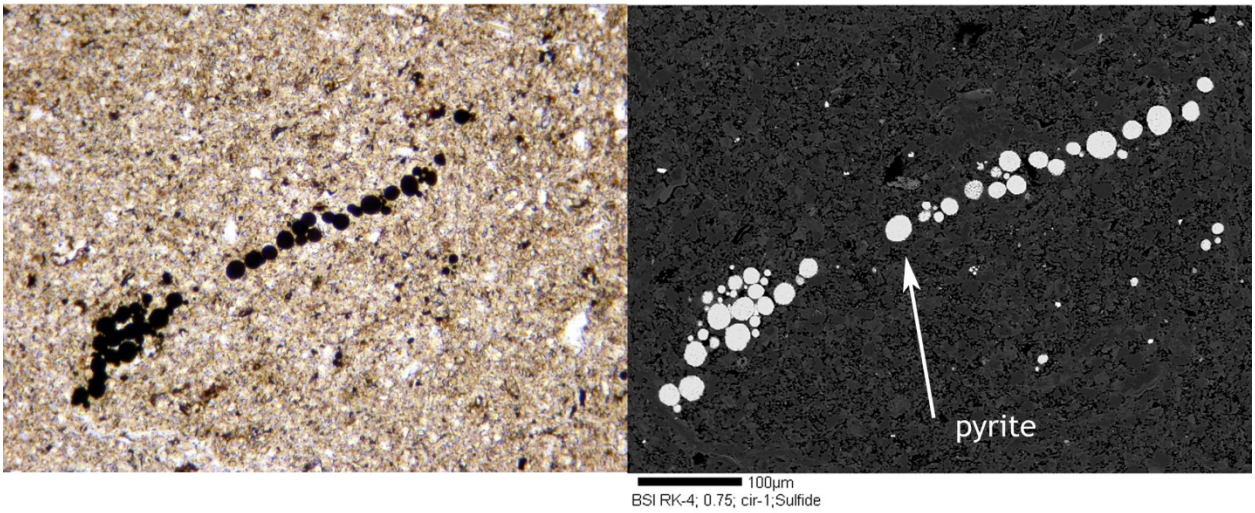

Circle 2

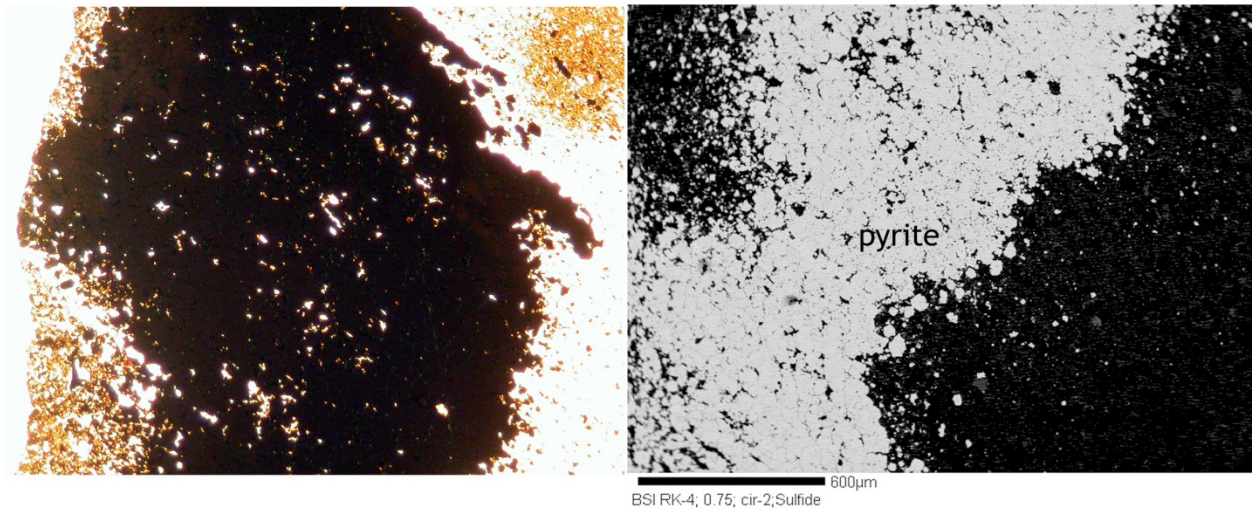

Figure 4.3E Mudstone images.

Mudstone 19 mm sample

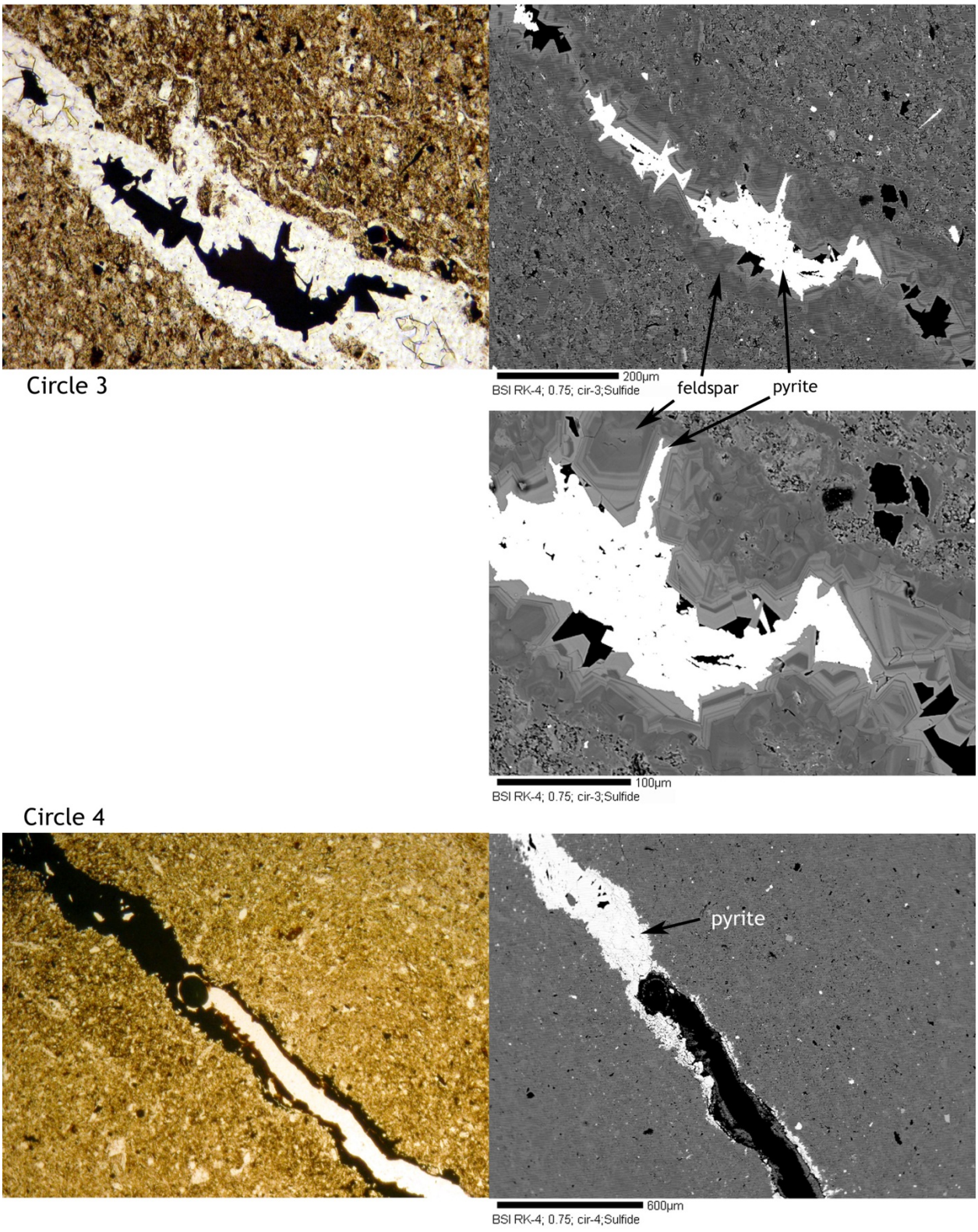

Figure 4.3F Mudstone images.

Mudstone 19 mm sample

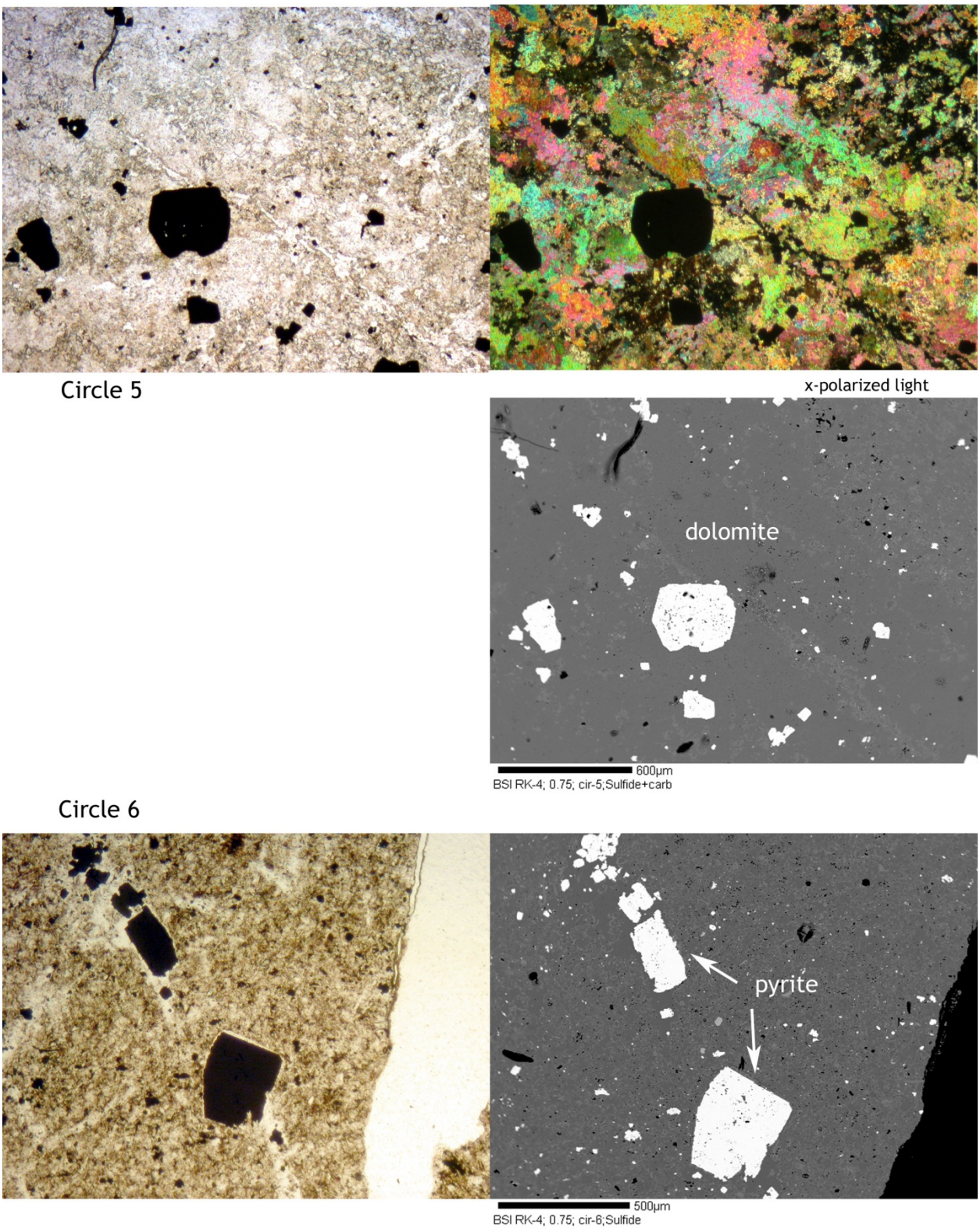

Figure 4.3G Mudstone images.

Mudstone 19 mm sample

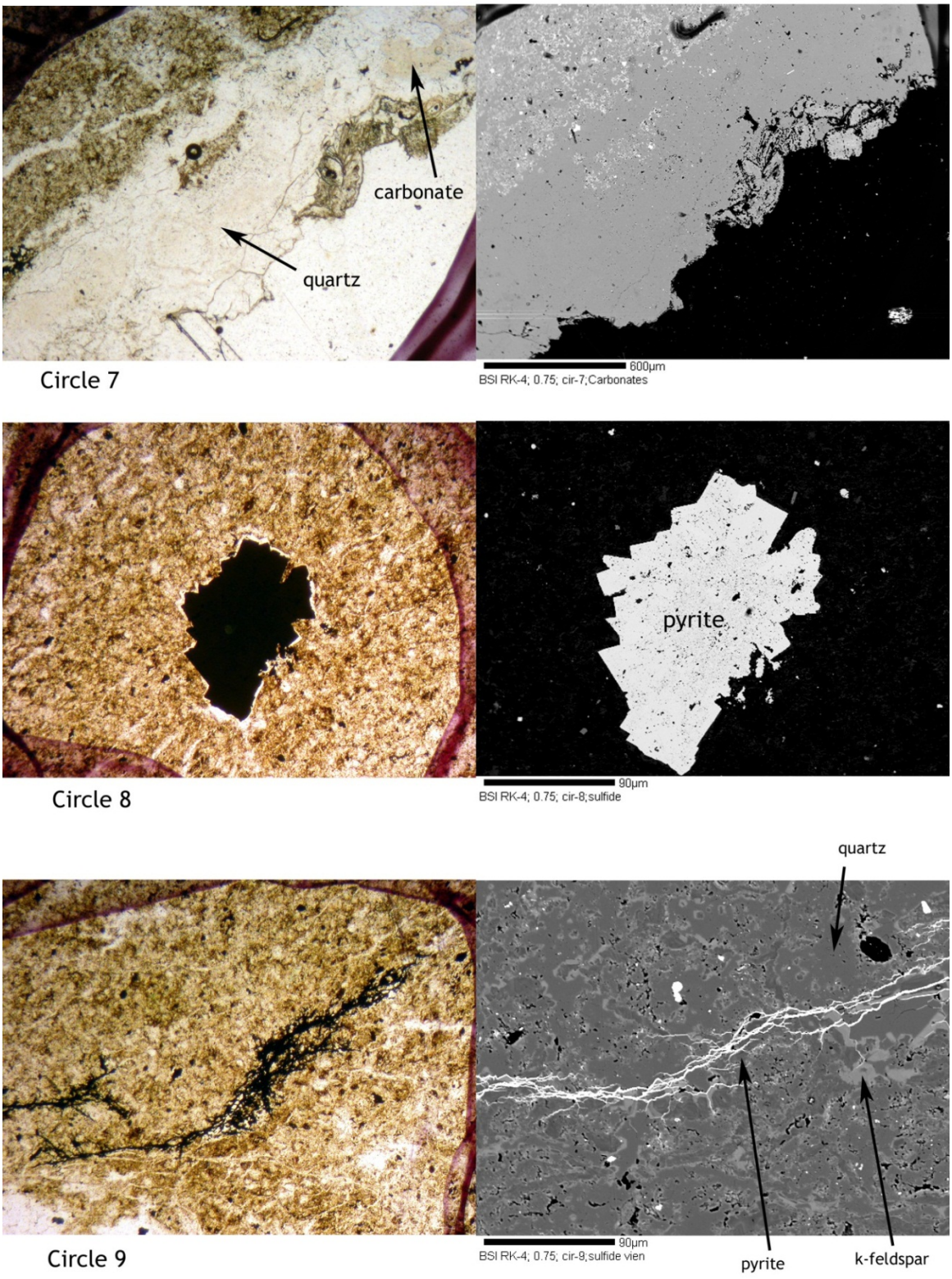

Figure 4.3H Mudstone images.

Mudstone 19 mm sample

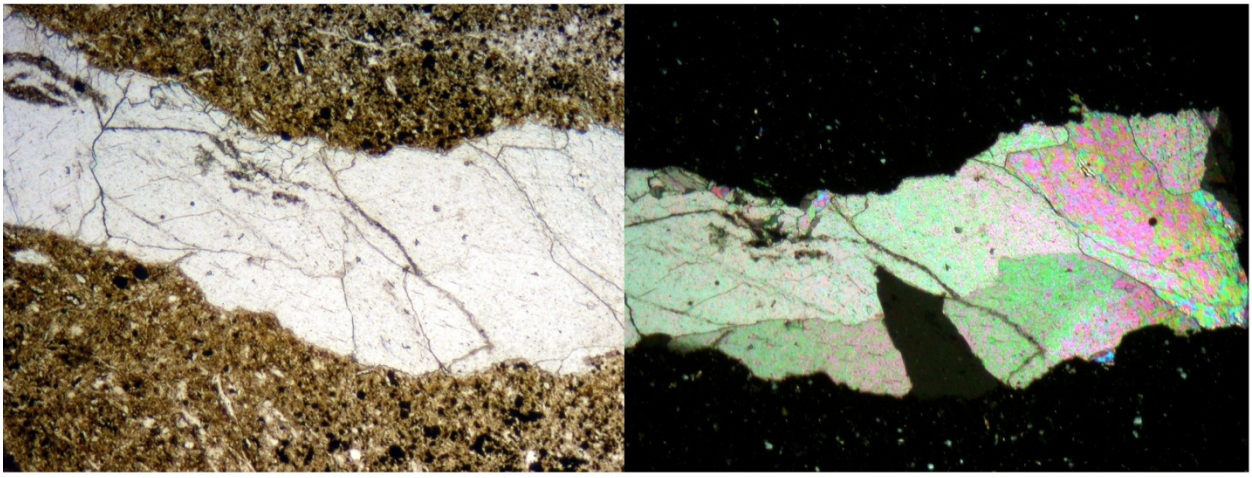

Circle 10

Dolomite

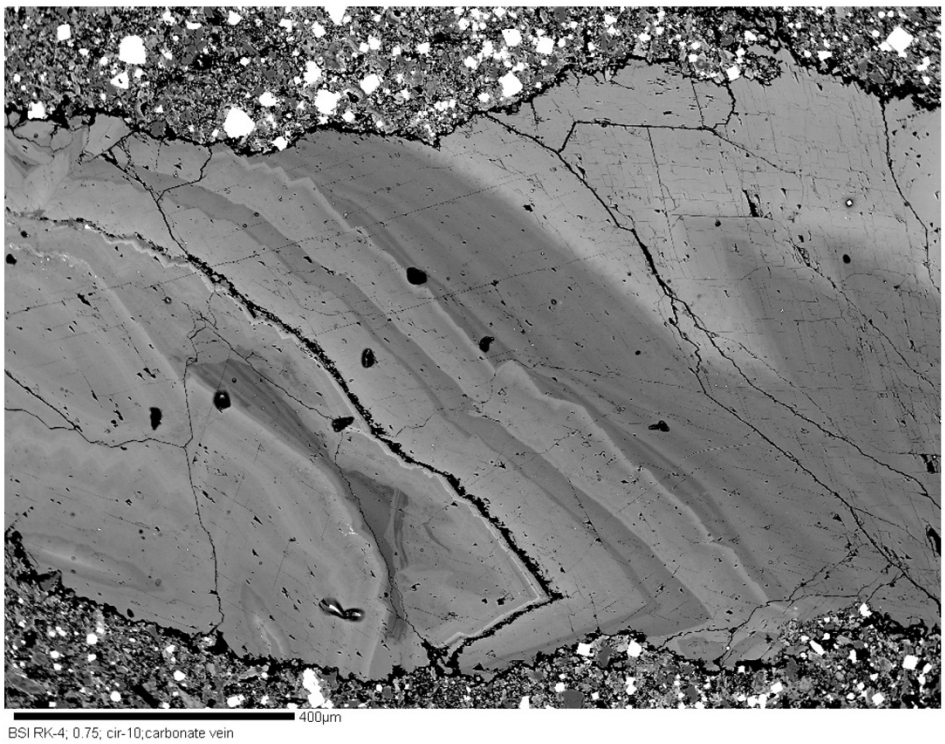

Figure 4.3I Mudstone images.

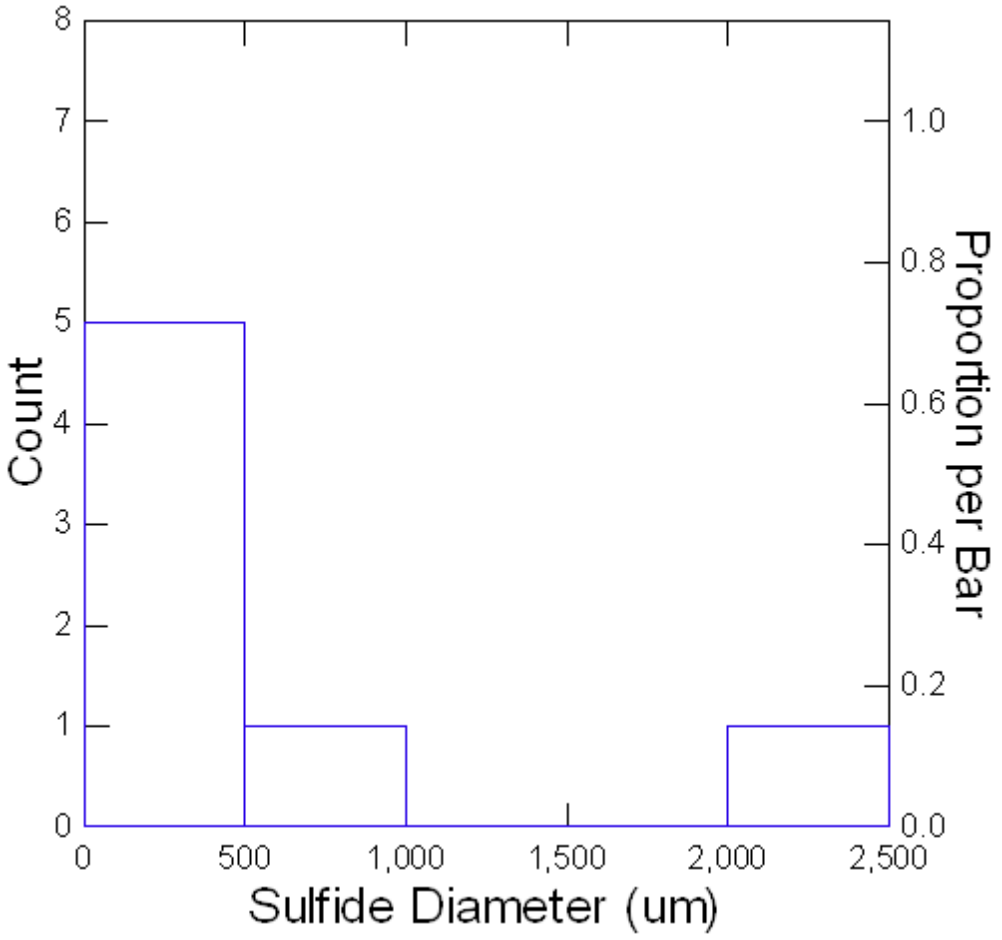

Figure 4.4 Norite sulfide mineral size distribution.

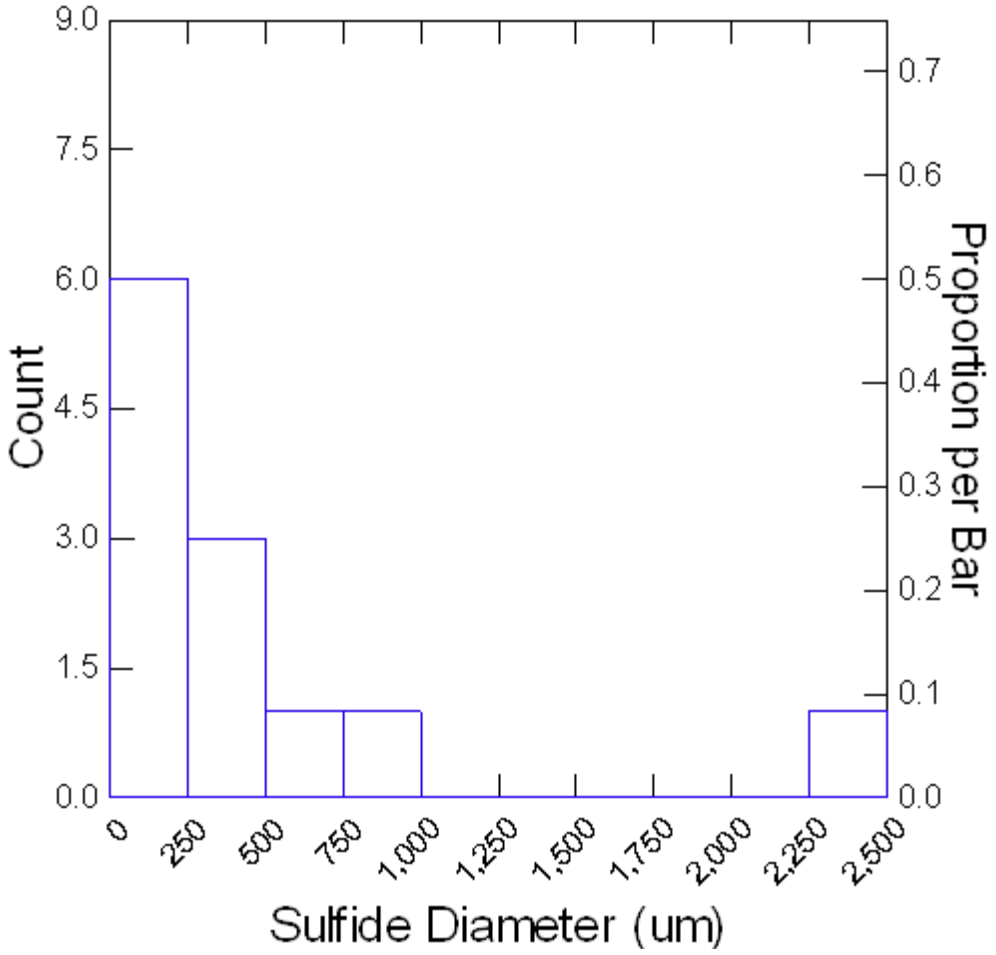

Figure 4.5 Mudstone sulfide mineral size distribution.

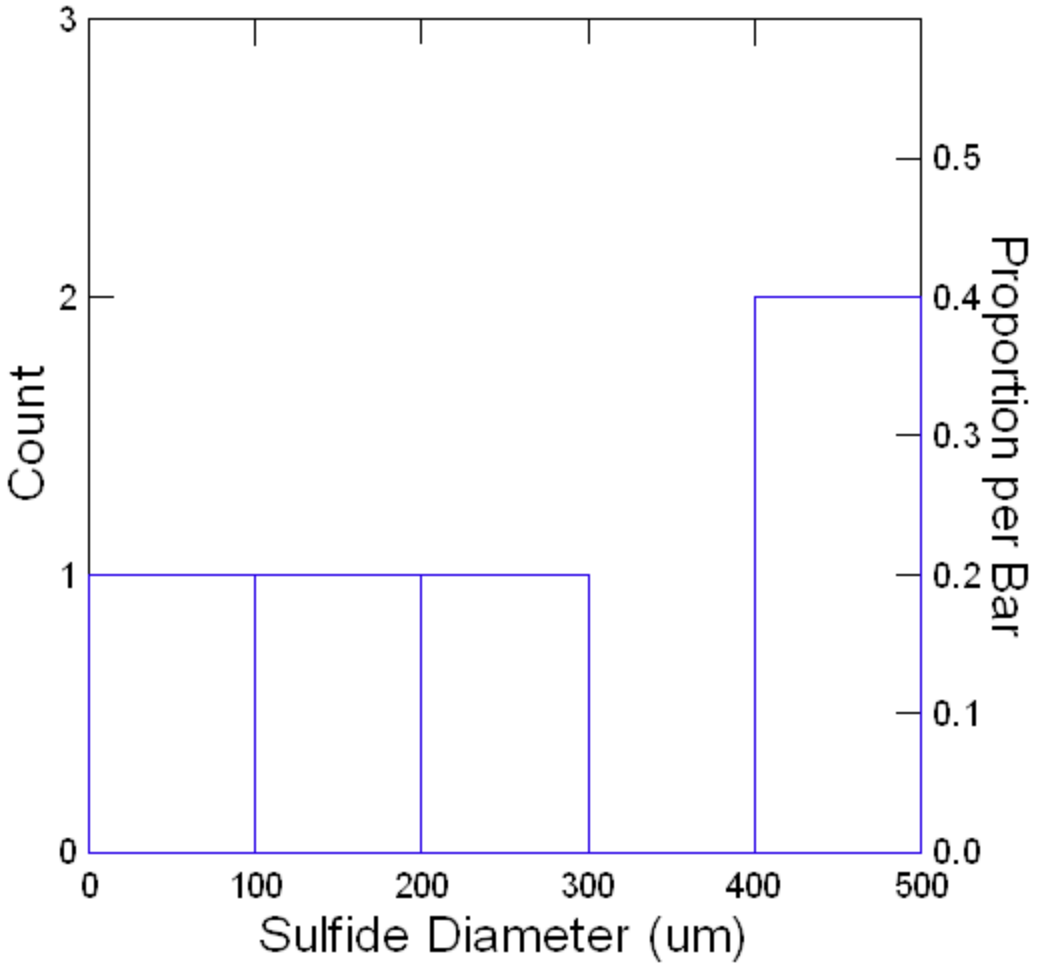

Figure 4.6 Diatreme sulfide mineral size distribution.

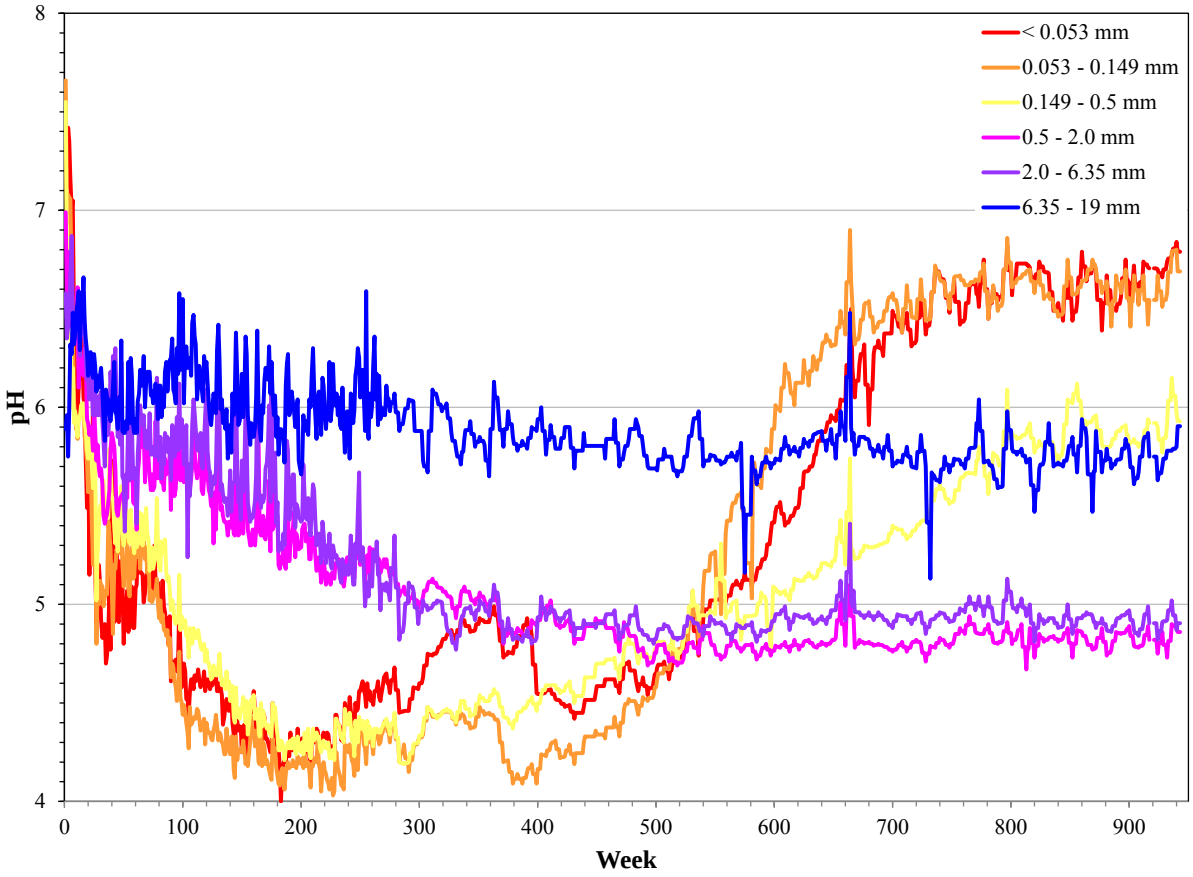

Figure 4.7 Norite pH time series plot.

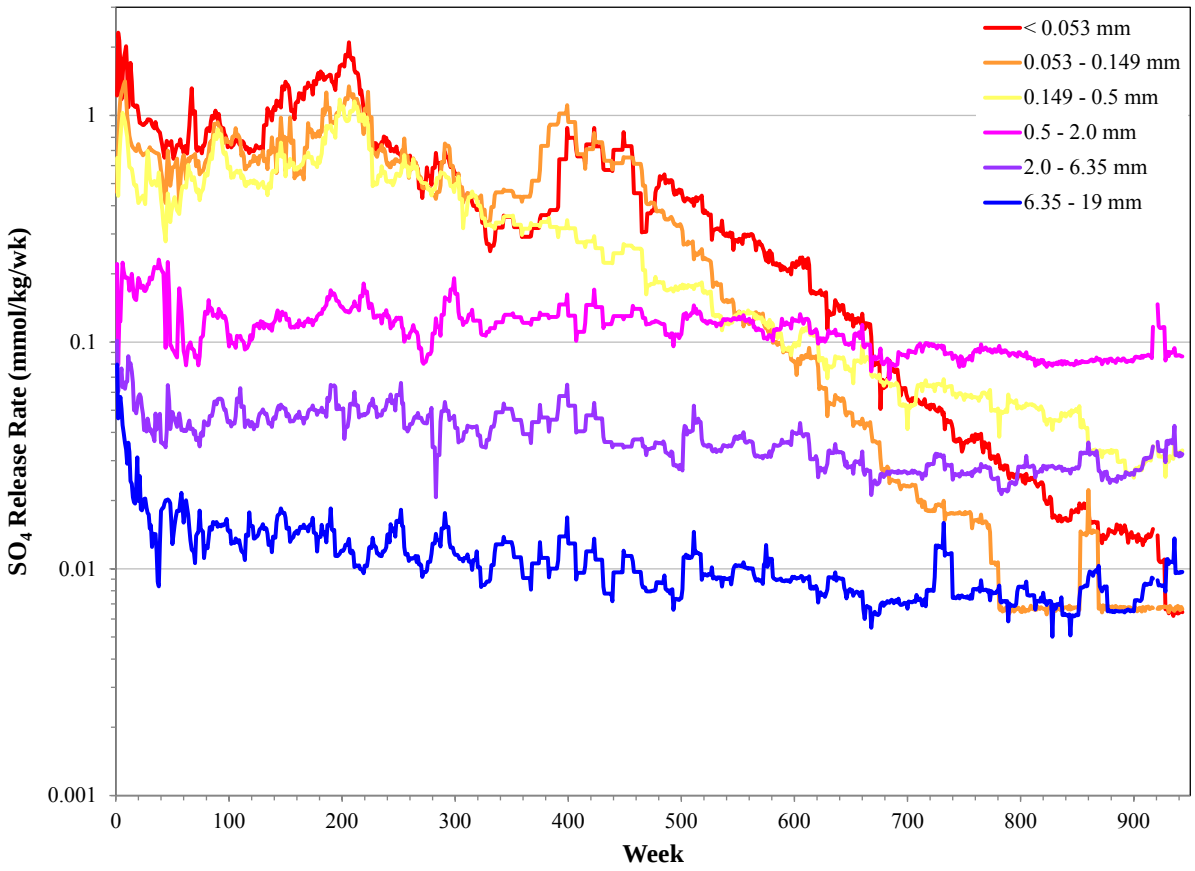

Figure 4.8 Norite SO_4 release rate time series plot.

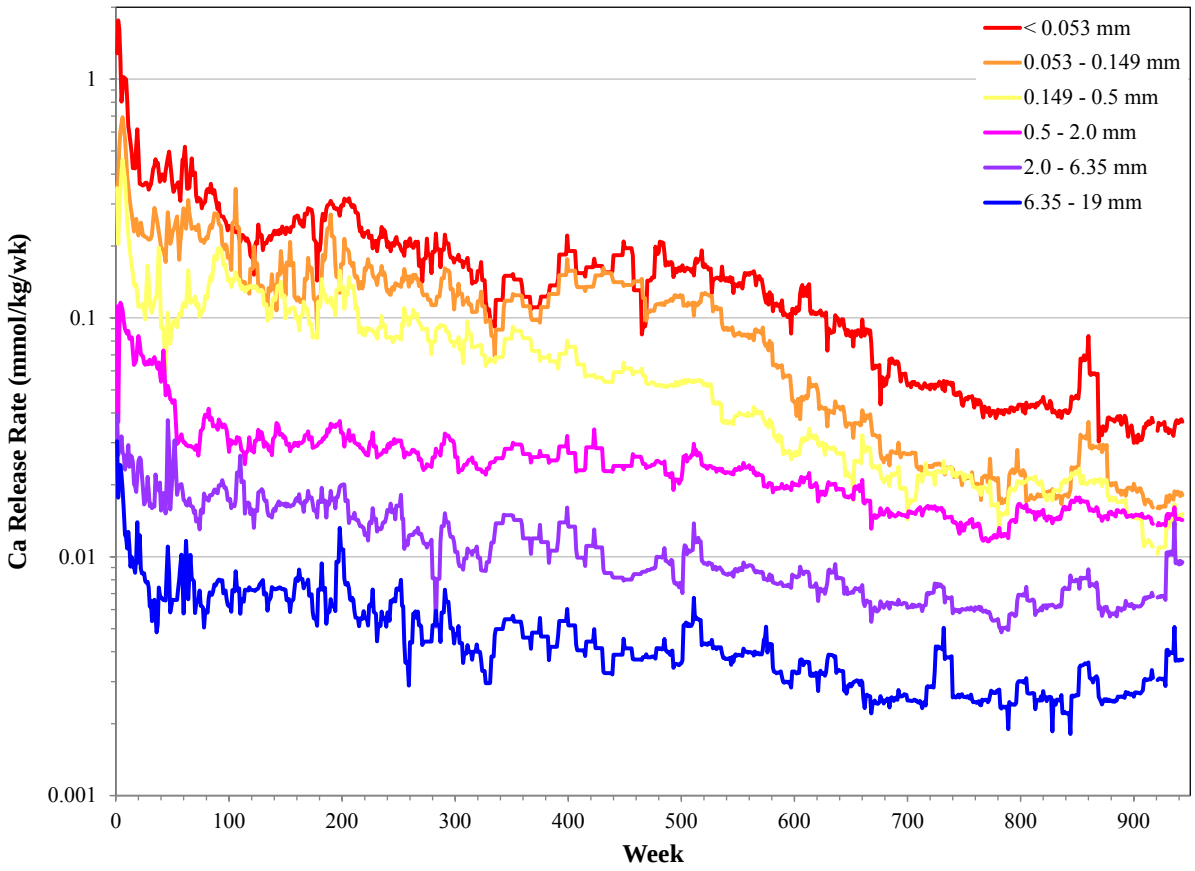

Figure 4.9 Norite Ca release rate time series plot.

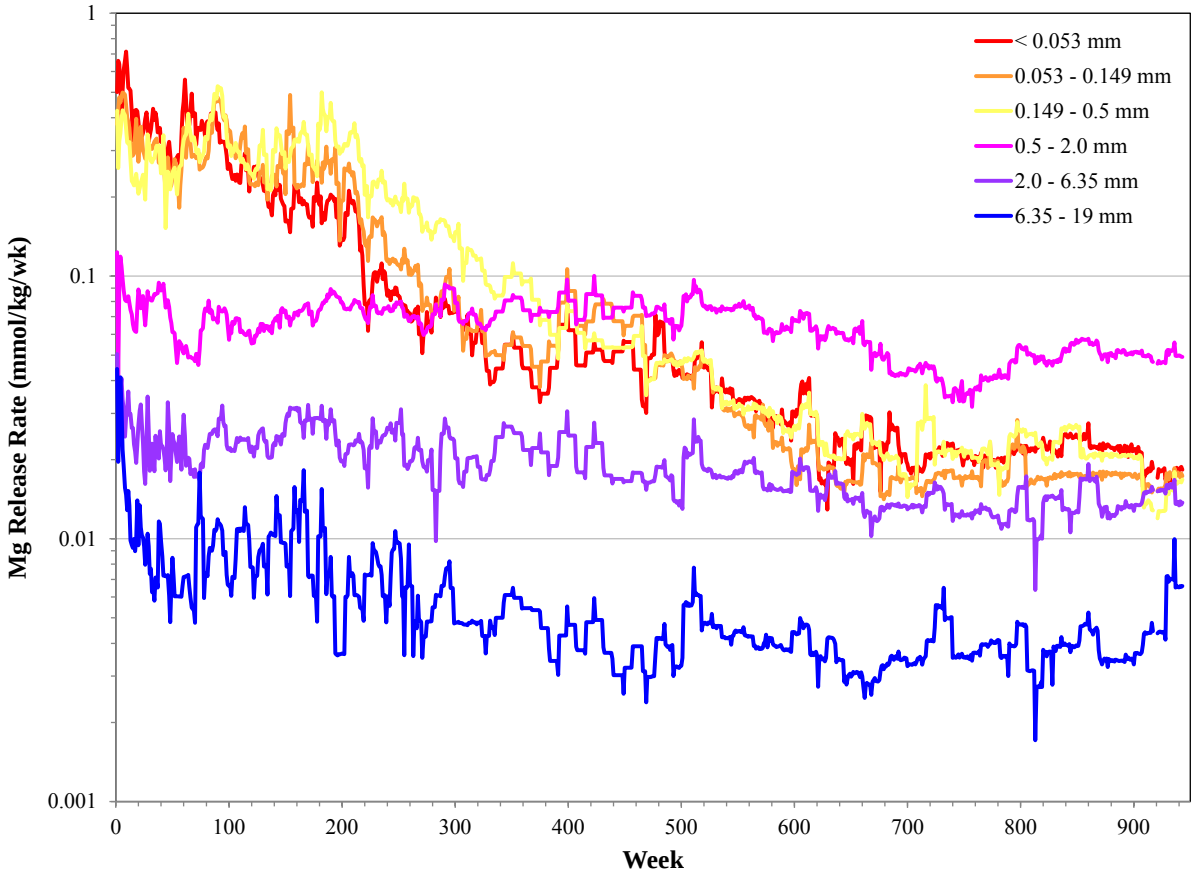

Figure 4.10 Norite Mg release rate time series plot.

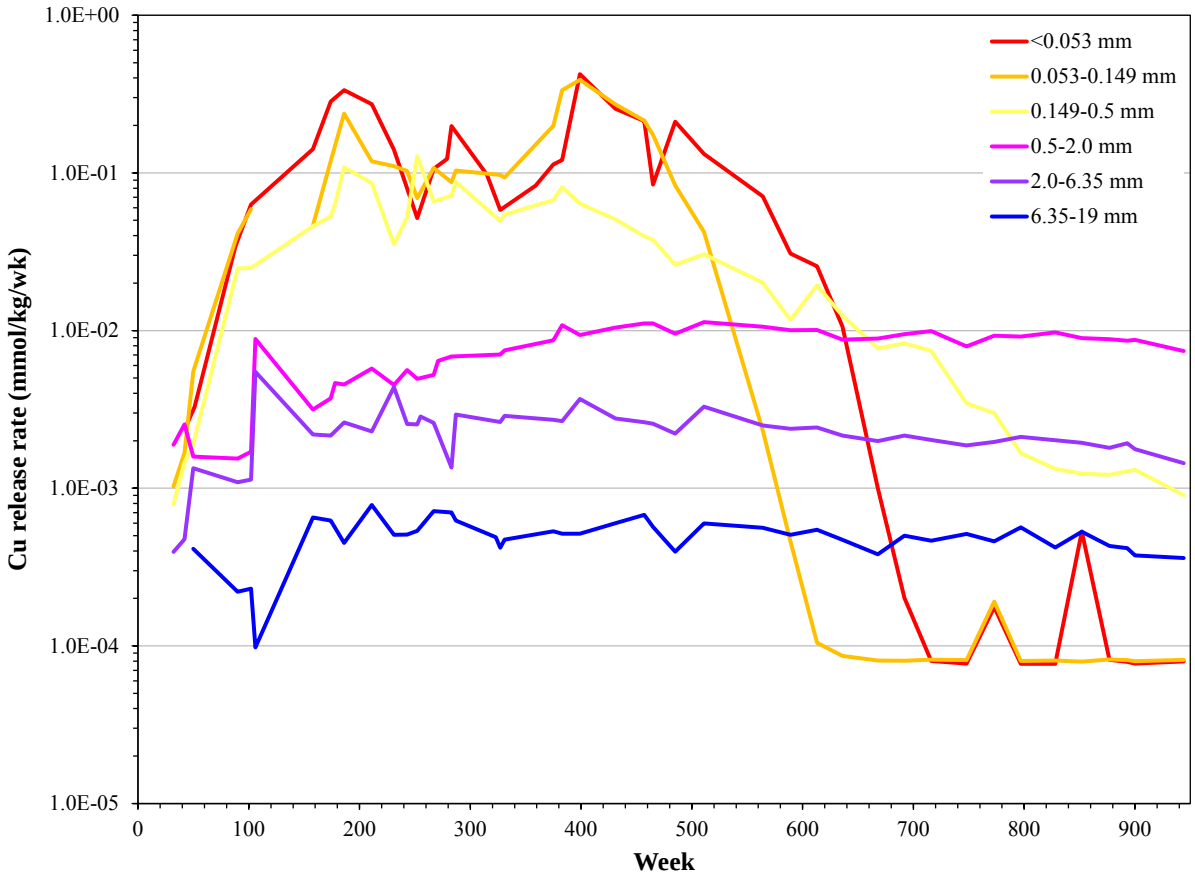

Figure 4.11 Norite Cu release rate time series plot.

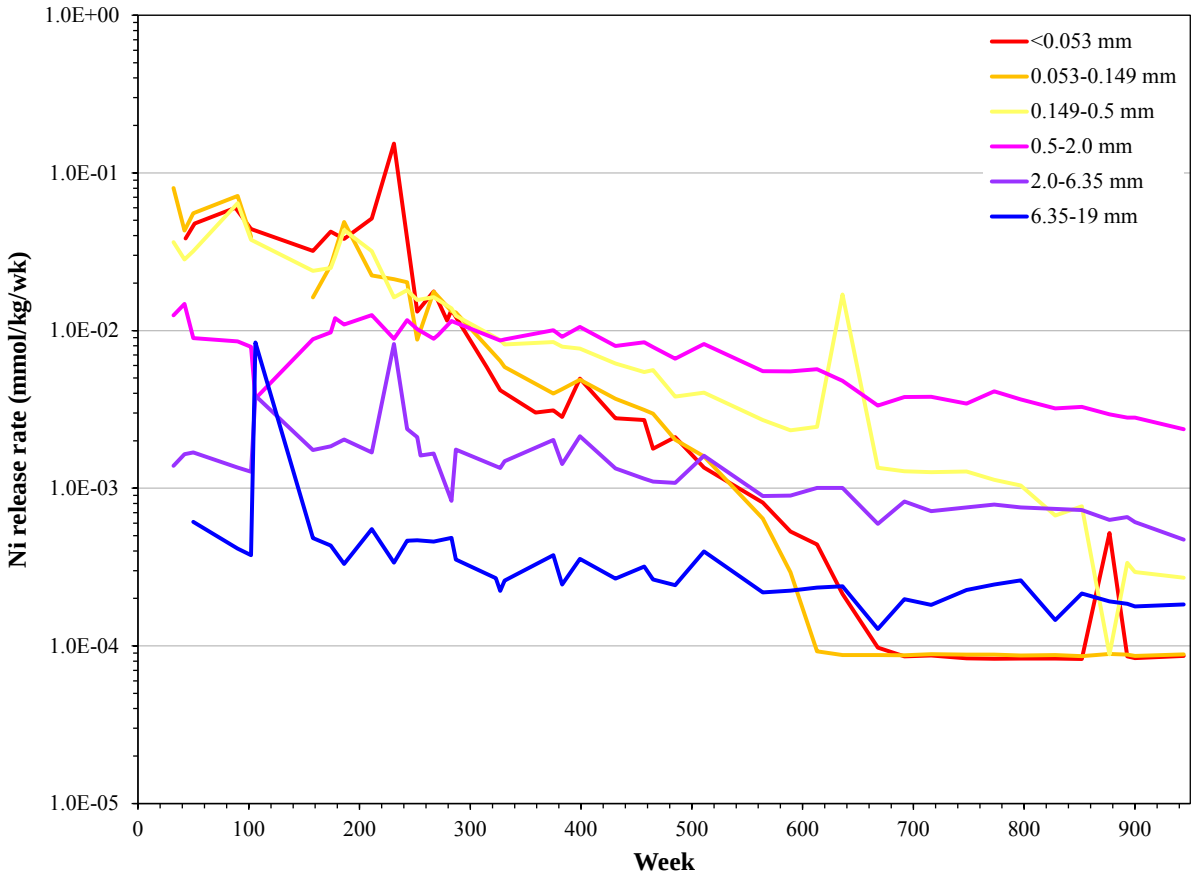

Figure 4.12 Norite Ni release rate time series plot.

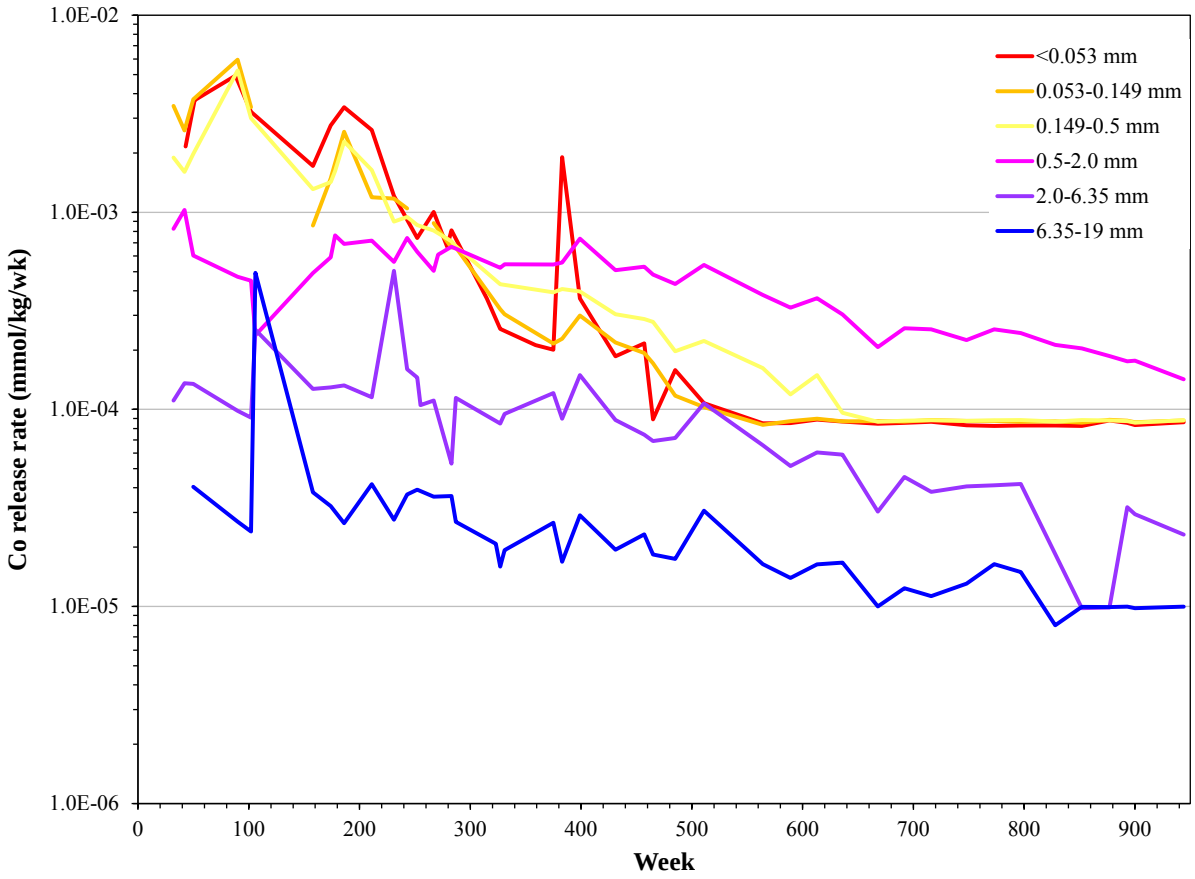

Figure 4.13 Norite Co release rate time series plot.

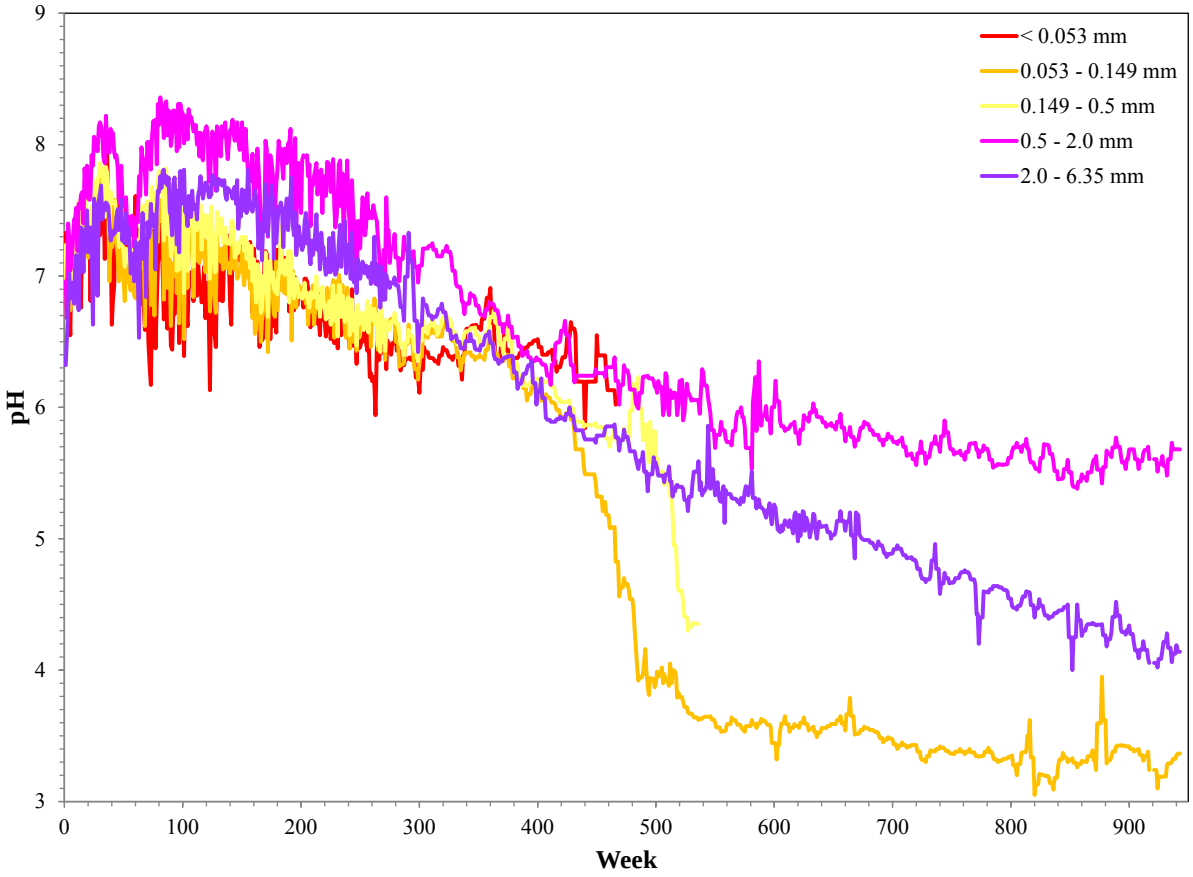

Figure 4.14 Diatreme pH time series plot.

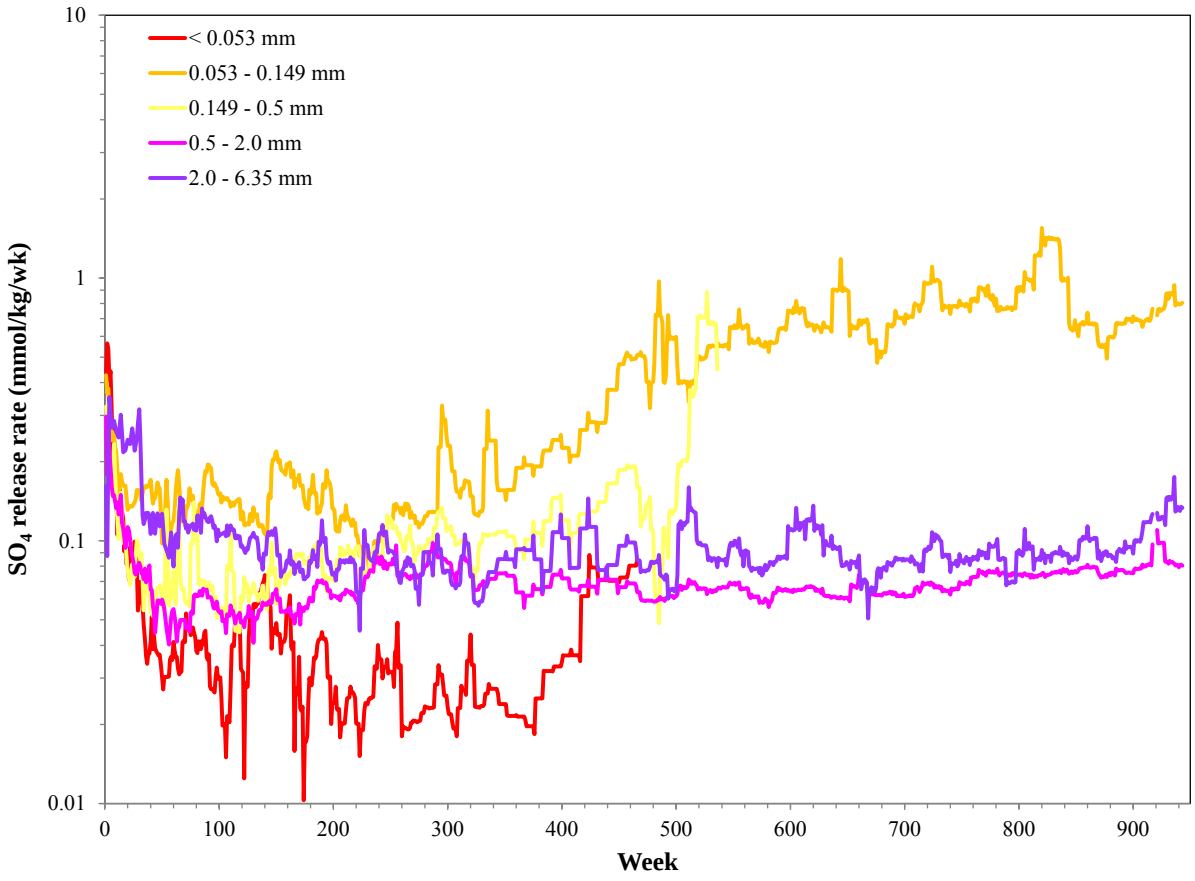

Figure 4.15 Diatreme SO_4 release rate time series plot.

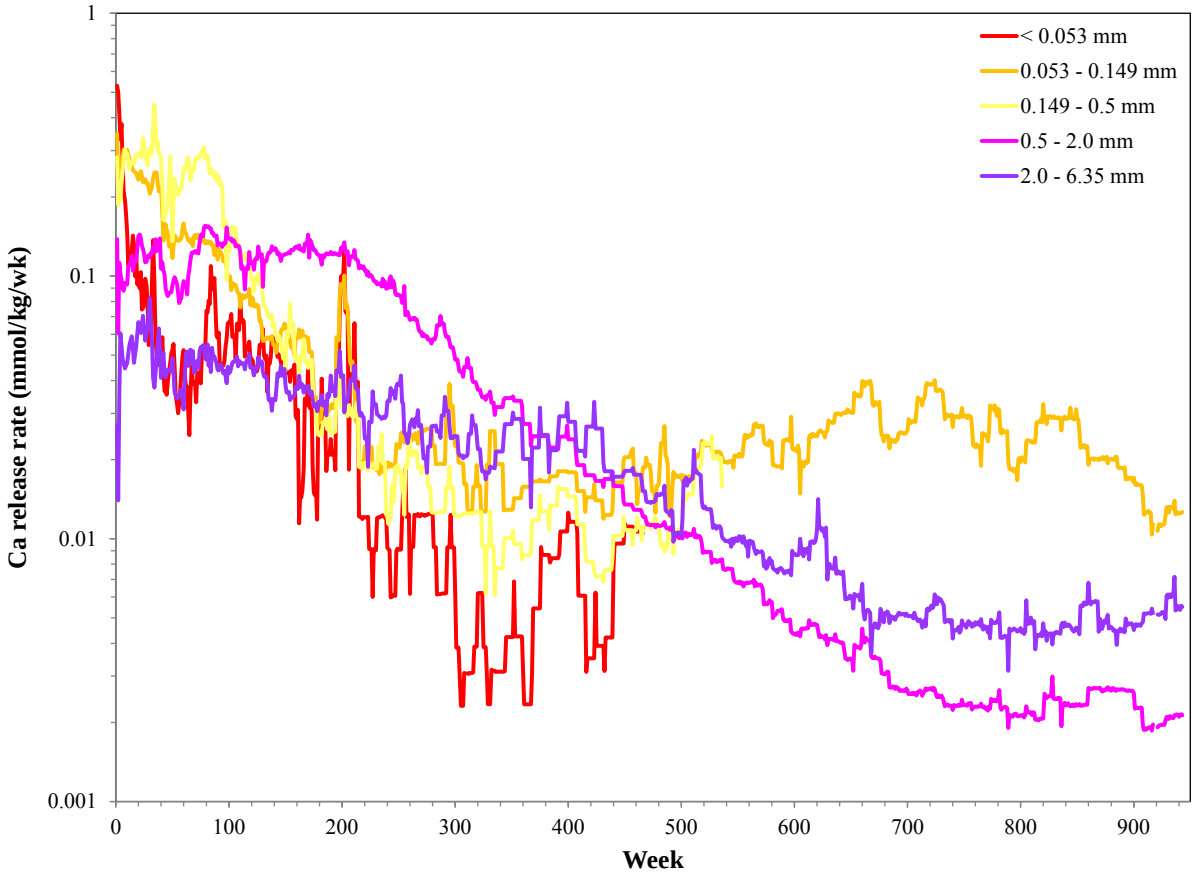

Figure 4.16 Diatreme Ca release rate time series plot.

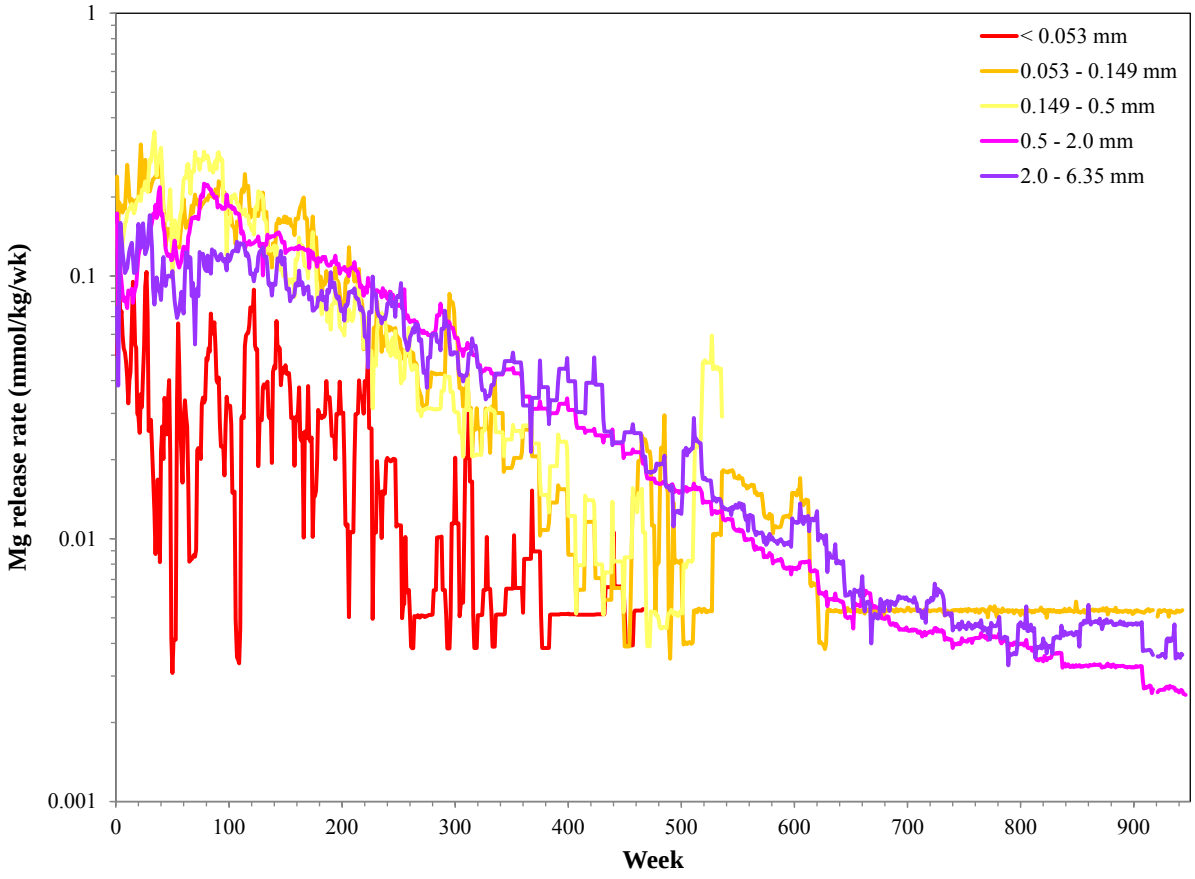

Figure 4.17 Diatreme Mg release rate time series plot.

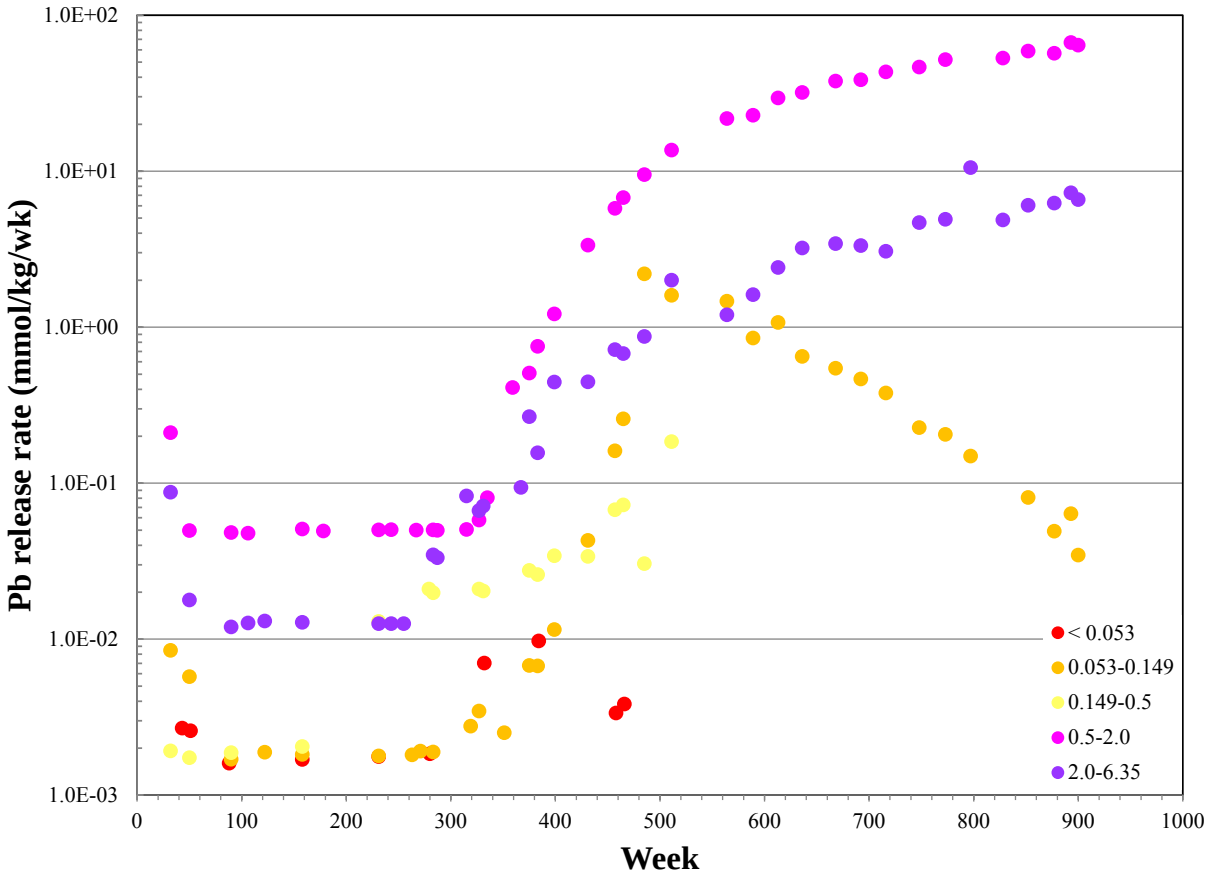

Figure 4.18 Diatreme Pb release rate time series plot.

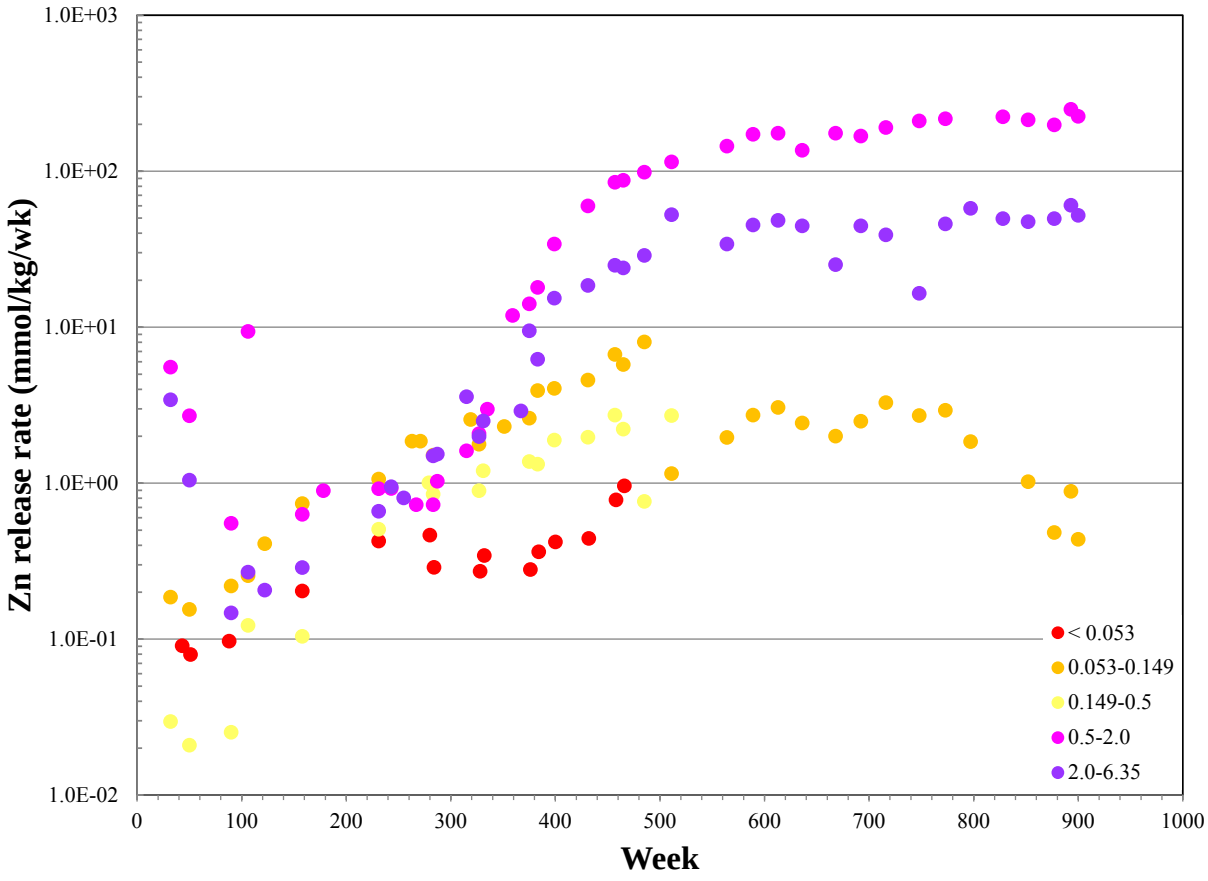

Figure 4.19 Diatreme Zn release rate time series plot.

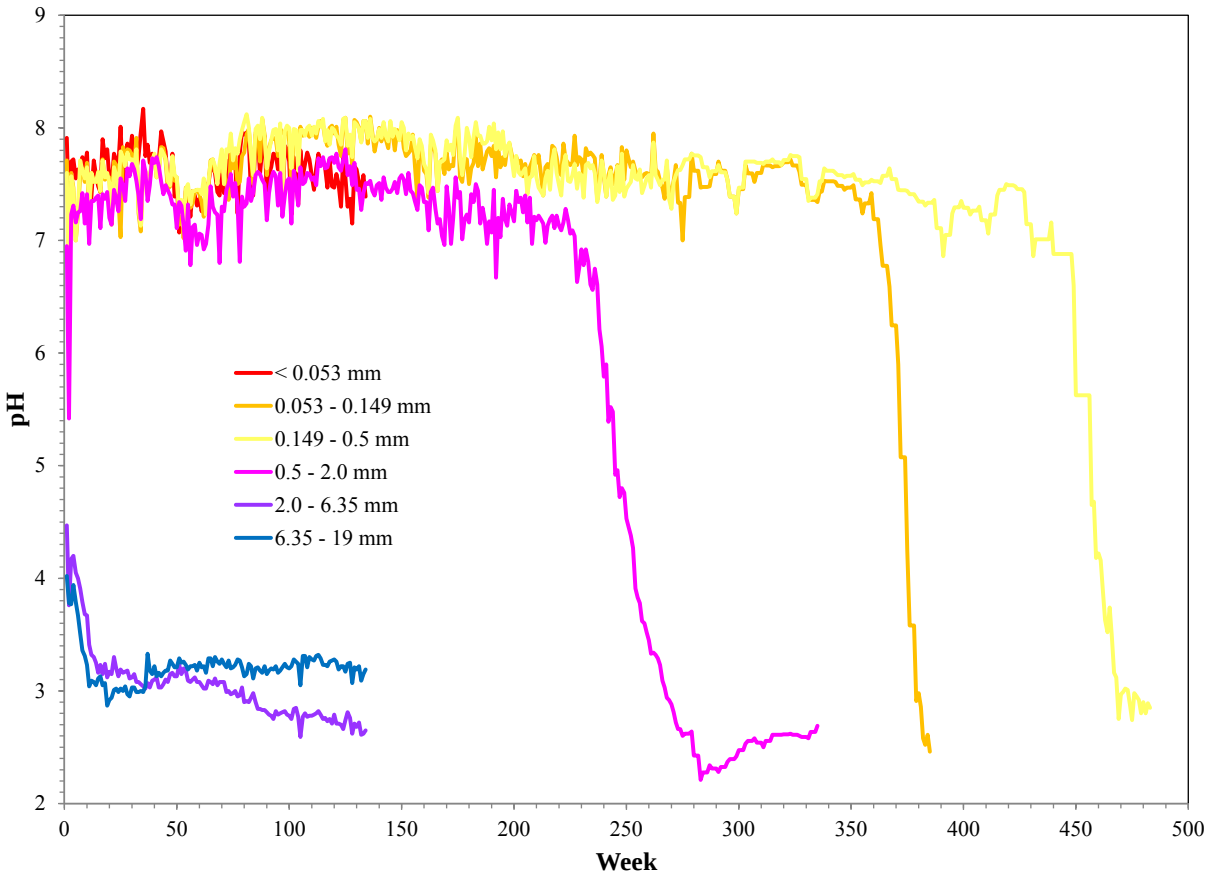

Figure 4.20 Mudstone pH time series plot.

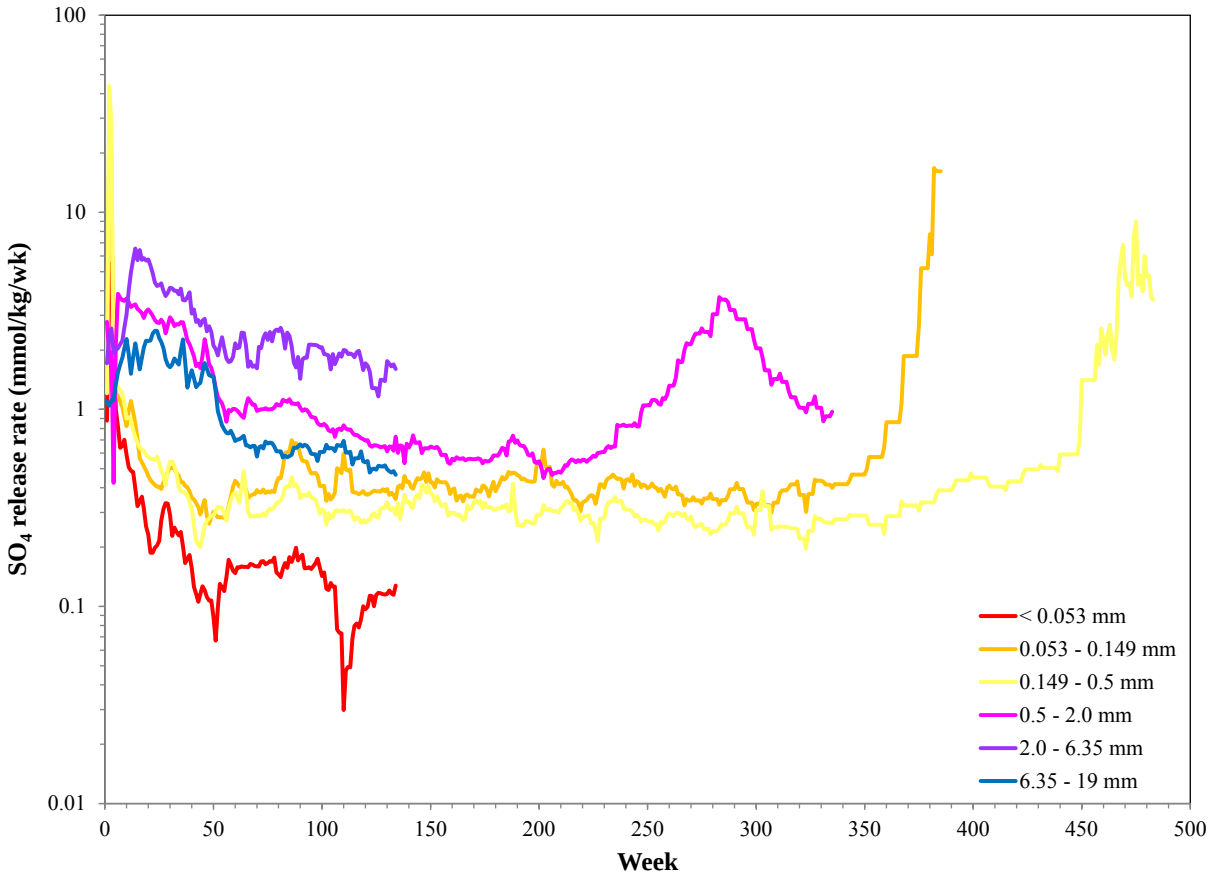

Figure 4.21 Mudstone SO_4 release rate time series plot.

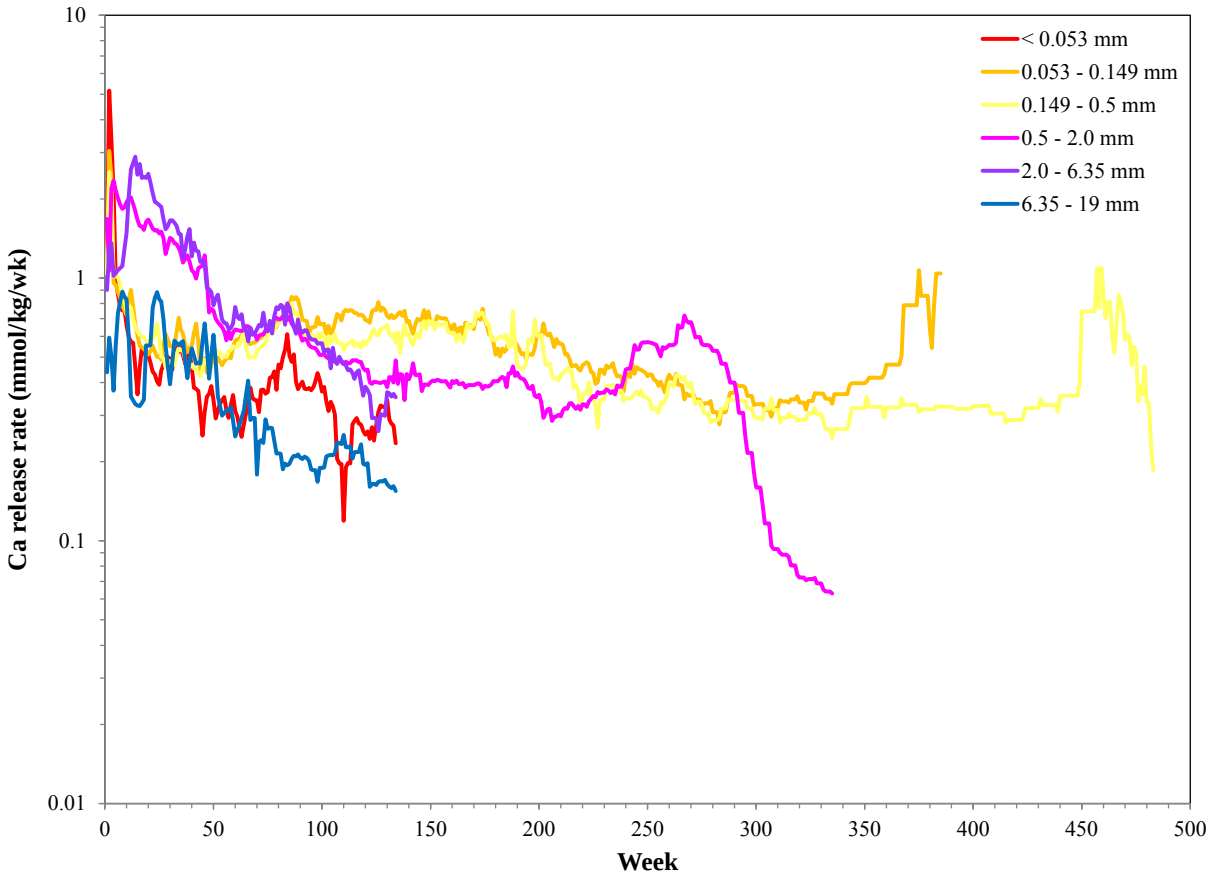

Figure 4.22 Mudstone Ca release rate time series plot.

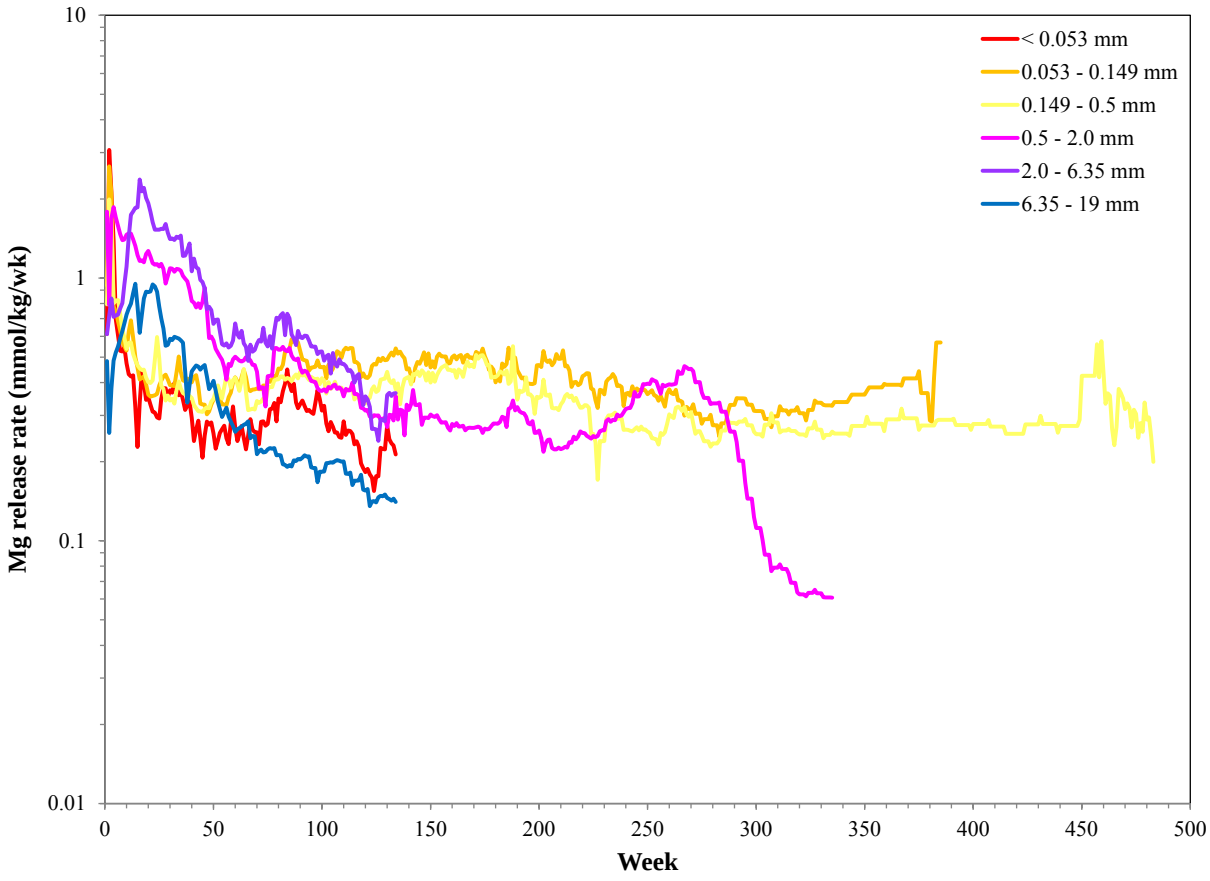

Figure 4.23 Mudstone Mg release rate time series plot.

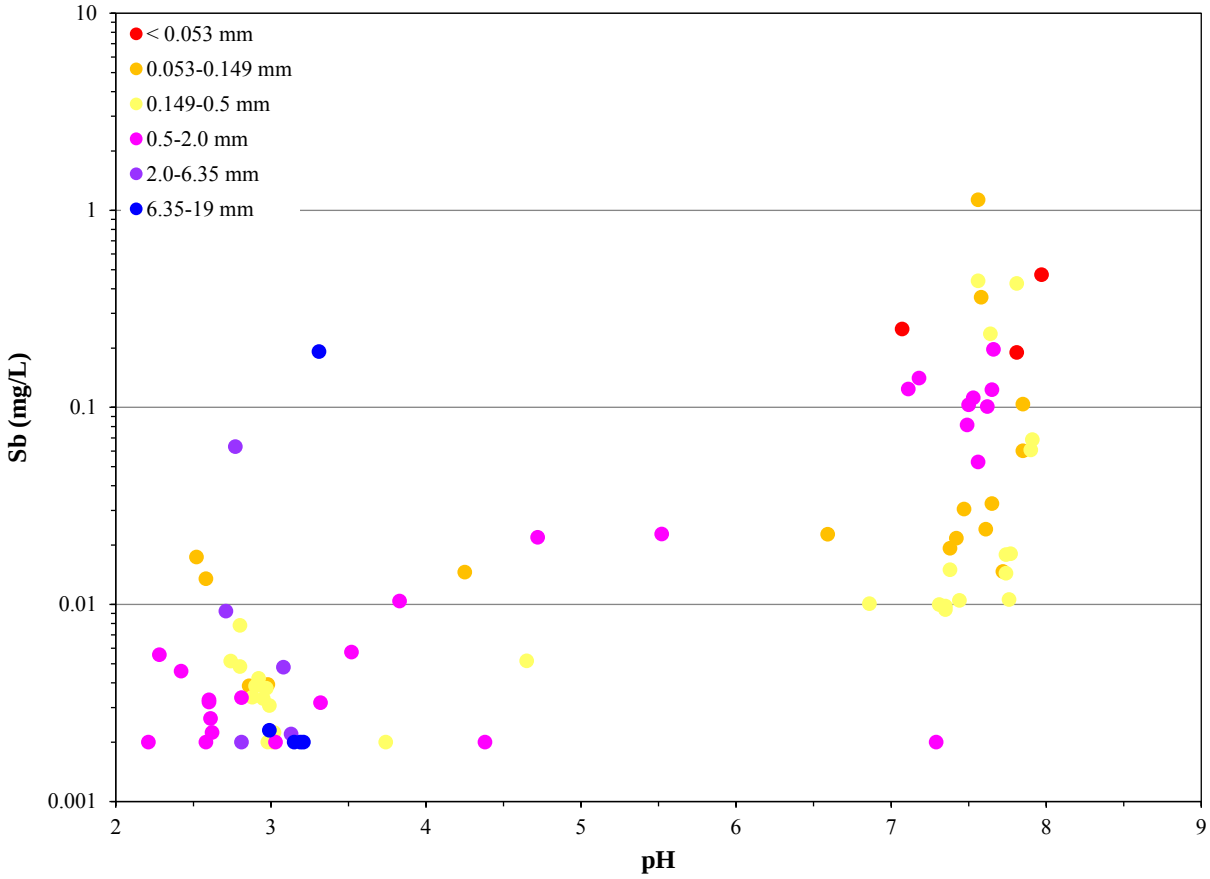

Figure 4.24 Mudstone Sb concentration as a function of pH.

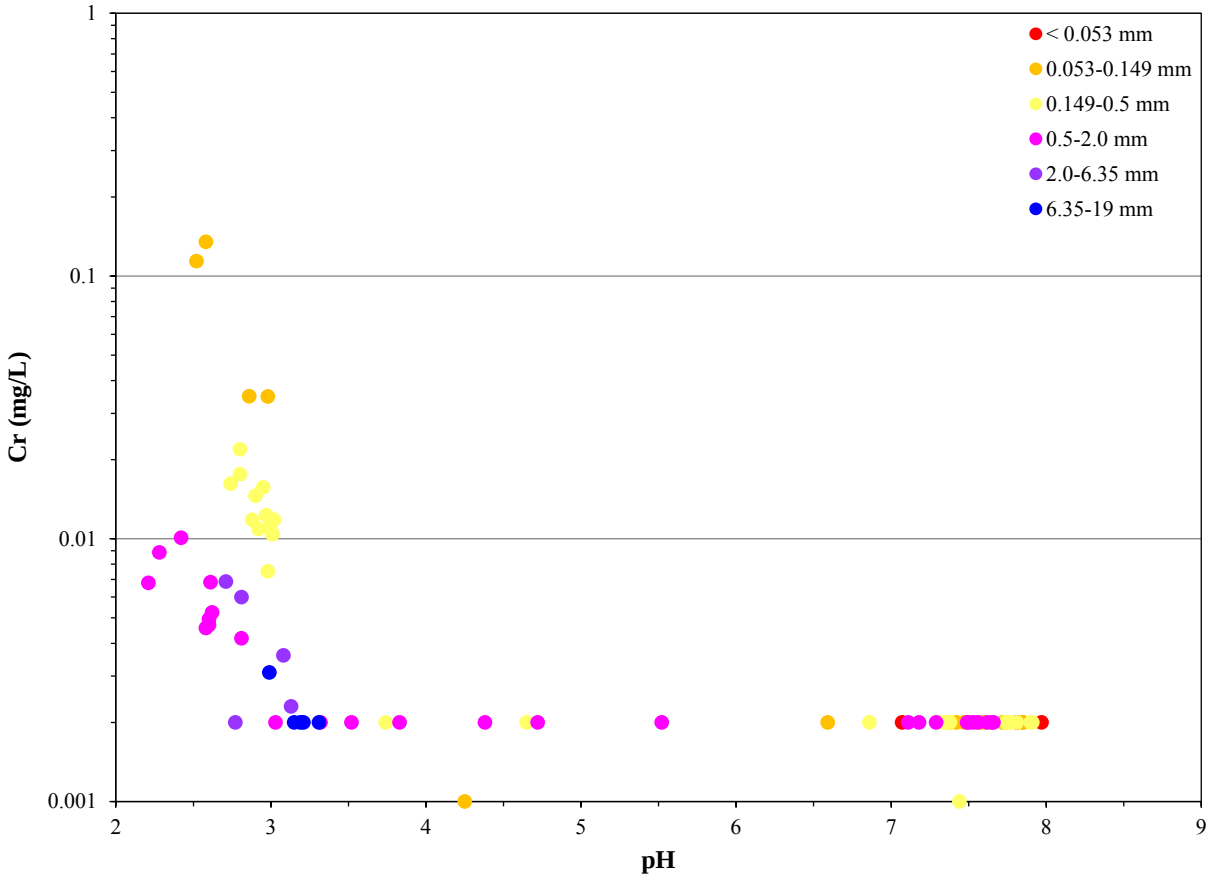

Figure 4.25 Mudstone Cr concentration as a function of pH.

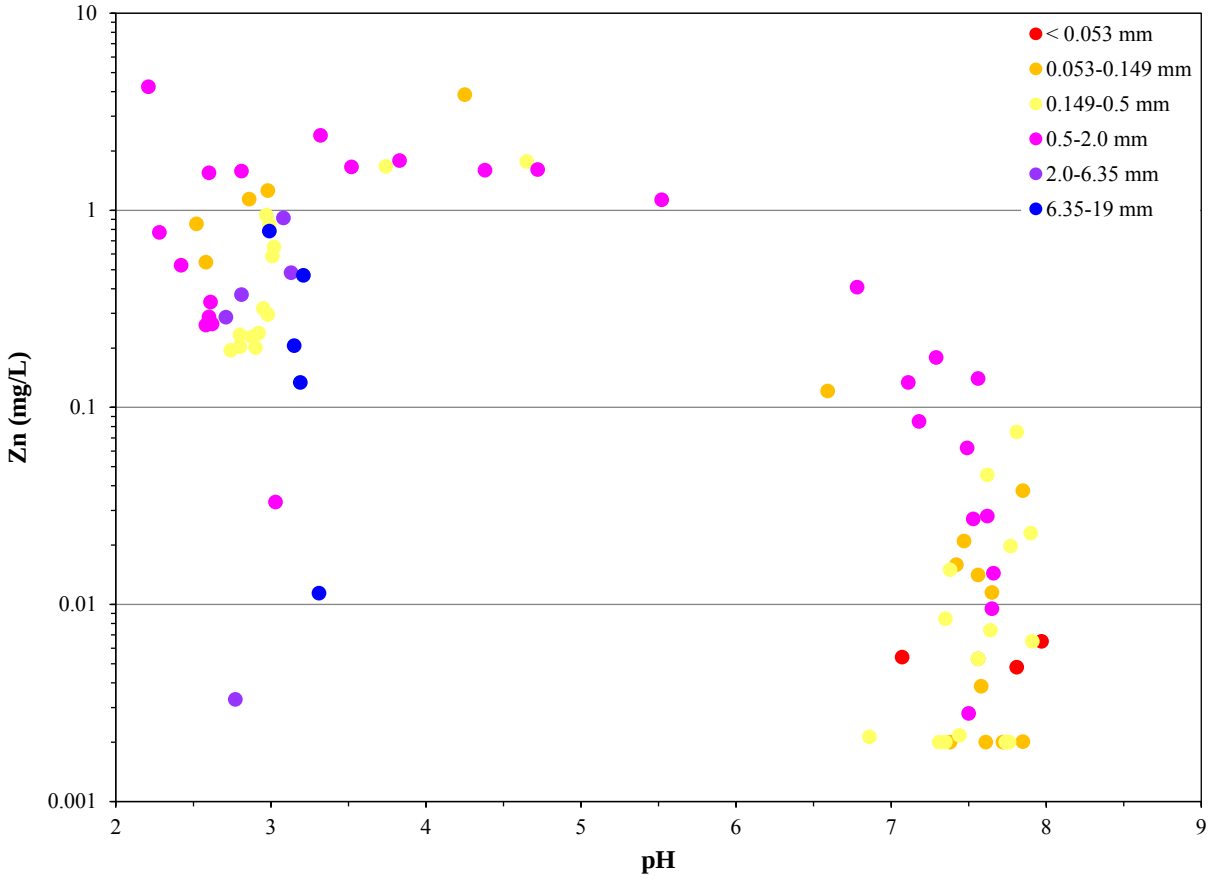

Figure 4.26 Mudstone Zn concentration as a function of pH.

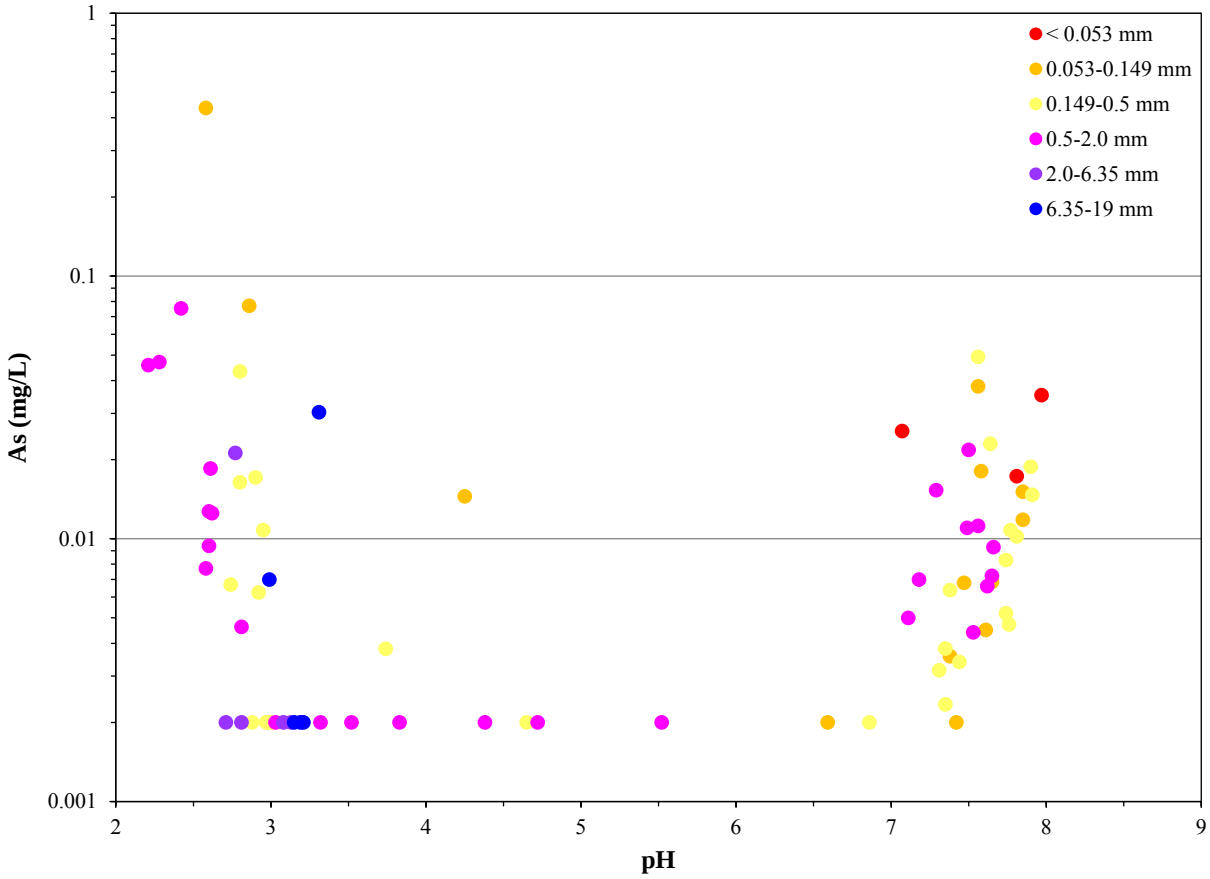

Figure 4.27 Mudstone As concentration as a function of pH.

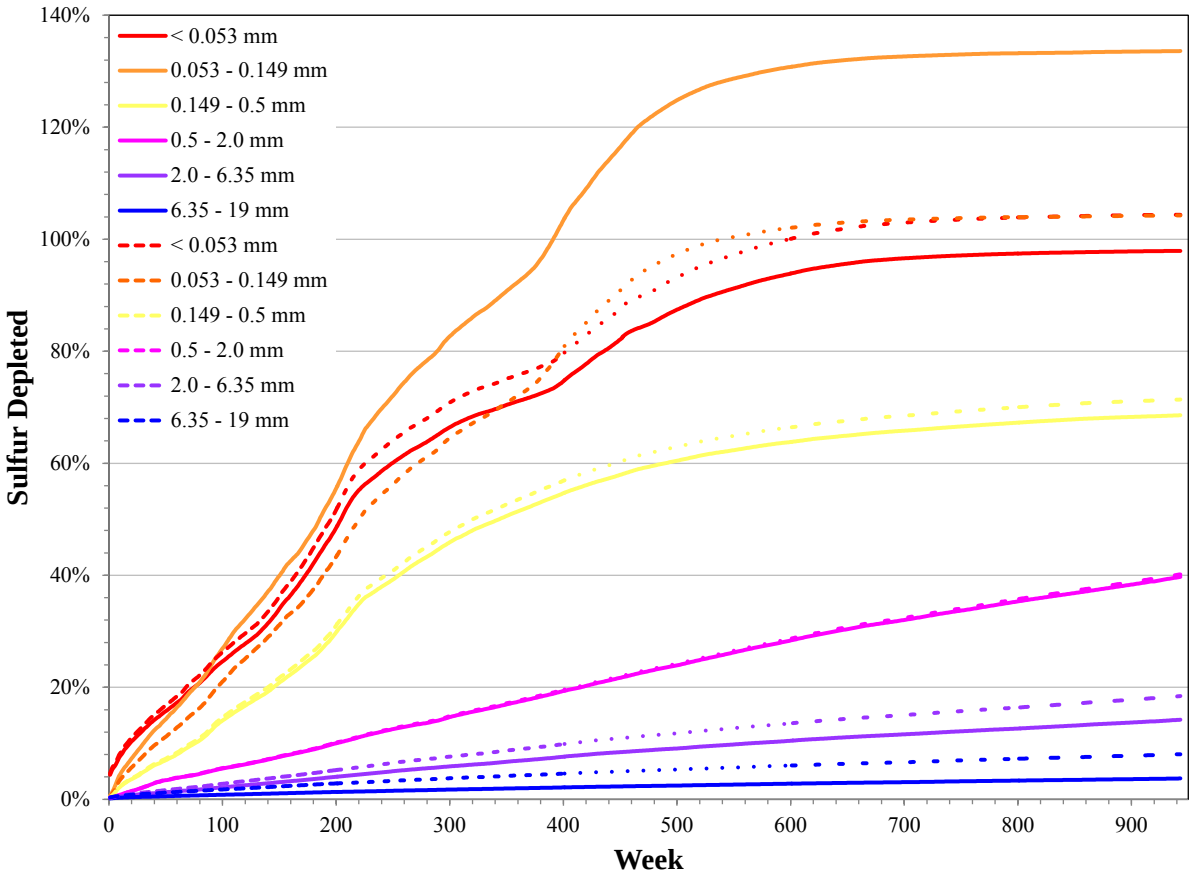

Figure 4.28 Norite cumulative sulfur release.
Solid lines represent Midland Research sulfur analyses and dashed lines are ACME sulfur analyses.

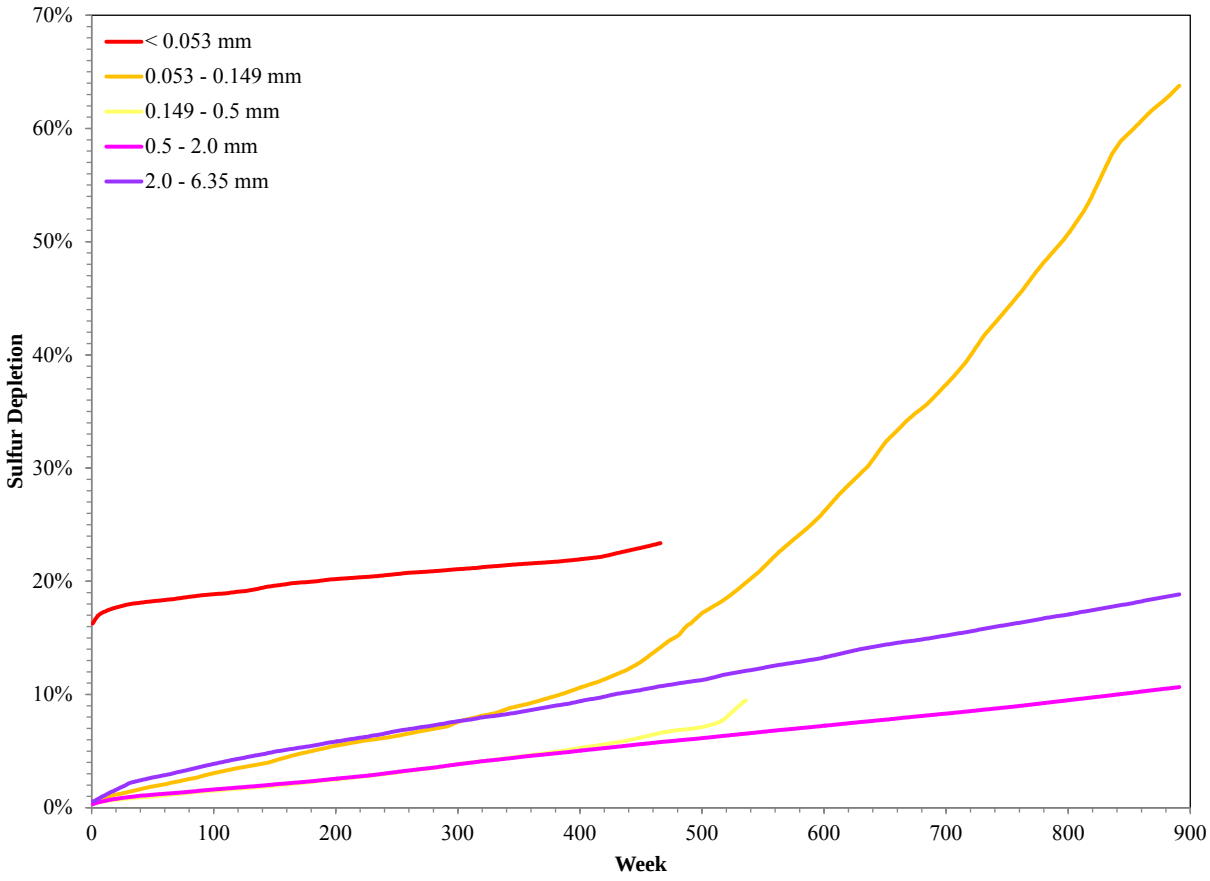

Figure 4.29 Diatreme cumulative sulfur release.

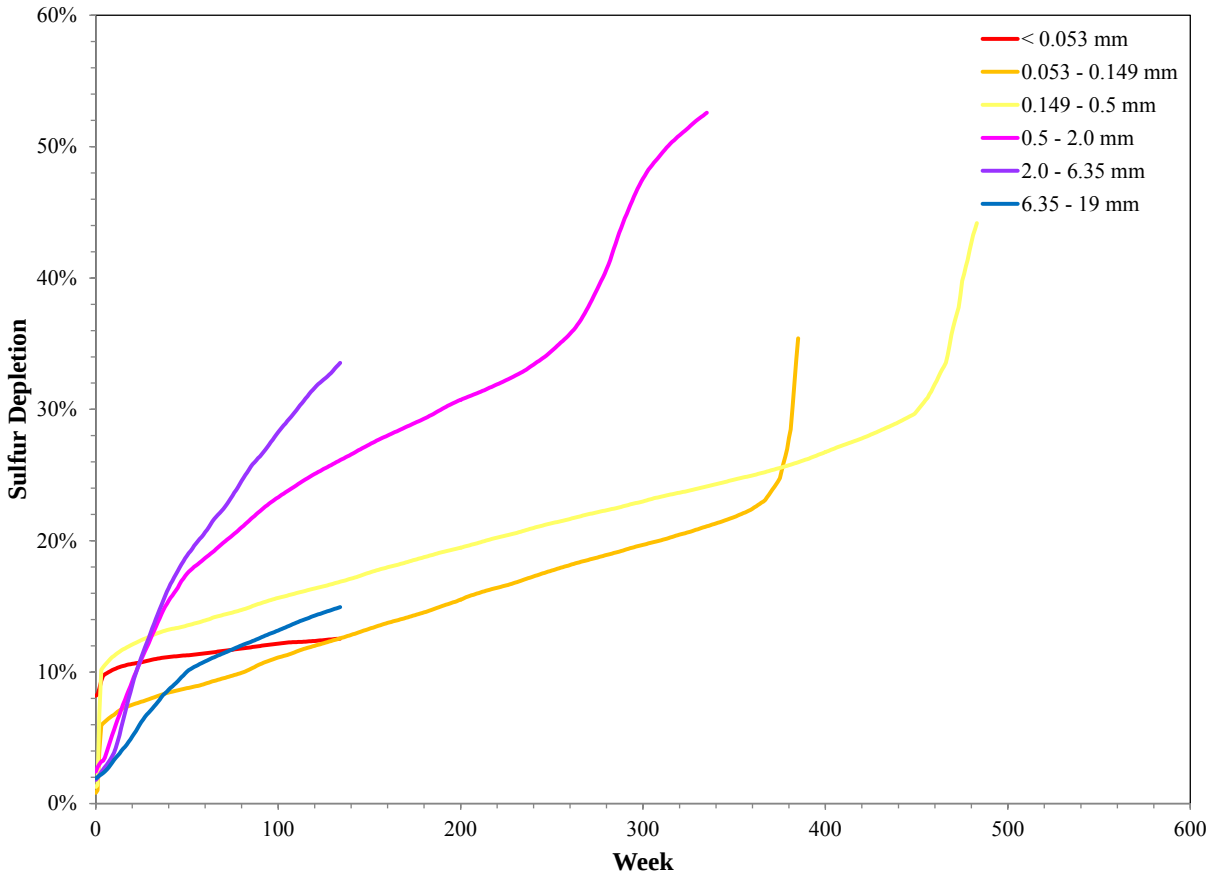

Figure 4.30 Mudstone cumulative sulfur release.

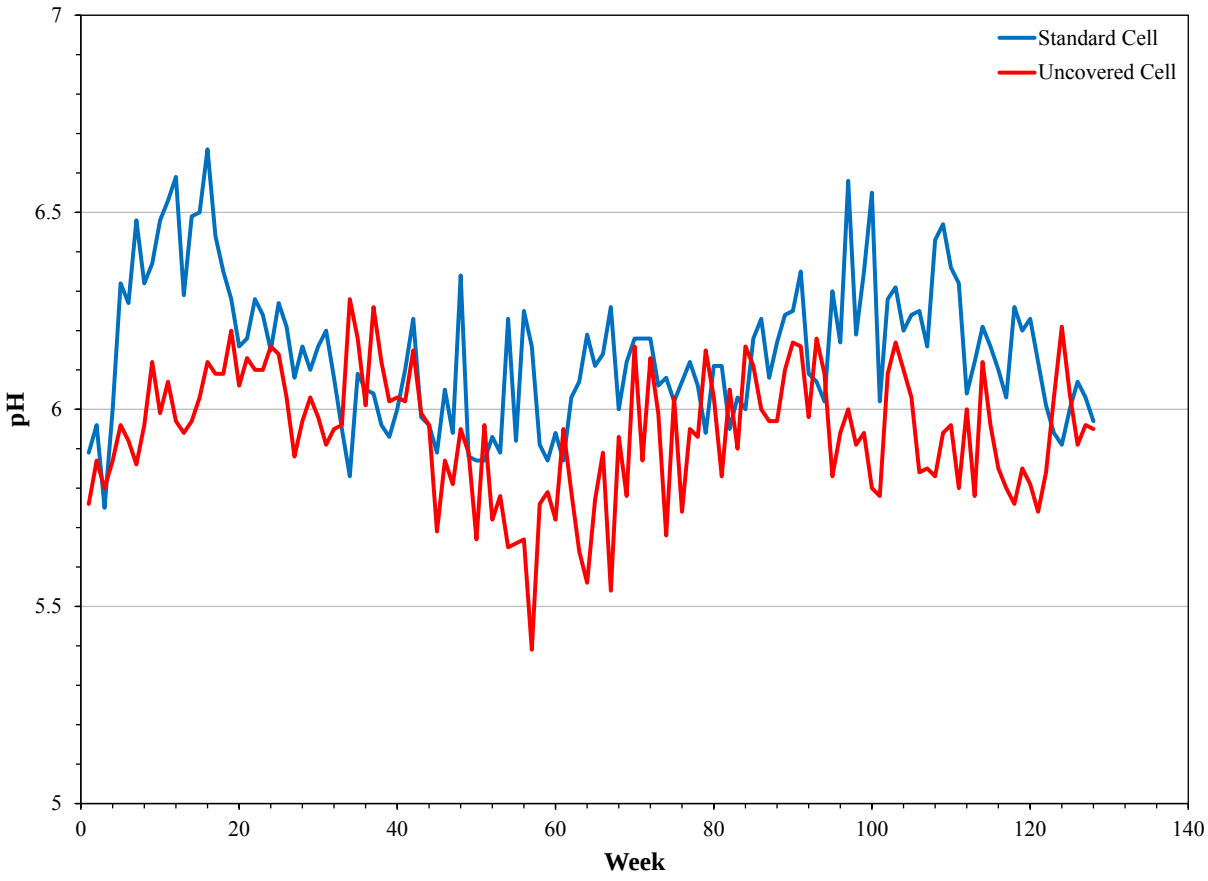

Figure 4.31 Norite 6.35-19 mm standard and uncovered samples leachate pH trends.

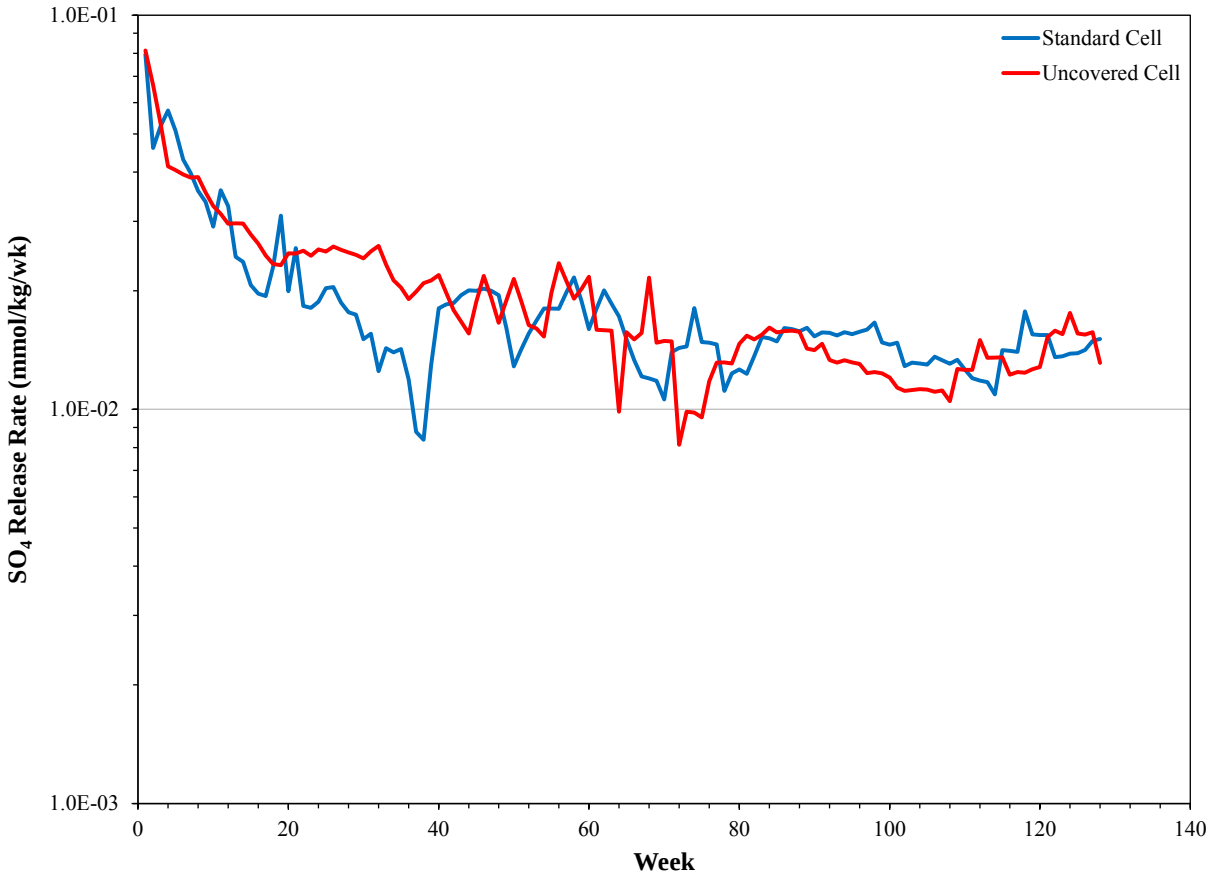

Figure 4.32 Norite 6.35-19 mm standard and uncovered SO_4 release rate trends.

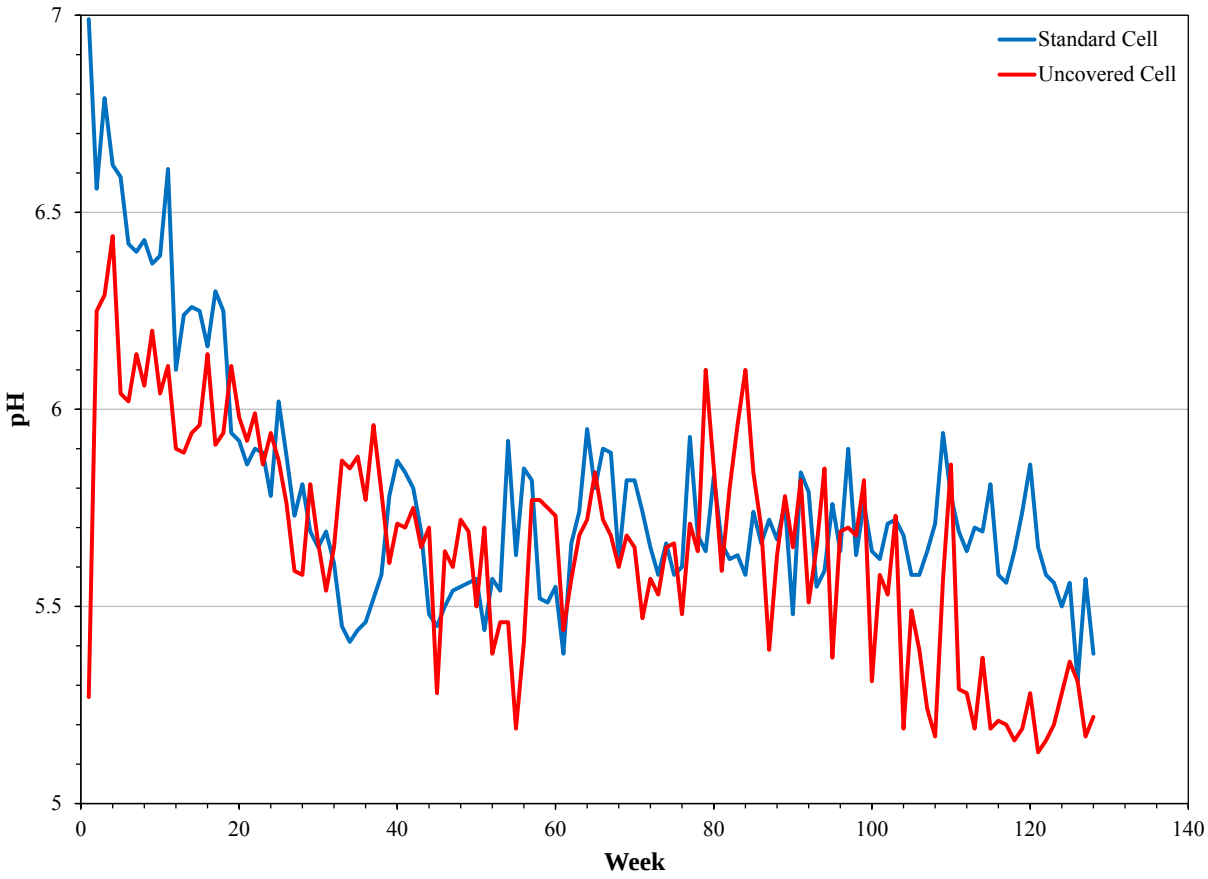

Figure 4.33 Norite 0.5-2.0 mm standard and uncovered samples leachate pH trends.

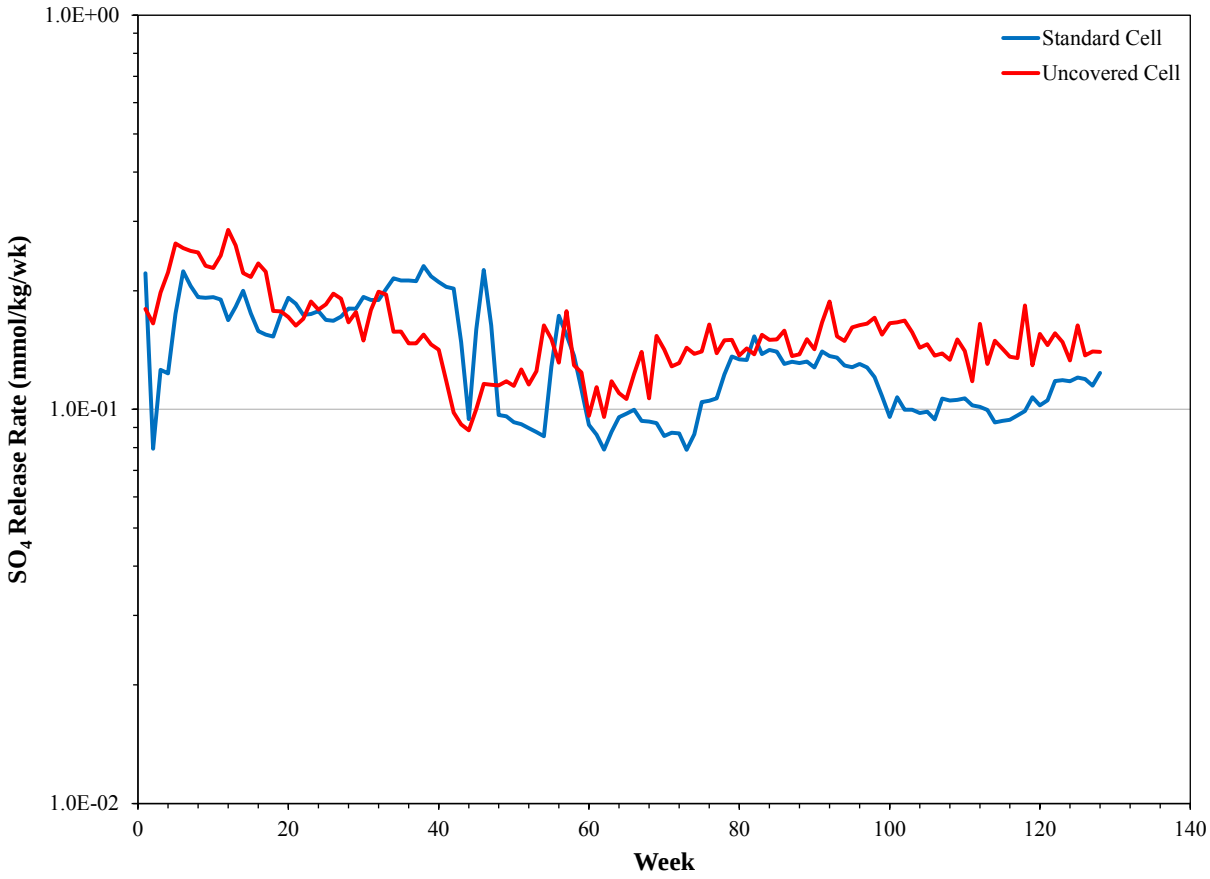

Figure 4.34 Norite 0.5-2.0 mm standard and uncovered SO_4 release rate trends.

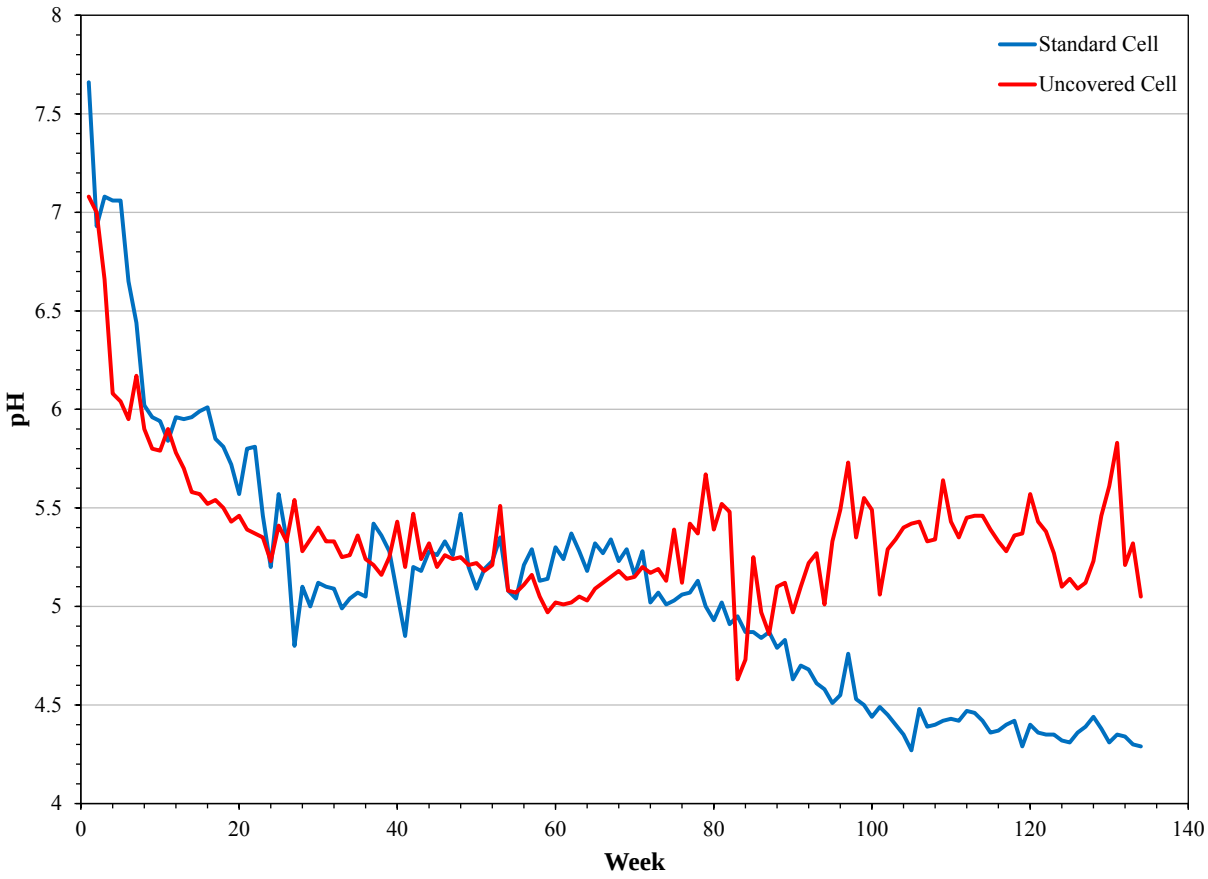

Figure 4.35 Norite 0.053-0.149 mm standard and uncovered samples leachate pH trends.

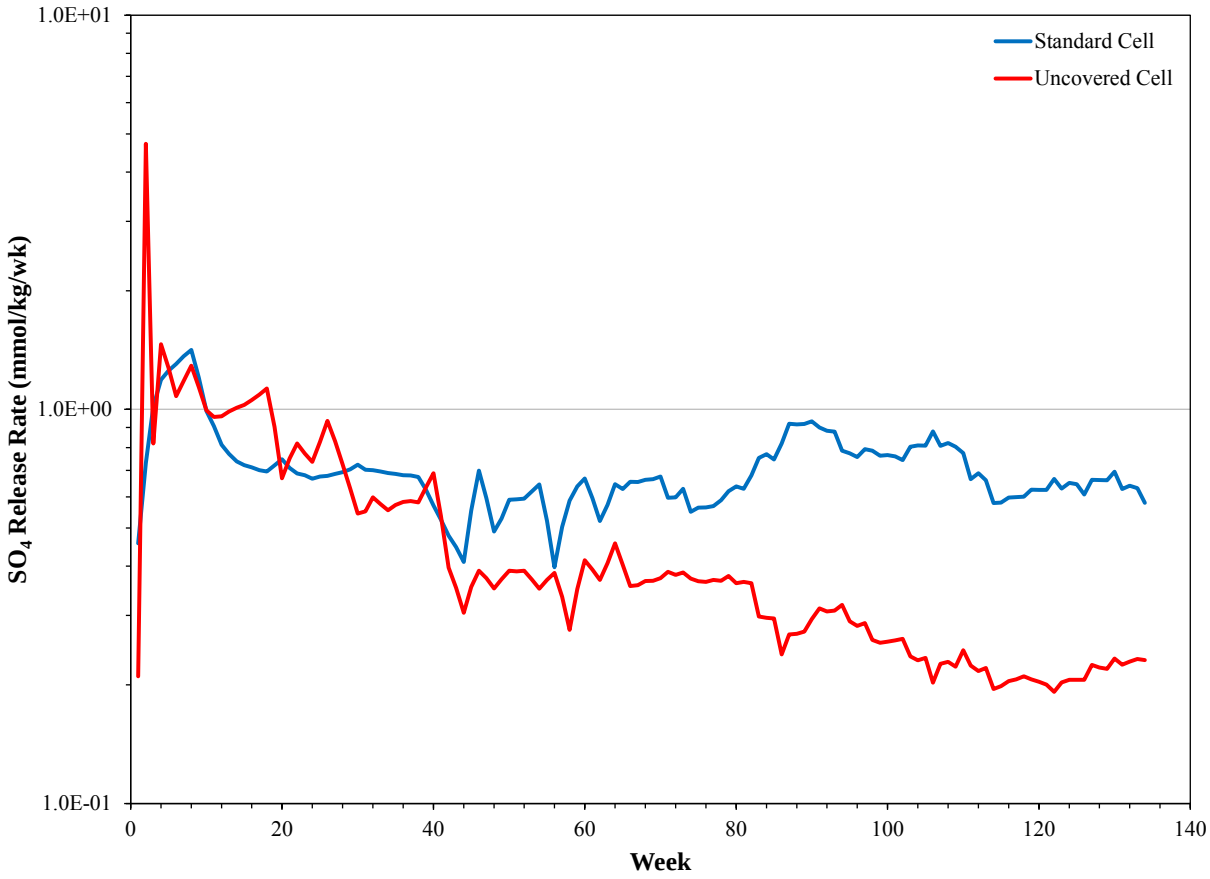

Figure 4.36 Norite 0.053-0.149 mm standard and uncovered SO_4 release rate trends.

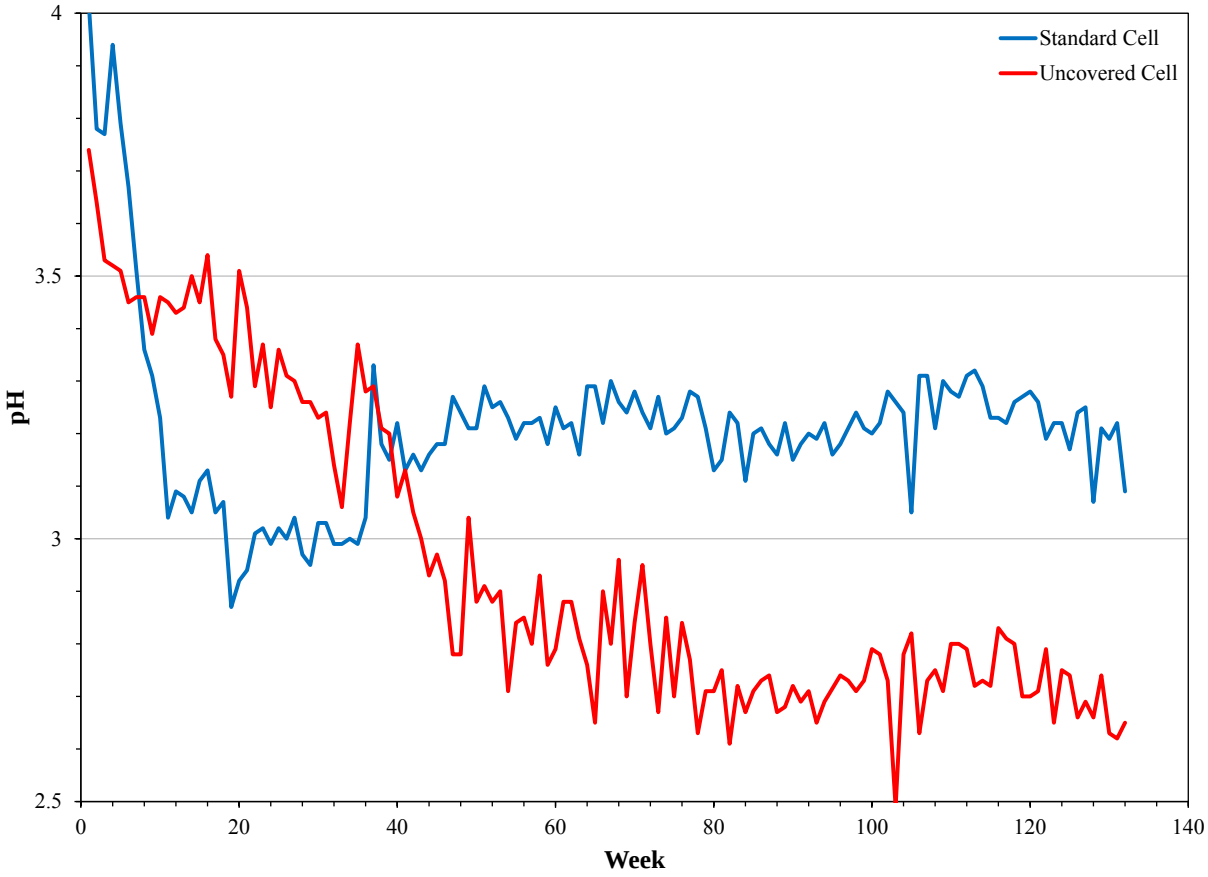

Figure 4.37 Mudstone 6.35-19 mm standard and uncovered samples leachate pH trends.

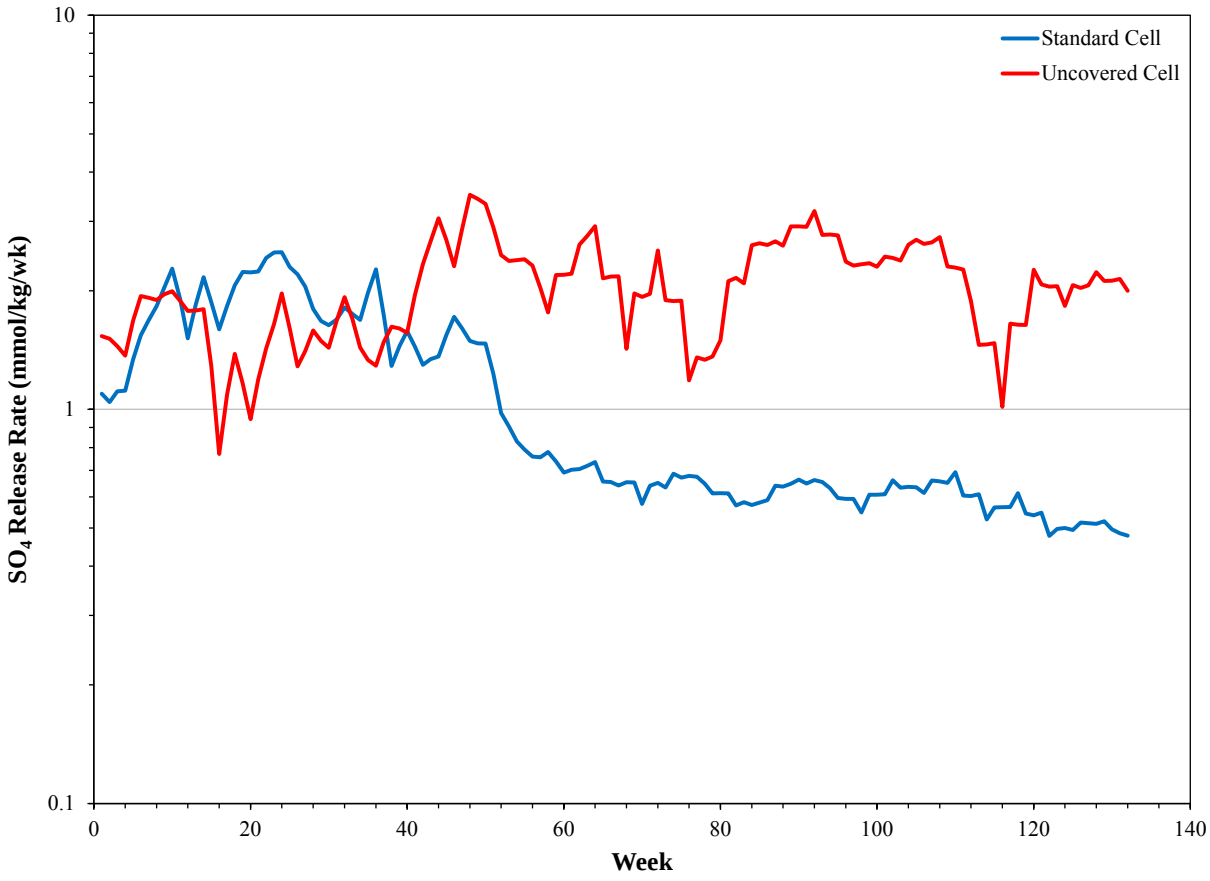

Figure 4.38 Mudstone 6.35-19 mm standard and uncovered SO_4 release rate trends.

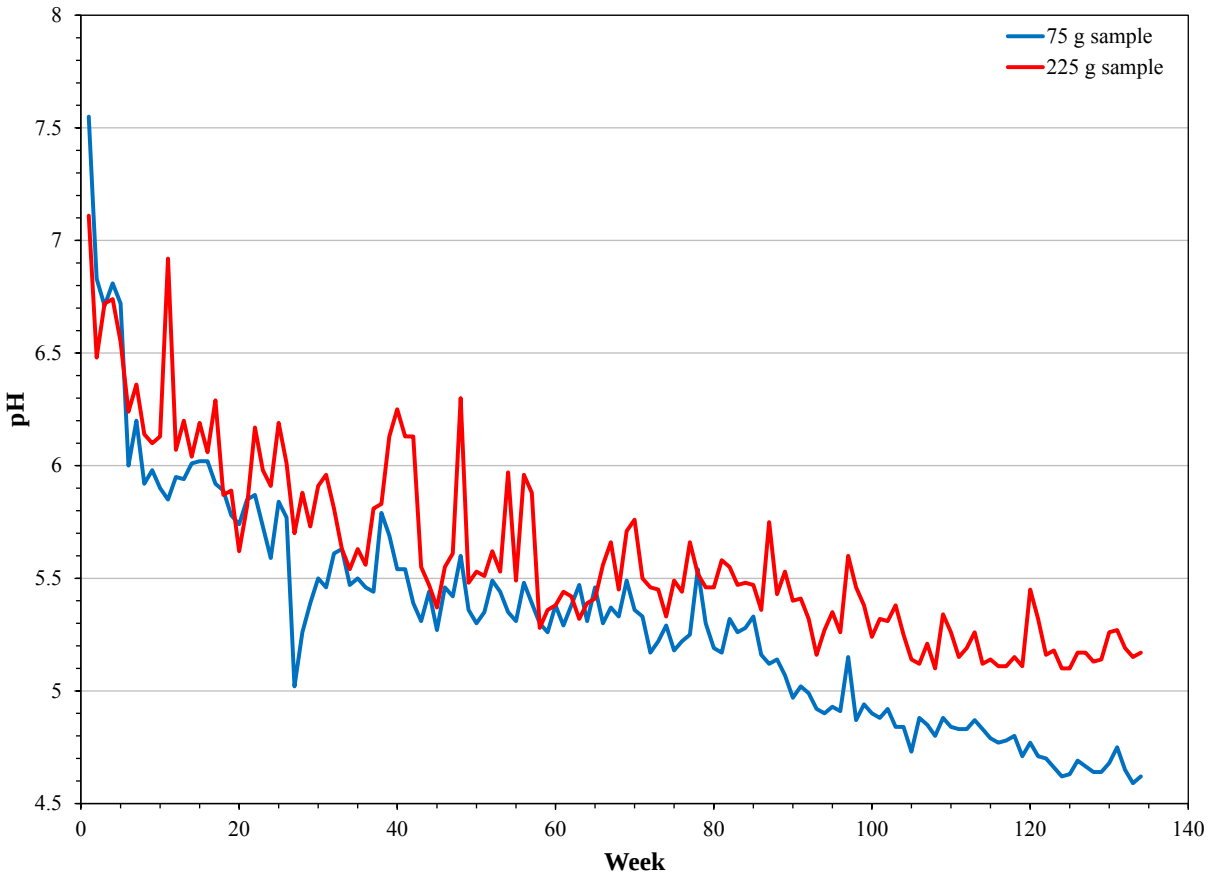

Figure 4.39 Norite standard and oversized samples leachate pH trends.

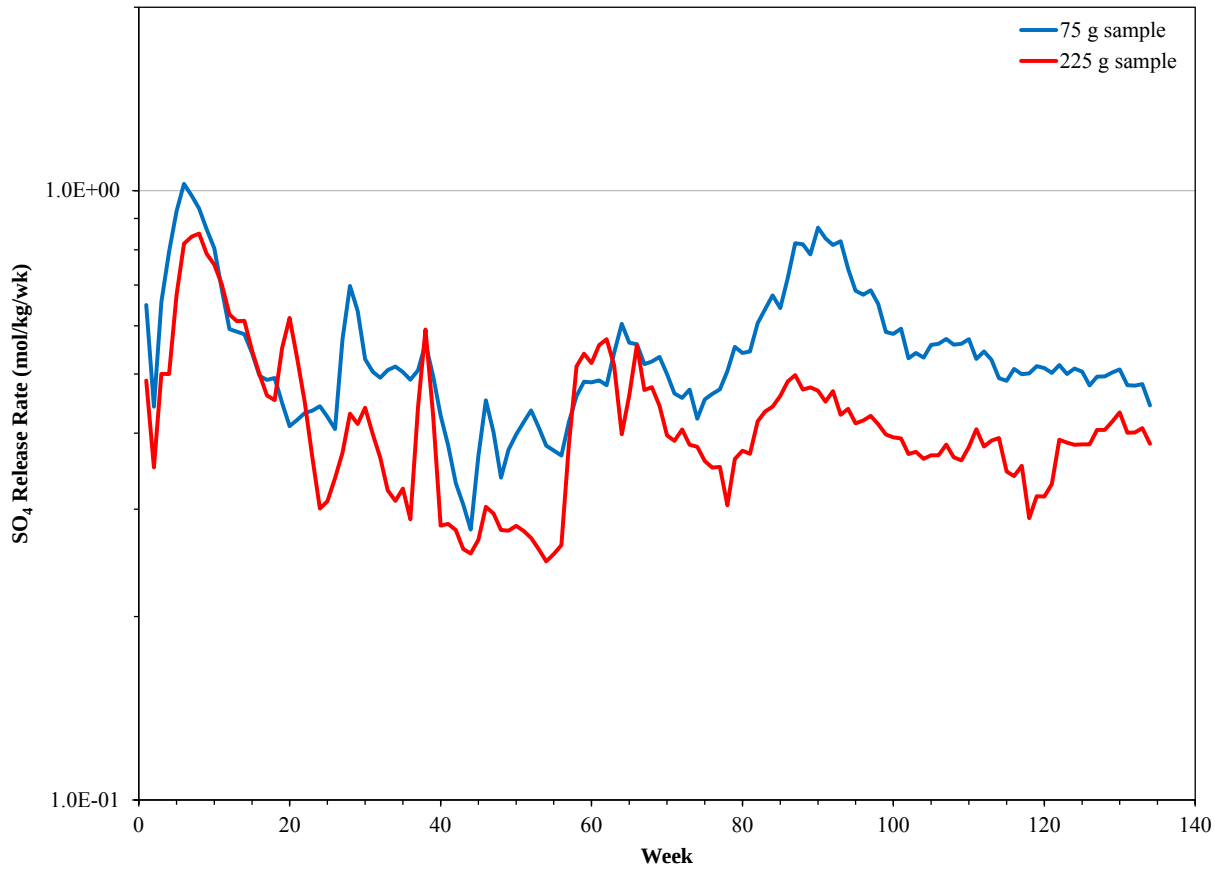

Figure 4.40 Norite standard and oversized samples SO_4 release rate trends

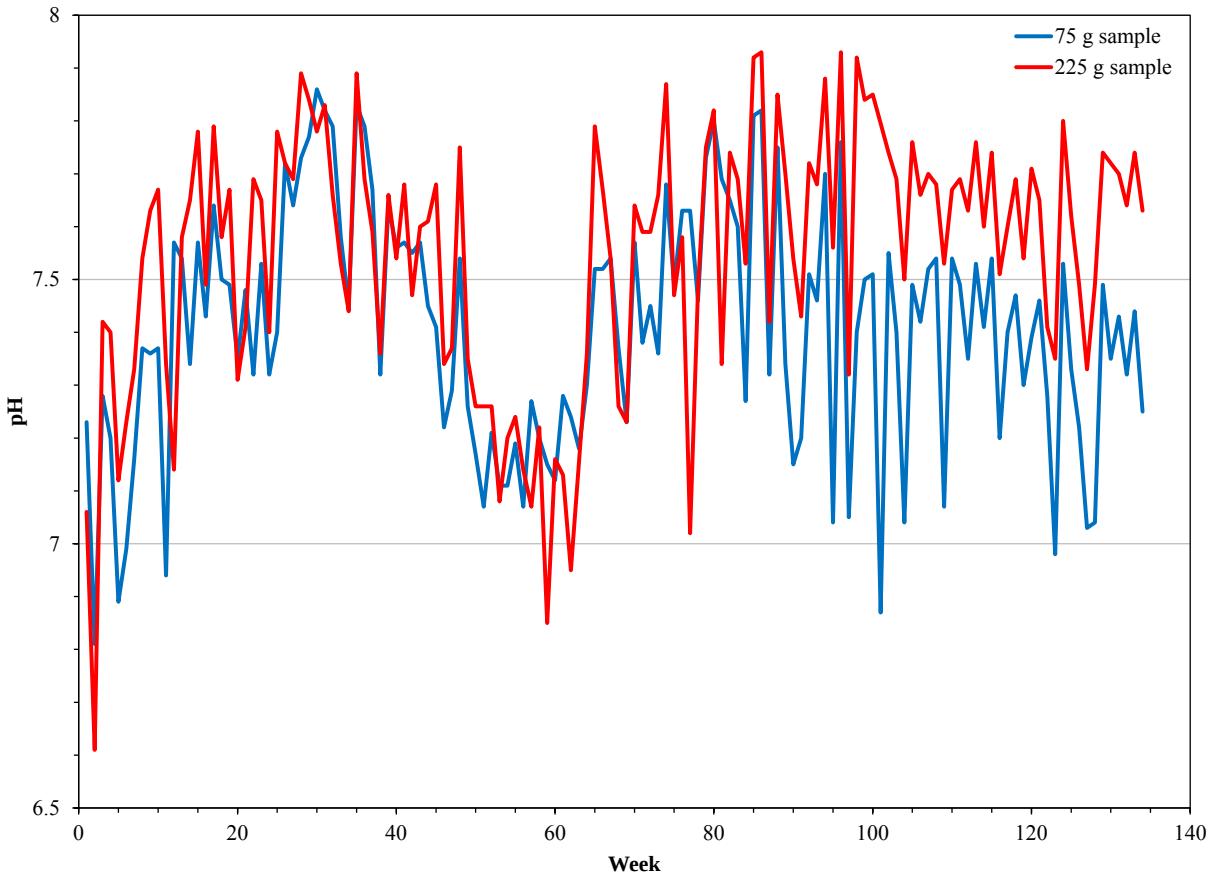

Figure 4.41 Diatreme standard and oversized samples leachate pH trends

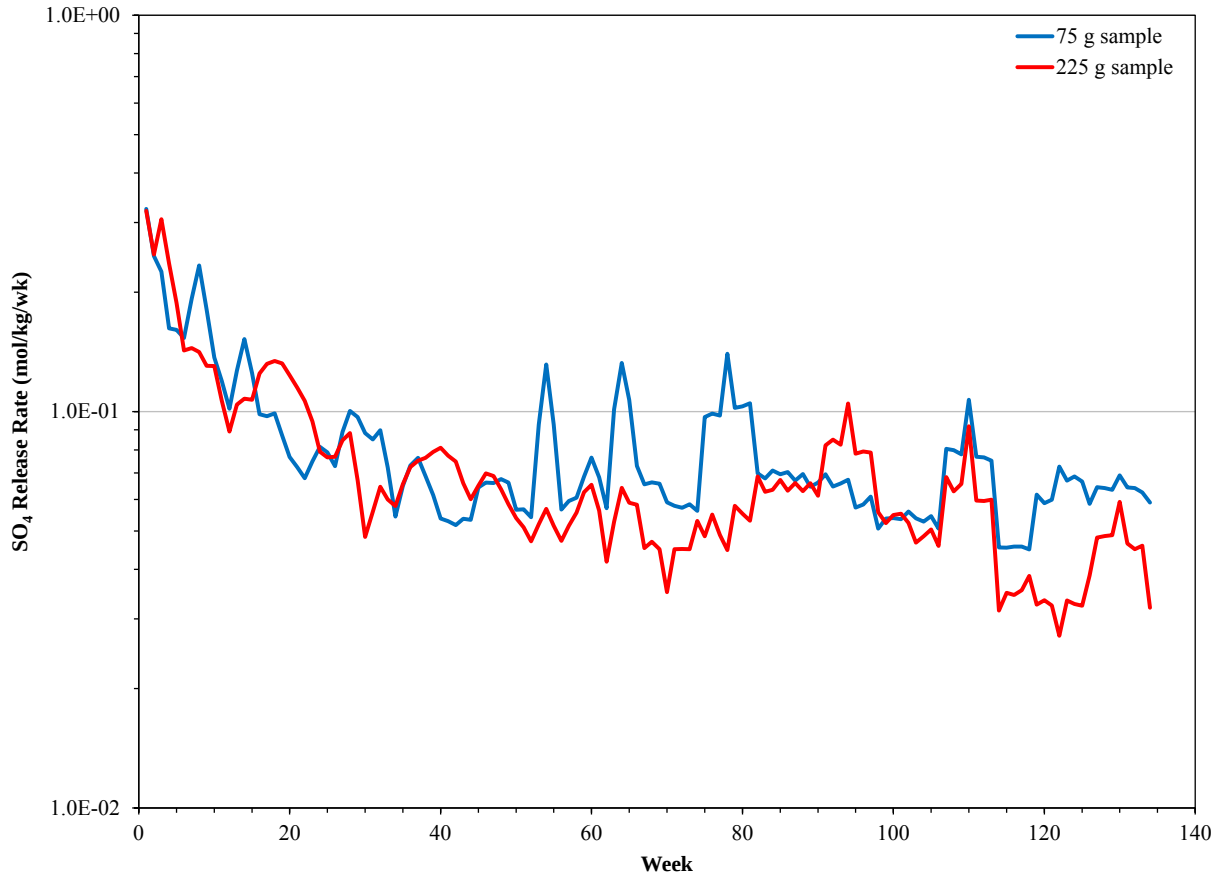

Figure 4.42 Diatreme standard and oversized samples SO_4 release rate trends

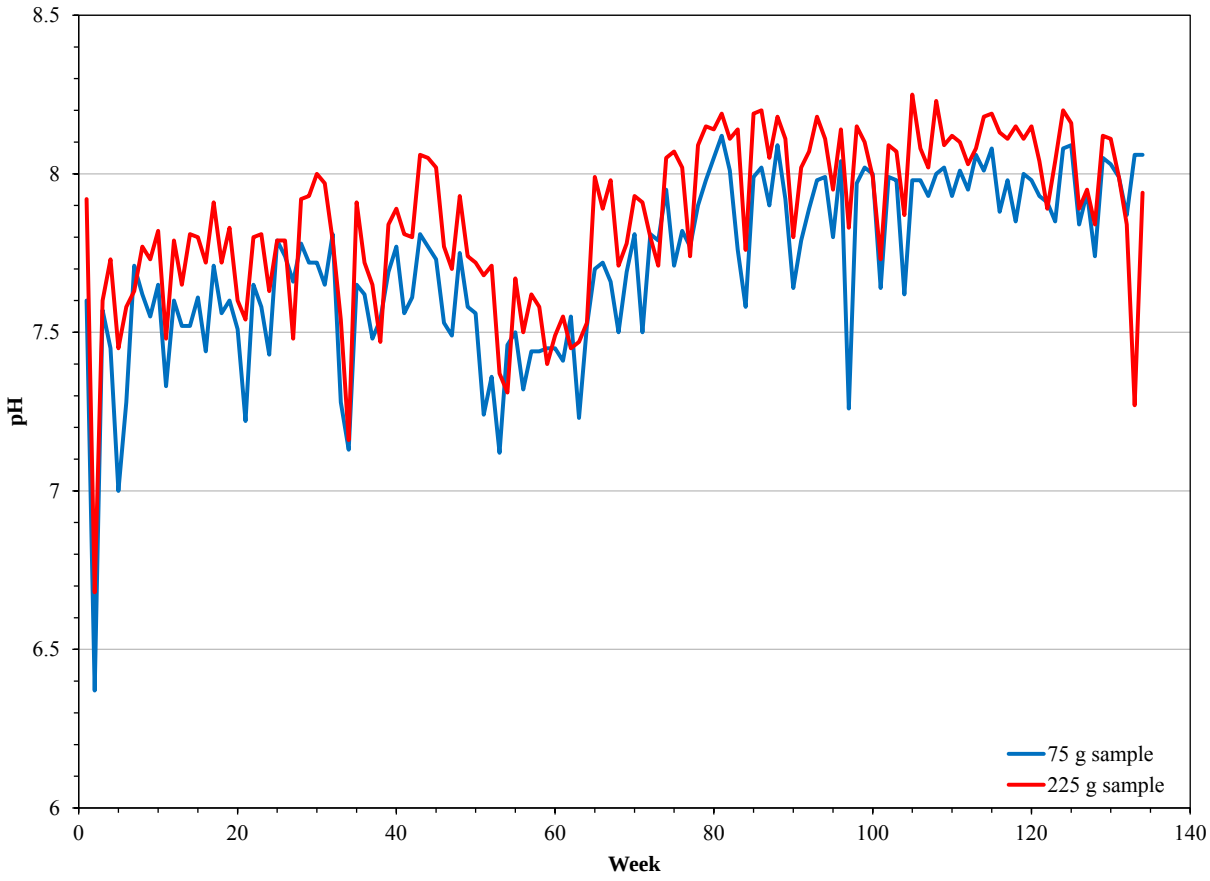

Figure 4.43 Mudstone standard and oversized samples leachate pH trends

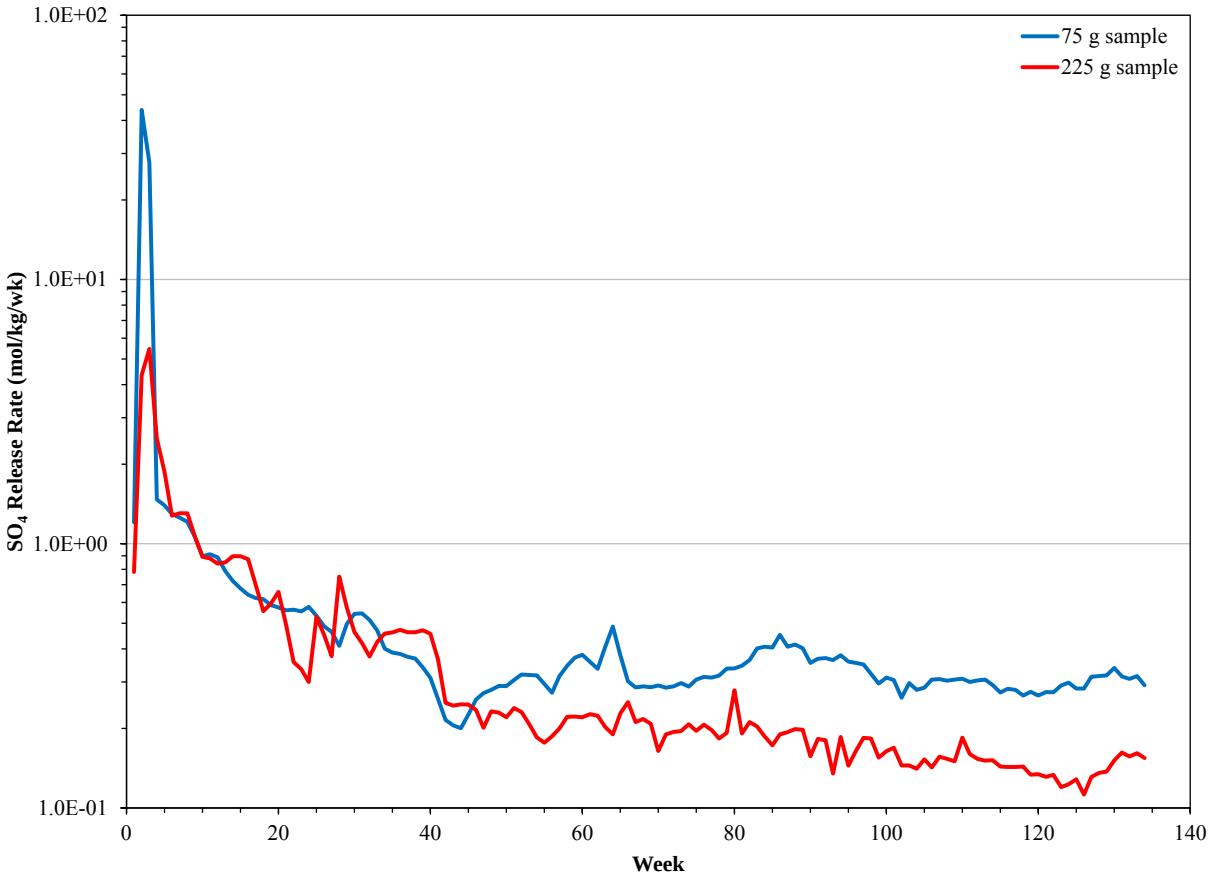

Figure 4.44 Mudstone standard and oversized samples SO_4 release rate trends

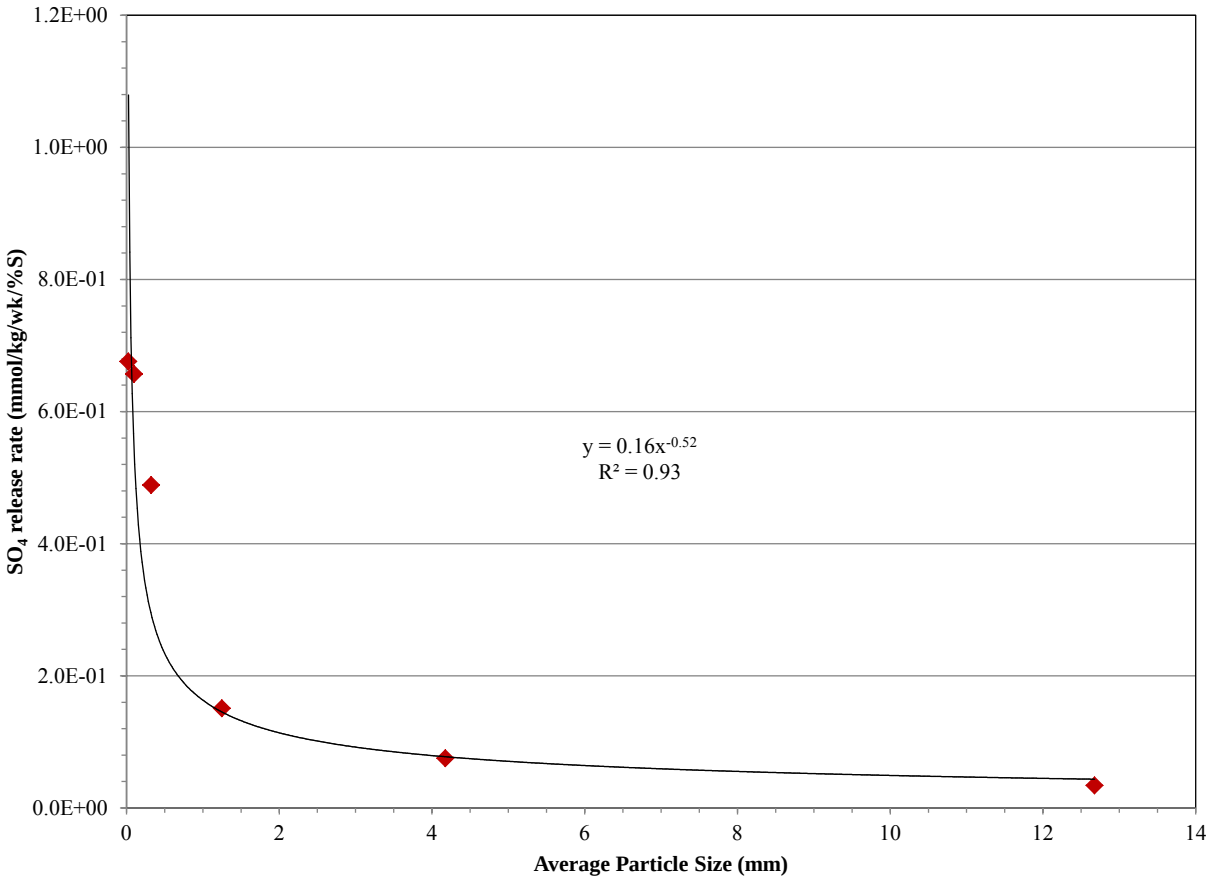

Figure 5.1 Norite SO_4 release rate as a function of particle size

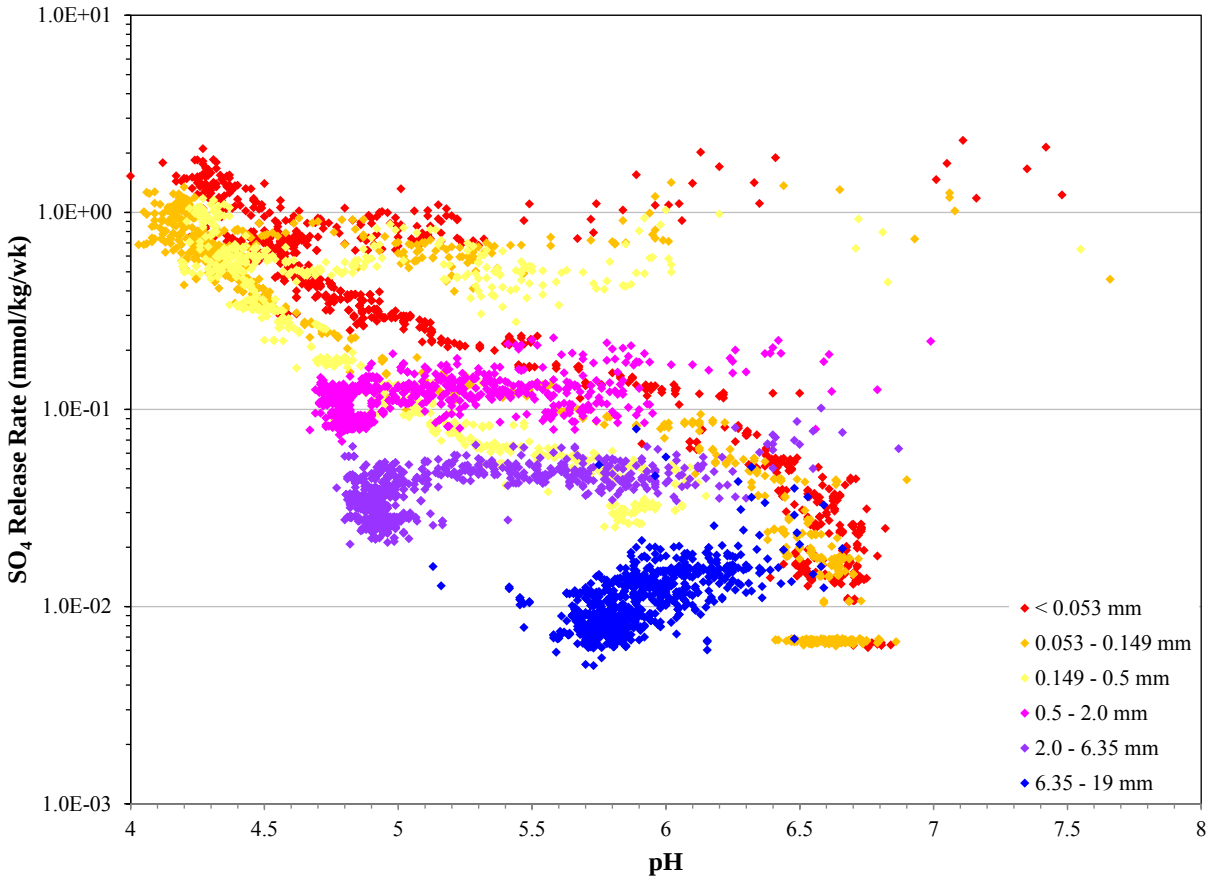

Figure 5.2 Norite SO_4 release rate and pH relationship

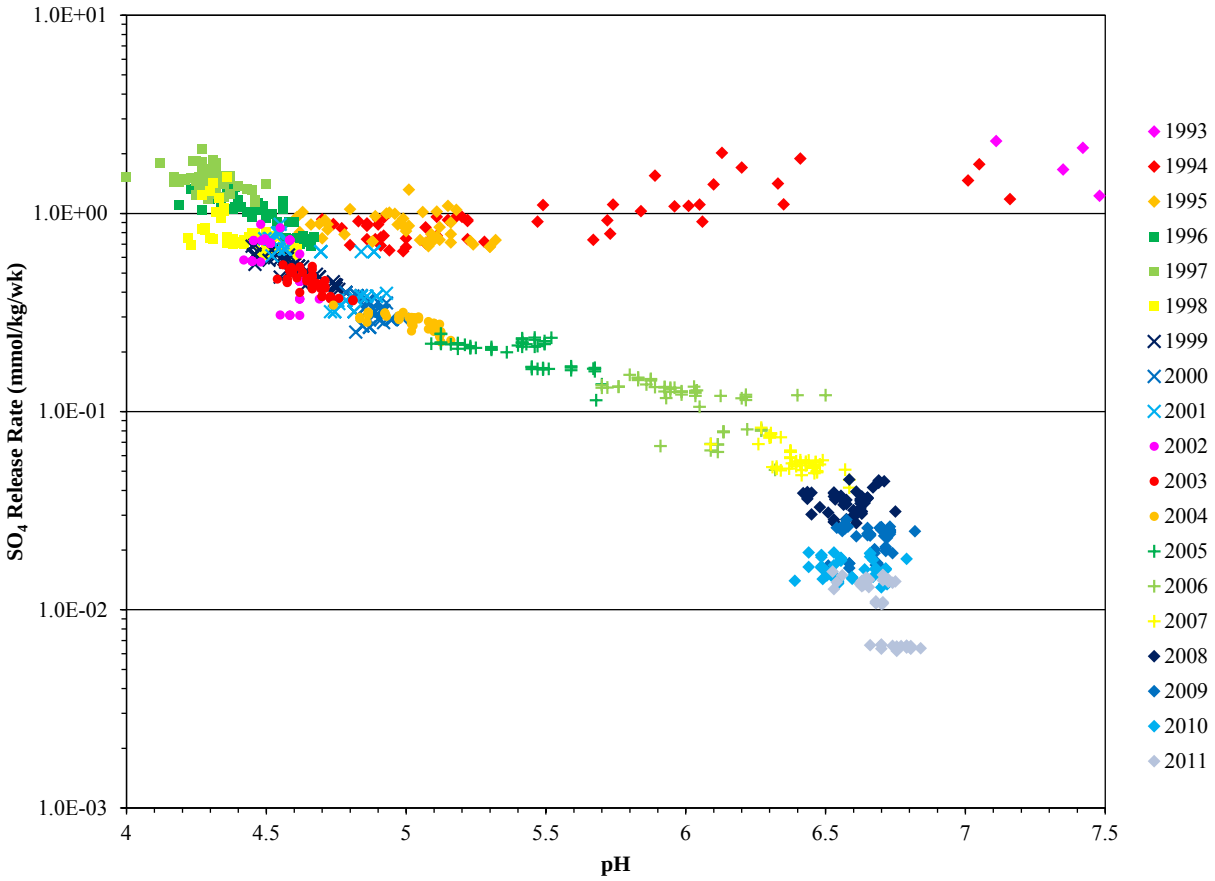

Figure 5.3 Annual norite SO_4 release rate and pH relationship

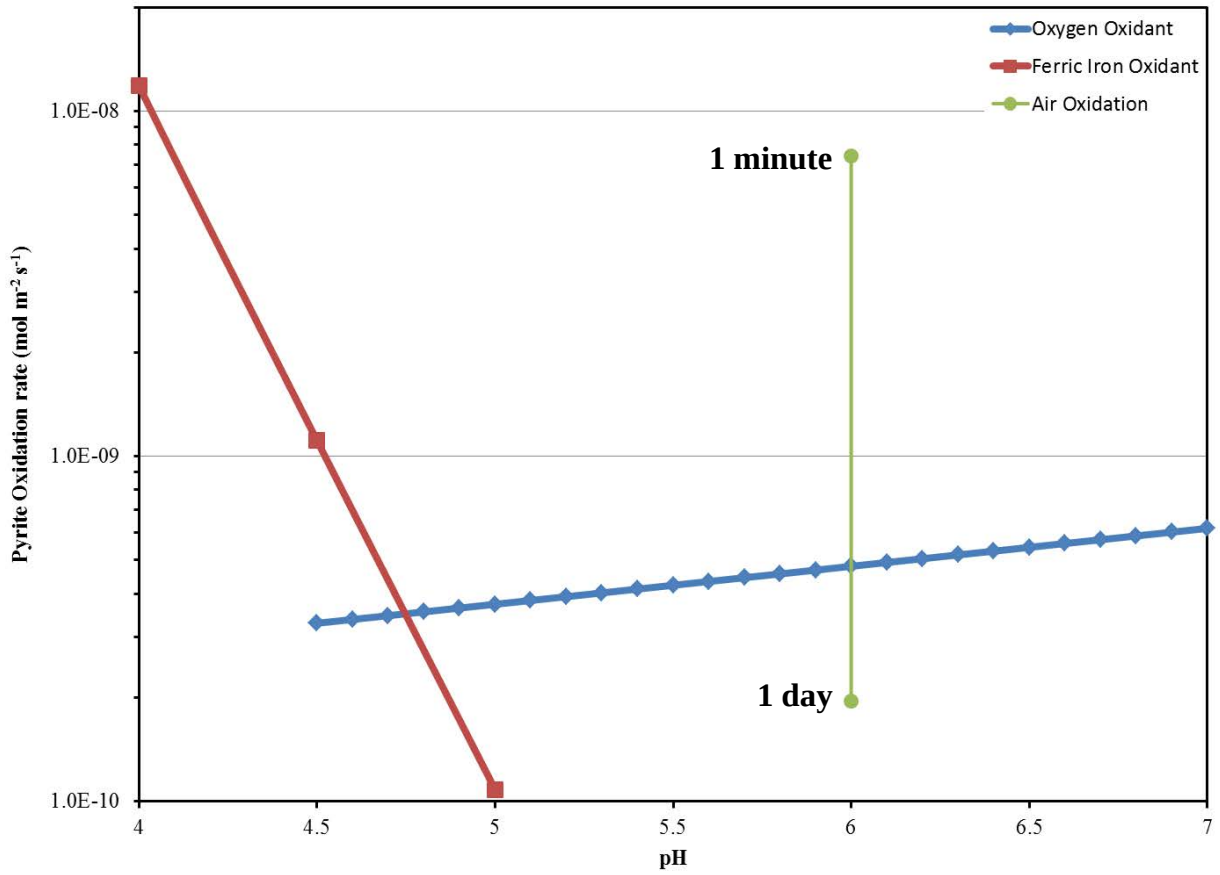

Figure 5.4 Pyrite oxidation rate as a function of fluid pH and oxidant.
Trends were calculated based on the equations of Williamson and Rimstidt (1994) and Jerz and Rimstidt (2004). Oxygen concentration was assumed to be in equilibrium with the atmosphere. And Fe species concentrations were calculated as equilibrium with Fe(OH)3 using the Geochemist's Workbench (Bethke and Yeakel, 2011).

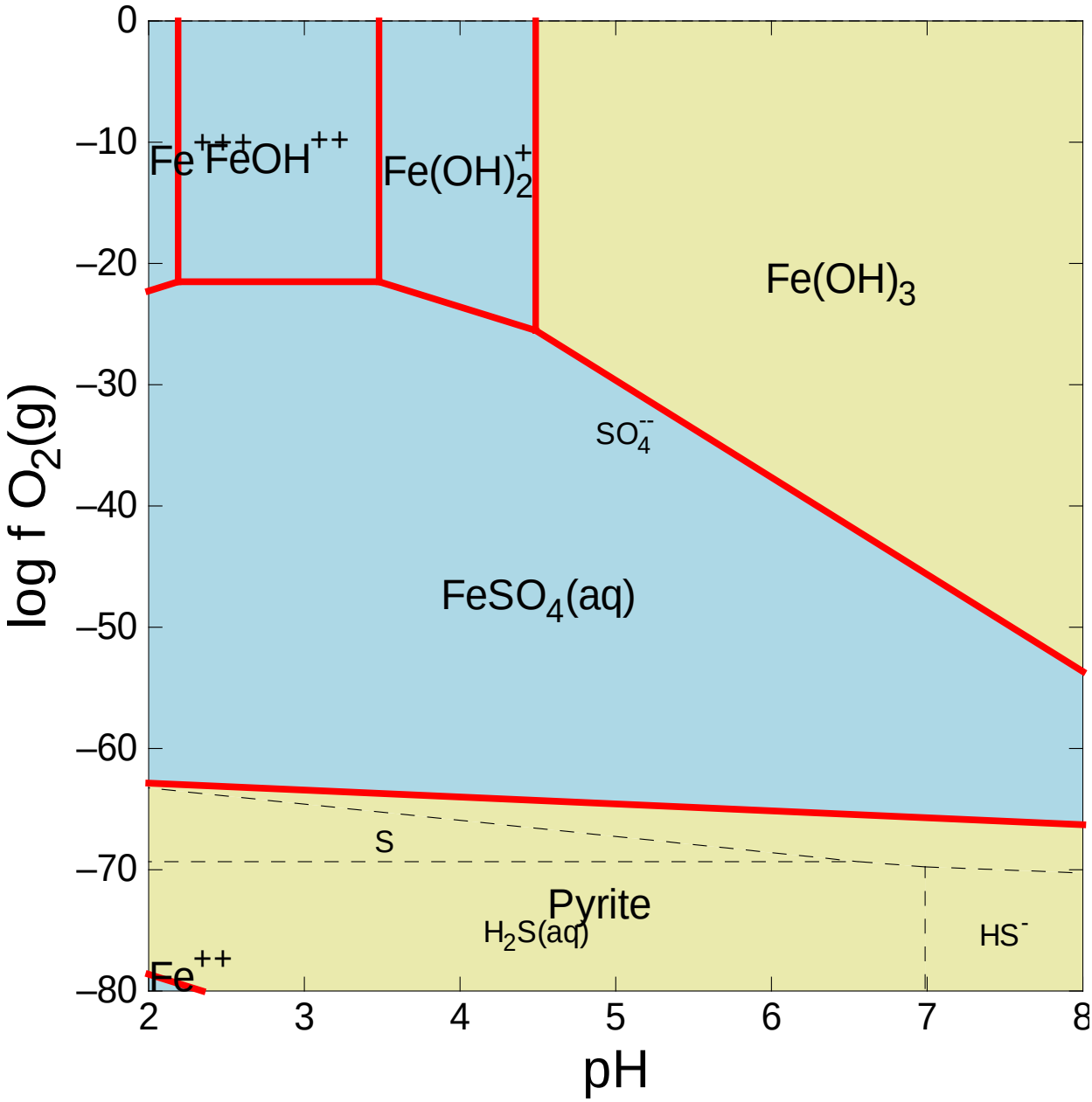

Figure 5.5 Oxidation state and fluid pH plot of dominant Fe species.
The diagram was calculated with Geochemist's Workbench (Bethke and Yeakel, 2011). Fe and SO_4 log activities were −4.5 and −2 respectively. These values represent the approximate values for the AMAX FL-6 leachate composition for a pH of about 4.5.

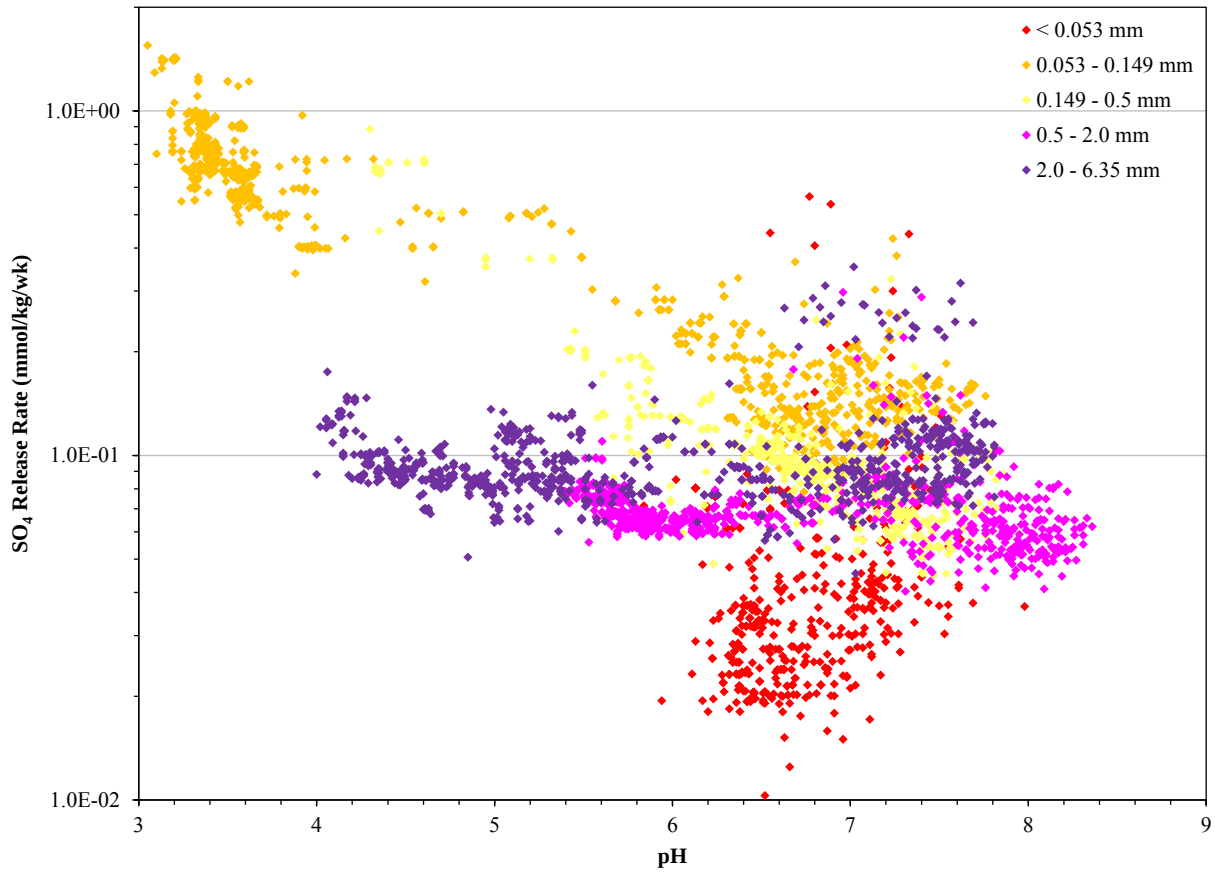

Figure 5.6 Diatreme SO_4 release rate and pH relationship.

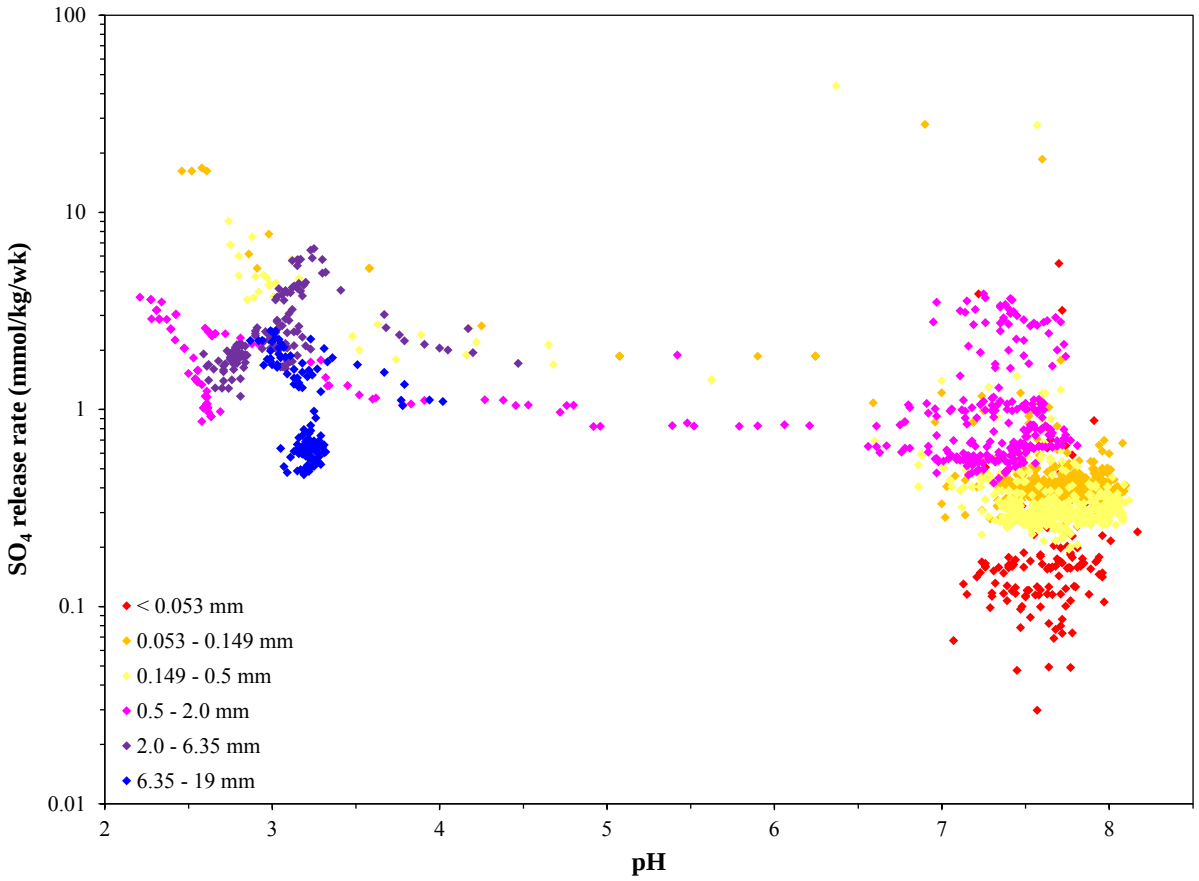

Figure 5.7 Mudstone SO_4 release rate and pH relationship.

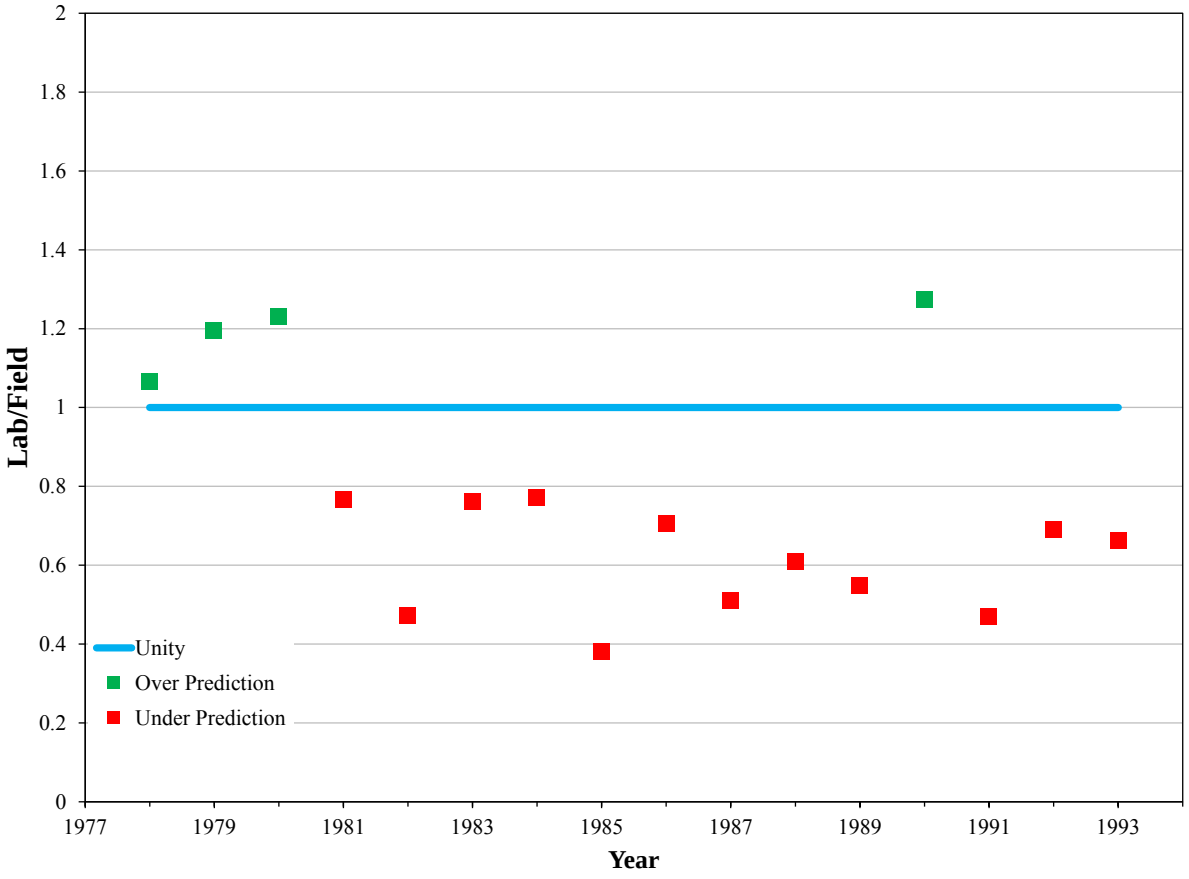

Figure 5.8 Comparison between laboratory predicted and field measured SO_4 release rates.

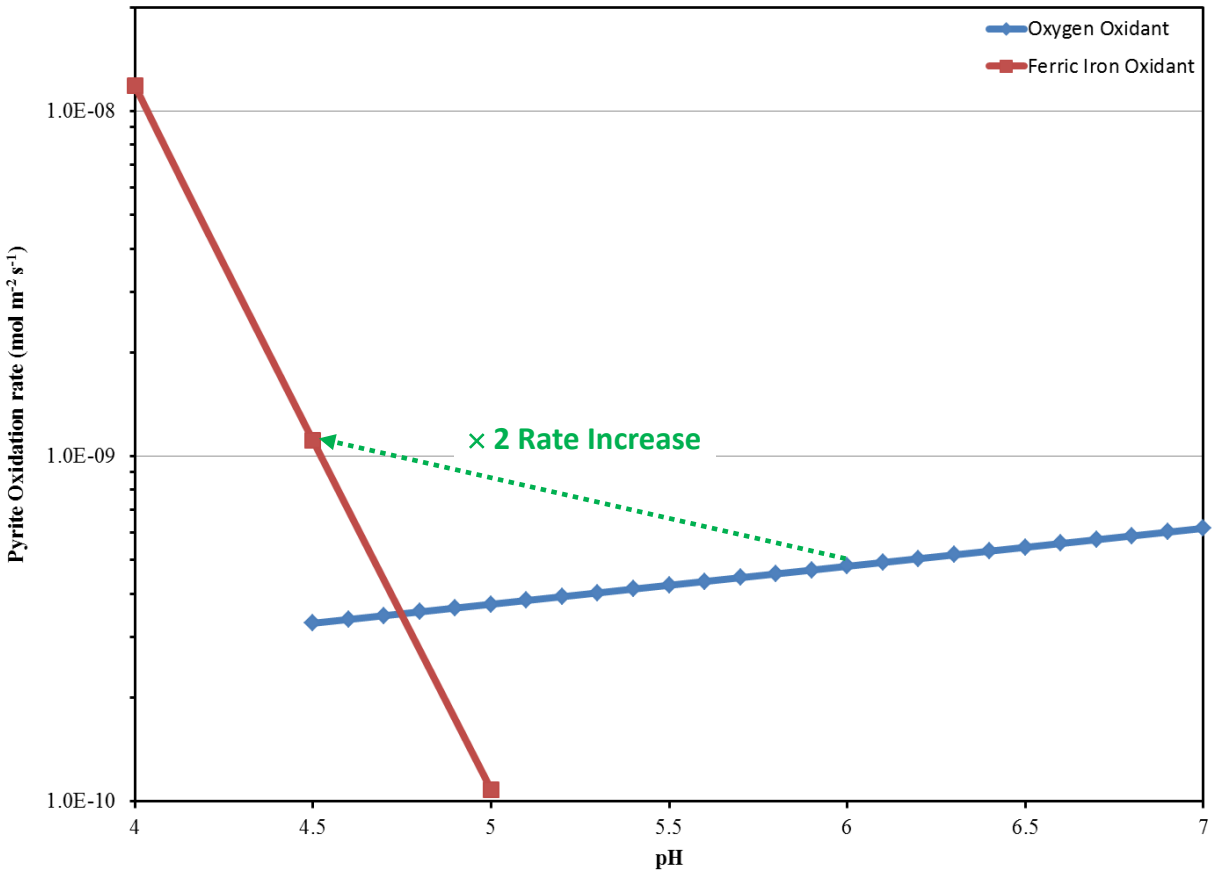

Figure 5.9 Pyrite oxidation as a function of fluid pH and oxidant.

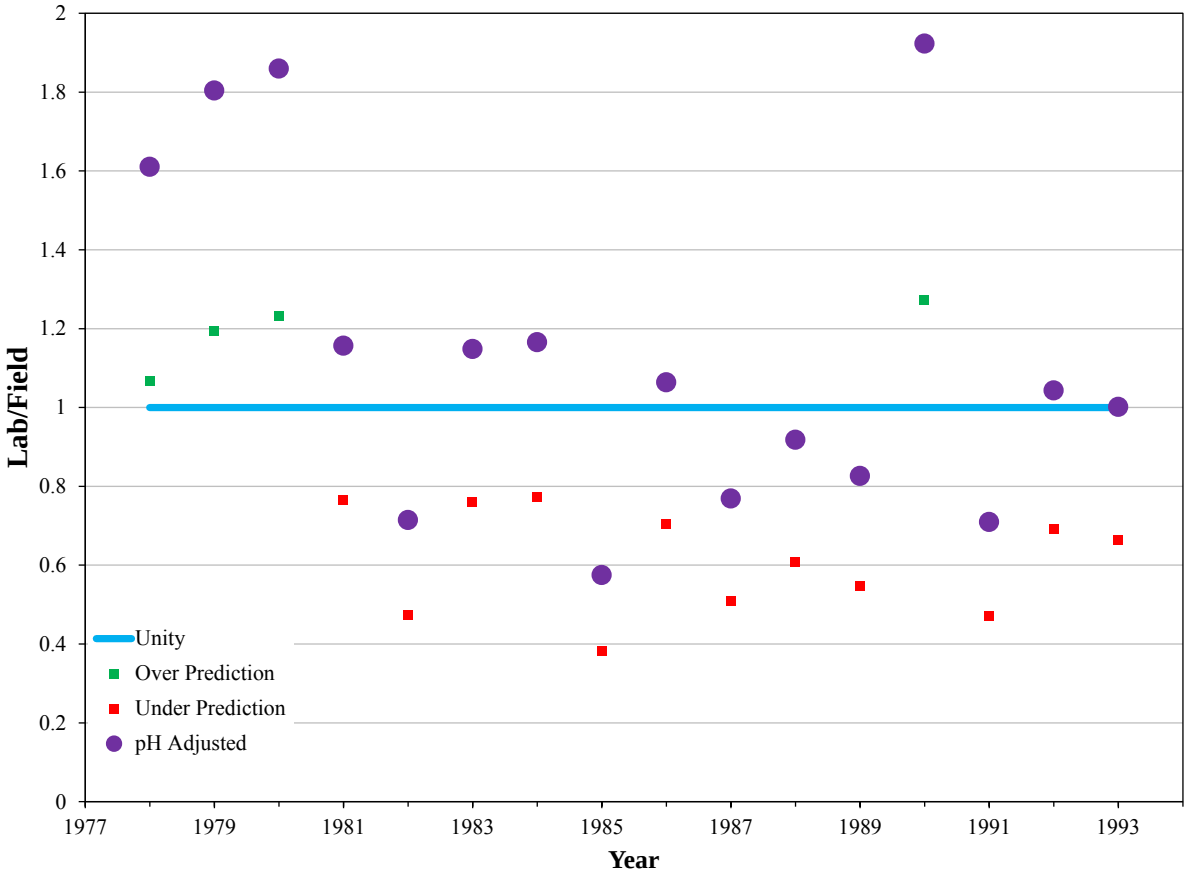

Figure 5.10 Comparison between laboratory predicted and field measured SO_4 release rates with adjustment for difference in laboratory fluid pH.

APPENDIX LIST

A1.1 Sulfur, Carbon and Major Oxide Analyses of Individual Particle Size Samples

Sample	Particle Size (mm)	S_{total}	S^{2-}	SO_4	C_{total}	CO_2	SiO_2	Al_2O_3	Fe_2O_3	MgO	CaO	Na_2O	K_2O	TiO_2	P_2O_5	MnO	LOI	FeO
norite	<0.053	1.41	1.13	0.28	0.25	0.14	43.69	13.85	18.64	8.23	6.45	1.58	0.95	2.47	0.45	0.17	2.1	
norite	0.053-0.149	1.11	0.76	0.35	0.18	0.61	44.58	14.65	18.92	8.18	6.25	1.82	1.00	2.46	0.22	0.16	0.4	
norite	0.149-0.5	1.24	0.80	0.44	0.15	0.06	45.01	14.98	17.68	8.67	6.60	1.91	0.89	1.73	0.18	0.15	1.2	
norite	0.5-2.0	0.87	0.52	0.35	0.13	<0.01	44.95	14.88	17.56	8.80	6.81	1.81	0.78	1.88	0.23	0.16	1.2	
norite	2.0-6.35	0.64	0.57	0.07	0.15	<0.01	45.50	15.24	17.09	8.78	6.96	1.79	0.79	1.95	0.25	0.17	0.7	
norite	6.35-19	0.43	0.31	0.12	0.08	0.02	45.52	15.11	16.76	9.51	7.58	1.62	0.67	1.80	0.25	0.17	0.9	
diatreme	<0.053	0.90	0.57	0.34	0.29	0.77	58.41	19.86	5.43	0.79	0.53	0.21	7.57	0.35	0.09	0.49	4.6	3.14
diatreme	0.053-0.149	1.88	1.53	0.35	0.45	1.45	67.97	12.86	5.12	0.47	0.87	0.67	6.91	0.16	0.10	0.58	2.7	2.54
diatreme	0.149-0.5	2.19	2.05	0.14	0.45	1.50	72.72	9.77	5.15	0.40	0.28	0.16	4.99	0.13	0.05	0.64	3.7	2.01
diatreme	0.5-2.0	1.87	1.69	0.18	0.51	1.72	74.61	9.52	4.68	0.43	0.36	0.14	4.36	0.16	0.07	0.76	3.6	2.34
diatreme	2.0-6.35	1.59	1.44	0.15	0.41	1.38	70.01	12.41	4.67	0.51	0.24	0.17	5.67	0.32	0.12	0.60	3.8	2.34
mudstone	<0.053	2.74	2.06	0.68	0.90	0.84	66.22	12.11	5.77	1.79	1.39	0.16	5.26	0.59	0.21	0.08	6	
mudstone	0.053-0.149	3.12	2.54	0.58	1.08	1.63	64.62	11.10	8.21	1.72	1.62	0.12	4.92	0.51	0.18	0.10	5.6	
mudstone	0.149-0.5	2.56	1.98	0.58	1.11	1.60	66.59	11.47	5.21	1.80	1.60	0.08	5.12	0.57	0.23	0.08	6.8	
mudstone	0.5-2.0	2.83	2.29	0.54	1.04	1.46	66.75	11.49	5.55	1.70	1.40	0.06	5.17	0.57	0.21	0.08	6.1	
mudstone	2.0-6.35	2.99	2.45	0.55	1.20	2.08	65.92	11.52	5.40	1.96	1.97	0.13	5.12	0.58	0.20	0.10	6.2	
mudstone	6.35-19	2.70	2.35	0.35	0.88	0.98	67.73	11.28	5.24	1.60	1.07	0.08	4.92	0.57	0.22	0.03	6.3	

Concentrations in wt%. LOI= loss on ignition. FeO determined by wet chemistry.

A1.2 Large Ion Lithophiles and Rare Earth Element Analyses of Individual Particle Size Samples

Sample	Particle Size (mm)	Rb	Sr	Cs	Ba	Sc	Y	La	Ce	Pr	Nd	Sm	Eu	Gd	Tb	Dy	Ho	Er	Tm	Yb	Lu	Hf	Ta	W
norite	<0.053	27	283	2.3	390	27	29.0	27.6	63.4	8.2	35.6	7.0	1.7	6.8	1.0	5.7	1.0	2.6	0.3	2.3	0.3	5.4	1.1	1.7
norite	0.053-0.149	28	304	1.8	440	29	19.3	18.8	41.7	5.1	18.9	3.9	1.6	3.7	0.6	3.6	0.6	1.9	0.3	1.7	0.3	2.8	1.0	0.7
norite	0.149-0.5	26	320	1.9	400	25	17.4	18.0	36.9	4.6	18.9	4.2	1.6	3.2	0.6	3.2	0.6	1.6	0.2	1.8	0.3	2.9	0.7	1.1
norite	0.5-2.0	21	285	1.5	345	26	19.2	17.2	36.9	4.5	19.1	3.9	1.5	3.7	0.6	3.7	0.7	2.0	0.3	1.8	0.3	2.9	0.7	0.2
norite	2.0-6.35	42	608	2.9	376	28	41.6	35.6	76.7	9.7	38.9	8.5	3.4	8.1	1.3	7.0	1.3	3.7	0.5	3.7	0.5	5.5	1.4	1.2
norite	6.35-19	19	260	1.1	358	28	18.9	16.6	34.5	4.1	17.4	3.4	1.5	3.9	0.5	3.4	0.6	1.8	0.3	1.8	0.3	2.2	0.6	1.1
diatreme	<0.053	336	185	9.7	1157	5	16.8	43.2	77.1	8.6	31.4	4.9	1.3	4.5	0.5	3.4	0.6	1.5	0.2	1.7	0.2	4.3	0.8	13.3
diatreme	0.053-0.149	257	206	3.4	1322	3	8.1	17.6	29.2	3.4	11.4	2.1	0.6	2.0	0.3	1.6	0.3	0.8	0.1	0.8	0.1	2.8	0.3	7.7
diatreme	0.149-0.5	190	146	3.0	904	1	6.4	14.7	24.9	2.7	11.3	1.4	0.5	1.3	0.2	1.2	0.2	0.7	0.1	0.6	0.1	1.9	0.2	5.6
diatreme	0.5-2.0	173	143	2.8	876	2	9.4	15.7	28.1	3.2	11.1	1.8	0.5	2.2	0.2	1.6	0.3	0.9	0.2	1.0	0.2	2.6	0.4	7.4
diatreme	2.0-6.35	223	206	4.4	1075	4	12.0	19.8	34.7	4.0	14.0	2.4	0.6	1.8	0.3	1.9	0.4	1.1	0.2	1.3	0.2	3.8	0.6	14.5
mudstone	<0.053	160	88	10.4	532	14	23.1	17.3	35.4	4.6	20.5	4.2	1.1	4.5	0.7	4.3	0.9	2.4	0.3	2.4	0.4	2.9	0.4	11.2
mudstone	0.053-0.149	149	111	9.0	495	14	20.3	16.7	31.0	4.0	17.0	3.5	0.9	3.9	0.5	3.6	0.8	2.0	0.3	1.9	0.3	2.4	0.4	8.8
mudstone	0.149-0.5	149	96	10.3	471	16	18.6	16.3	31.3	4.0	18.0	3.4	0.8	3.5	0.5	3.6	0.8	1.9	0.3	1.9	0.3	2.6	0.4	10.7
mudstone	0.5-2.0	159	87	10.4	468	15	19.9	16.9	33.0	4.1	18.2	3.7	0.9	4.0	0.6	3.8	0.8	2.0	0.3	1.8	0.3	2.6	0.4	10.2
mudstone	2.0-6.35	142	106	9.7	475	16	19.8	16.1	31.6	3.9	17.3	2.9	0.9	3.6	0.5	3.6	0.7	1.9	0.3	1.8	0.3	2.6	0.4	10.2
mudstone	6.35-19	144	67	10.4	459	15	20.3	16.5	32.1	4.1	17.3	3.7	0.9	3.8	0.6	3.5	0.7	1.9	0.3	2.2	0.3	2.6	0.4	9.2

Concentrations in parts per million (mg/kg)

A1.3 High Field Strength Elements and Ore Metal Analyses of Individual Particle Size Samples

Sample	particle size (mm)	V	Co	Ni	Cu	Zn	Ga	As	Se	Zr	Nb	Mo	Ag	Cd	Sn	Sb	Au[1]	Hg	Tl	Pb	Bi	Th	U
norite	<0.053	266	121	1259	6656	146	20	23	3.4	190	19	6	2.0	0.9	1.0	2.1	39	0.14	0.3	16	0.8	4.5	1.1
norite	0.053-0.149	269	102	904	4641	102	20	12	2.2	101	16	3	1.2	0.6	1.0	2.5	15	0.08	0.2	7	0.4	1.6	0.7
norite	0.149-0.5	233	111	1078	5011	98	23	8	2.8	98	12	2	1.4	0.5	<1.0	0.4	8	0.04	0.2	6	0.2	2.0	0.5
norite	0.5-2.0	223	98	930	4048	88	23	5	1.8	113	12	2	1.1	0.6	<1.0	0.3	11	0.04	0.1	4	0.5	0.9	0.4
norite	2.0-6.35	471	167	529	2804	81	39	4	1.4	210	26	2	0.7	0.4	<1.0	0.2	5	0.02	0.1	4	0.4	2.4	1.0
norite	6.35-19	234	79	431	2365	90	21	5	1.1	75	10	2	0.6	0.4	<1.0	0.1	7	0.02	0.1	6	0.2	0.8	0.5
diatreme	<0.053	50	5	12	169	3636	25	54	<0.5	134	11	10	11.8	12.0	7.0	1.8	137	0.62	0.5	1298	1.8	11.9	3.7
diatreme	0.053-0.149	21	5	9	228	5591	11	75	<0.5	93	6	7	11.7	15.7	3.0	1.2	460	0.18	0.4	1584	1.8	6.0	2.1
diatreme	0.149-0.5	18	4	4	173	5549	10	68	<0.5	66	5	5	11.5	17.1	<1.0	1.2	188	0.61	0.3	1987	2.3	4.3	1.7
diatreme	0.5-2.0	20	4	4	202	7092	12	56	<0.5	85	6	8	13.0	20.4	<1.0	1.5	92	4.36	0.2	3322	2.4	5.3	2.1
diatreme	2.0-6.35	37	4	4	231	4374	15	47	<0.5	119	8	9	10.0	12.9	1.0	1.0	124	0.04	0.2	1751	2.1	9.2	3.2
mudstone	<0.053	148	18	115	124	291	14	333	1.6	103	7	2	1.3	0.8	2.0	213	252	7.83	1.5	70	0.4	4.4	1.9
mudstone	0.053-0.149	137	17	85	95	244	14	333	1.6	98	7	3	1.5	0.5	7.0	206	262	6.32	2.1	48	0.4	5.0	1.6
mudstone	0.149-0.5	153	13	76	73	159	13	334	1.3	89	7	2	1.3	0.3	1.0	94	237	4.95	1.8	25	0.2	5.2	1.5
mudstone	0.5-2.0	155	13	76	57	112	16	337	1.6	98	7	1	1.1	0.2	2.0	81	198	2.97	1.3	19	0.2	5.7	1.4
mudstone	2.0-6.35	141	15	86	65	113	13	355	1.4	91	6	1	1.0	0.2	2.0	45	204	2.68	1.1	9	0.1	2.9	1.7
mudstone	6.35-19	147	19	86	63	99	14	348	1.8	93	7	1	1.1	0.2	1.0	168	203	2.50	1.4	8	0.2	3.7	1.5

Concentrations in parts per million (mg/kg) [1]= Au concentration in parts per billion (ug/mg)

A1.4 Sulfur, Carbon and Major Oxide Analyses of Leached Particle Size Samples

Sample	particle size (mm)	S_{total}	SO_4	C_{total}	CO_2	SiO_2	Al_2O_3	Fe_2O_3	MgO	CaO	Na_2O	K_2O	TiO_2	P_2O_5	MnO	Cr_2O_3	Ba	LOI
diatreme	<0.053	1.47	0.09	0.29	0.15	62.27	15.68	7.61	0.48	0.3	0.25	7.02	0.5	0.16	0.25	0.008	1650	4.5
mudstone	<0.053	3.31	0.18	0.75	0.19	66.71	11.6	6.2	1.28	0.71	0.27	5.54	0.57	0.21	0.04	0.022	1014	6.5
mudstone	0.053-0.149	2.34	0.13	0.66	<0.01	67.67	11.36	6.87	1.02	0.4	0.25	5.57	0.54	0.17	0.02	0.016	579	5.9
mudstone	0.149-0.5	1.85	0.09	0.66	<0.01	69.47	11.87	4.92	1.03	0.24	0.1	5.8	0.58	0.17	0.02	0.016	570	5.7
mudstone	0.5-2.0	1.36	0.07	0.71	<0.01	69.14	11.83	5.32	1.02	0.15	0.08	5.65	0.6	0.17	0.01	0.017	514	5.8
mudstone	2.0-6.35	1.95	0.15	0.66	0.12	68.36	11.45	5.44	1.02	0.35	0.1	5.63	0.58	0.19	0.01	0.014	485	6.6
mudstone	6.35-19	2.83	0.56	1.06	1.47	66.41	11.62	5.41	1.51	1.38	0.06	5.57	0.59	0.18	0.07	0.016	501	7

Concentrations in wt%, Ba concentration in parts per million (mg/kg). LOI= loss on ignition

A1.5 Sulfur, Sulfate, and Carbon Dioxide Analyses of Individual Particle Size Samples

sample	particle size (mm)	S_{total}	SO_4	CO_2
diatreme	<0.053	0.95	0.16	0.96
	0.053-0.149	1.98	0.04	1.32
	0.149-0.5	2.34	0.03	1.6
	0.5-2.0	1.9	0.05	1.73
	2.0-6.35	1.5	0.04	1.46
mudstone	<0.053	2.83	0.28	0.88
	0.053-0.149	3.01	0.08	1.64
	0.149-0.5	2.61	0.07	1.68
	0.5-2.0	2.79	0.11	1.4
	2.0-6.35	3.52	0.13	1.27
	6.35-19	3.46	0.14	1.89
norite	<0.053	1.51	0.08	0.32
	0.053-0.149	0.87	0.08	0.1
	0.149-0.5	1.29	0.09	0.06
	0.5-2.0	0.88	0.07	0.05
	2.0-6.35	0.83	0.06	0.09
	6.35-19	0.93 (0.3)*	0.03	<0.01

Concentrations in wt%. Analyses performed by Midland Research.
*=Original value. Sample was rerun because of prior knowledge of the bulk sample composition of the AMAX FL-6 rock pile. The 0.93 value is likely more accurate.

A1.6 Mineral Modal Abundance and Average Mineral Composition of Individual Particle Size Samples

Sample	Mineral	Modal %	n	SiO_2	Al_2O_3	TiO_2	FeO	MgO	MnO	K_2O	Na_2O	CaO	Cr_2O_3	NiO	CO_2	H_2O	Total %
Diatreme	Quartz	71	75	99.1	0.1	0.02	0.06	0.00	0.01	0.01	0.00	0.01					99.3
Diatreme	K-feldspar	16	17	65.1	18.4	0.03	0.12	0.01	0.02	16.13	0.67	0.02					100.5
Diatreme	Muscovite	9	9	48.0	31.5	0.11	2.34	1.01	0.14	10.23	0.12	0.09				6.5	100.0
Diatreme	Kutnahorite	3	3				13.35	3.26	28.10			13.68			41.6		100.0
Diatreme	Quartz	43	43	99.1	0.1	0.02	0.03	0.00	0.01	0.02	0.01	0.01					99.2
Diatreme	K-feldspar	31	31	64.4	19.2	0.05	0.11	0.02	0.08	15.85	0.41	0.03					100.2
Diatreme	Muscovite	16	16	45.4	30.5	0.27	3.99	0.89	1.93	8.70	0.14	0.05				8.2	100.0
Diatreme	Rhodochrosite	2	2				25.16	2.68	30.93			3.27			38.0		100.0
Diatreme	Siderite	5	5				48.36	2.10	7.38			3.64			38.5		100.0
Mudstone	Quartz	29	31	100.1	0.2	0.02	0.15	0.01	0.00	0.00	0.01	0.02					100.5
Mudstone	K-feldspar	16	17	68.7	18.6	0.00	0.26	0.02	0.02	13.15	0.01	0.26					101.1
Mudstone	Mixed Mica	26	28	63.2	17.8	0.36	1.88	1.58	0.04	5.92	0.10	0.17				8.9	100.0
Mudstone	Siderite	1	1				43.61	2.42	0.46			0.02			53.5		100.0
Mudstone	Dolomite	8	9				2.50	20.32	2.17			35.54			39.5		100.0
Mudstone	Quartz	60	66	99.3	0.5	0.01	0.03	0.00	0.06	0.09	0.05	0.02					100.0
Mudstone	K-feldspar	38	42	64.8	18.7	0.10	0.17	0.00	0.00	15.77	1.06	0.12					100.7
Norite	Ilmenite[1]	8	9	0.0	0.1	52.09	47.29	0.25	0.40	0.01	0.03	0.01	0.08	0.03			100.5
Norite	Plagioclase	13	14	54.6	29.6	0.02	0.41	0.04	0.01	0.28	5.11	10.95					101.0
Norite	Plagioclase[2]	24	25	53.6	29.7	0.09	0.48	0.03	0.02	0.19	4.07	4.78				7.0	100.0
Norite	K-feldspar	4	4	64.9	19.6	0.05	0.32	0.01	0.01	10.75	2.70	0.28					98.7
Norite	Hypersthene	15	16	50.3	1.0	0.23	33.09	14.16	0.41	0.01	0.01	0.48	0.10				99.7
Norite	Olivine	19	20	37.3	0.0	0.05	29.66	32.79	0.40	0.01	0.01	0.03	0.07	0.17			100.5
Norite	Biotite	2	2	34.7	15.2	6.67	23.26	7.74	0.05	7.82	0.06	0.02				4.5	100.0
Norite	Cordierite	9	9	49.1	33.5	0.03	8.36	8.47	0.06	0.01	0.31	0.15				0.9	100.8
Norite	Plagioclase	48	53	53.1	29.6	0.05	0.21	0.02	0.02	0.34	4.61	11.67					99.6
Norite	Hypersthene	6	7	50.8	0.6	0.26	25.91	20.42	0.51	0.01	0.01	1.24	0.11				99.8
Norite	Augite	1	1	52.9	1.4	0.36	10.03	14.16	0.20	0.02	0.25	20.92					100.2
Norite	Olivine	36	40	35.0	0.0	0.07	31.31	32.43	0.41	0.01	0.01	0.07	0.11	0.25			99.6
Norite	Biotite	8	9	35.9	14.5	4.63	11.98	17.59	0.08	9.50	0.13	0.03				5.7	100.0

Oxide values in wt%. n= number of spot analyses for modal % determination.

*= Samples analyzed were a split from the 2.0-6.35 mm sample, sample with no asterisk were taken from a whole rock thin section.

[1]= Ilmenite has an excess 0.16 wt% O, [2]= The plagioclase in this sample is altered, this plagioclase mode represents the altered modal %.

A1.7 Sulfide Mineral Modal Abundance and Average Mineral Composition

Sample	Mineral	Modal %	Counts	Fe	Ni	S	Cu	Total
Diatreme*	Pyrite	2	2	47	0.035	53	0.032	100
Diatreme	Pyrite	4	4	47	0.067	53	0.096	100
Mudstone*	Pyrite	20	22	47	0.048	53	0.16	100
Mudstone	Pyrite	3	3	47	0.12	53		100
Norite*	Pyrrhotite	7	7	64	0.030	37	0.28	101
Norite	Mixed Sulfide	1	1	58		35	7.8	100

Concentrations in wt%. n= number of spot analyses for modal % determination.
*= Samples analyzed were a split from the 2.0-6.35 mm sample, sample with no asterisk were taken from a whole rock thin section.

A1.8 Sulfide Mineral Compositions

Sample	Sample Size	Mineral	Fe	Ni	S	Cu	Total
diatreme	2.0-6.35	pyrite	45.87	0.00	53.59	0.00	99.46
diatreme	2.0-6.35	pyrite	46.81	0.05	52.62	0.00	99.49
diatreme	2.0-6.35	pyrite	46.62	0.05	53.15	0.23	100.06
diatreme	2.0-6.35	pyrite	46.36	0.00	53.66	0.07	100.09
diatreme	2.0-6.35	pyrite	46.32	0.00	52.82	0.00	99.13
mudstone	2.0-6.35	pyrite	45.67	0.00	53.28	0.00	98.95
mudstone	2.0-6.35	pyrite	46.70	0.03	53.16	0.09	99.98
mudstone	2.0-6.35	pyrite	46.23	0.00	53.45	0.00	99.68
mudstone	2.0-6.35	pyrite	46.26	0.15	52.72	0.00	99.13
mudstone	6.35-19	pyrite	46.63	0.05	52.90	0.00	99.58
mudstone	6.35-19	pyrite	45.86	0.00	53.37	0.00	99.23
mudstone	6.35-19	pyrite	45.51	0.03	52.87	0.07	98.48
mudstone	6.35-19	pyrite	45.47	0.21	52.65	0.22	98.55
mudstone	6.35-19	pyrite	47.14	0.00	53.40	0.03	100.56
mudstone	6.35-19	pyrite	46.31	0.01	52.90	0.13	99.35
norite	2.0-6.35	pyrrhotite	60.87	0.00	39.15	0.00	100.02
norite	2.0-6.35	pyrrhotite	60.59	0.35	37.95	0.00	98.90
norite	2.0-6.35	pyrrhotite	62.17	0.00	35.96	0.03	98.16
norite	2.0-6.35	pyrrhotite	60.30	0.14	38.11	0.05	98.60
norite	2.0-6.35	chalcopyrite	31.23	0.00	33.72	36.30	101.25
norite	2.0-6.35	chalcopyrite	31.89	0.03	33.39	34.33	99.63
norite	2.0-6.35	chalcopyrite	31.02	0.00	33.61	35.95	100.58
norite	2.0-6.35	cubanite	41.87	0.00	35.14	22.76	99.77
norite	2.0-6.35	cubanite	42.23	0.08	35.28	23.71	101.29

Values in wt%.

A1.9 Carbonate Mineral Compositions

Sample	Sample Size	Mineral	FeO	MgO	MnO	CaO	CO_2	Total
diatreme	2.0-6.35	Mn-siderite	29.33	4.49	27.30	1.25	37.63	100
diatreme	2.0-6.35	Mn-siderite	31.34	4.01	24.68	1.19	38.79	100
diatreme	2.0-6.35	Mn-siderite	43.42	4.82	10.64	2.81	38.32	100
diatreme	2.0-6.35	Mn-siderite	36.32	3.60	18.83	3.40	37.86	100
mudstone	2.0-6.35	dolomite	0.49	16.18	2.53	32.79	48.01	100
mudstone	2.0-6.35	dolomite	1.08	18.12	2.39	32.92	45.50	100
mudstone	2.0-6.35	dolomite	0.37	16.41	3.12	33.31	46.79	100
mudstone	2.0-6.35	dolomite	0.14	17.41	2.21	31.77	48.47	100
mudstone	6.35-19	dolomite	0.04	20.84	1.16	29.54	48.42	100
mudstone	6.35-19	dolomite	0.21	20.31	1.53	29.74	48.21	100
mudstone	6.35-19	dolomite	0.12	19.44	0.74	30.30	49.40	100
mudstone	6.35-19	dolomite	3.01	16.96	1.40	31.03	47.59	100
norite	2.0-6.35	calcite	0.07	0.00	0.03	56.01	43.89	100
norite	2.0-6.35	calcite	0.15	0.00	0.00	56.48	43.37	100

Values in wt%.

A1.10 Average Mineral Modal Abundance for Norite, Mudstone, and Diatreme

Sample	Plagioclase	Olivine	Pyroxene	Cordierite	Quartz	K-spar	Mica	Oxide	Carbonate	Sulfide	total
Norite	43	28	11	5	--	--	5	4	--	4	100
Mudstone	--	--	--	--	45	27	13	--	5	12	102
Diatreme	--	--	--	--	71	16	9	--	3	3	101